MASTER'S DISSERTATION

Lund University

Mechanical and Thermal Characterisation of Polymer Films Exposed to Filling Products

Name	Email
Erik Vu	kem13evu@student.lu.se

Submitted : February 1, 2019

Center for Analysis and Synthesis
Master's Dissertation

Mechanical and Thermal Characterisation of Polymer Films Exposed to Filling Products

Erik Vu

Supervisor: BAOZHONG ZHANG
PhD; Center for Analysis and Synthesis, LTH

ESKIL ANDREASSON
Technology Specialist, Tetra Pak®

ANNMAGRET ASP
Material Engineer, Tetra Pak®

ANNA SVENSSON
Development engineer, PhD, Tetra Pak®

Examiner: PATRIC JANNASCH
Professor; Center for Analysis and Synthesis, LTH

Contacting the division:
Center for Analysis and Synthesis
Lund University
Box 124, SE-221 00 Lund
Getingevägen 60
Sweden

Homepage:
http://www.materialkemi.lth.se/index.html

Abstract

Knowledge on how polymeric materials changes or are affected when exposed to products is of interest and importance for many commercial applications. Understanding the product interaction with packaging materials is the key to preventing errors and increasing the quality of products. At Tetra Pak®, product packaging is created to make food and drink safe and accessible everywhere. Therefore, packaging solutions for products must be constantly developed and improved in order to meet customer needs. Today's packaging contains many different polymeric materials and it does not look like it will change in the near future. Therefore, it is of importance to find an experimental working method to test and perform simulations, that are as close as possible to real behaviour of the material.

In this thesis, several experimental methods have been used to study the interaction between different products on low density polyethylene. Methods such as Wide-Angle X-ray Scattering (WAXS), tensile tests, thickness measurement, product uptake and Differential Scanning Calorimetry (DSC) have been used to study the interaction with products at Tetra Pak® and LTH. From the experimental tests, it was difficult to observe large difference in crystallinity and mechanical properties in the short period of the experiment. However, large differences could be seen in the thickness variation, which may be important to look into in the future as it may have a major impact on test results.

Abstrakt

Kunskap om hur polymera material förändras eller påverkas vid exponering för produkter är av intresse och betydelse för många kommersiella applikationer. Att förstå hur olika produkter integrera med förpackningsmaterial är nyckeln till att förebygga fel och öka produktkvaliteten. På Tetra Pak ® tillverkas och utvecklas produktförpackningar för att göra mat och dryck säkert och tillgängligt överallt i världen. Därför måste innovativa förpackningslösningar för produkter kontinuerligt utvecklas och förbättras för att möta kundernas behov. Dagens förpackning innehåller många olika polymermaterial och det ser inte ut som om det kommer att förändras inom en snar framtid. Därför är det viktigt att hitta en experimentell arbetsmetod för att testa och utföra simuleringar, som är så nära verkligheten som möjligt för att förstå polymer-materialets verkliga beteende.

I denna rapport har flera experimentella metoder använts för att studera interaktionen mellan olika produkter på en lågdensitetspolyeten material. Metoder som Wide-Angle X-ray Scattering (WAXS), dragprovsmätning, tjockleksmätning, produktupptagning och Differential Scanning Calorimetry (DSC) har använts för att studera produkt interaktionen på både Tetra Pak ® och LTH. Från experimentella tester var det svårt att observera någon stor skillnad i kristallinitet och i mekaniska egenskaper under den korta perioden av experimentet. Dock kan stora skillnader ses i tjockleksvariationen, vilket kan vara viktigt att undersöka i framtiden eftersom det kan ha en stor inverkan på testresultaten.

Acknowledgement

First and foremost, this thesis would not have been possible without the help of some very important people. My supervisors at Tetra Pak® and LTH; Eskil Andreasson, AnnMagret Asp, Anna Svensson and Baozhong Zhang. A special thanks for helping me with ideas, advises, recommendations and observations during this thesis work. Thank you for letting me be a part of a truly exceptional collaboration between Lund University and Tetra Pak®, as well as giving me the opportunity to learn a lot more about polymers, materials and many new interesting experimental methods. I could not have asked for a more competent, interested and encouraging supervisors.

I want to thank all the people at the division of polymer and material chemistry at LTH for making WAXS, DSC and SEM experiments possible. A special thanks to Reine Wallenberg for taking you time to show me the SEM instrument, Olga Gordivska for teaching me how to use WAXS, Smita Mankar and Thanh Huong Pham for helping me in using DSC and TGA.

Furthermore, a special thanks to Daniella Nae for helping me with the sample preparation and helping me with your expertise on materials, Jonas Galea for your support and guidance throughout the project and many interesting conversations and Björn Walter for his research on DIC.

Finally, I would like to thank my family, friends and many more who have always supported me and have been a part of making this thesis a success.

Erik Vu, Lund, Nov 2018

Contents

Page

1 Introduction **1**
- 1.1 Background and motivation . . . 1
- 1.2 Objective and vision . . . 2
- 1.3 Experimental Methods . . . 3
- 1.4 Limitations . . . 3

2 Theory **4**
- 2.1 Hierarchical Length Scales in Polymer Films . . . 4
- 2.2 Polymers . . . 5
  - 2.2.1 Blown film process . . . 6
- 2.3 Product Interactions . . . 7
  - 2.3.1 Mass transport processes . . . 8
- 2.4 Theoretical Framework . . . 10
  - 2.4.1 Product uptake . . . 10
  - 2.4.2 Thickness Measurement . . . 10
  - 2.4.3 Wide Angle X-ray Scattering (WAXS) . . . 11
  - 2.4.4 Differential scanning calorimetry (DSC) . . . 14
  - 2.4.5 Tensile testing . . . 17
  - 2.4.6 Digital Image Correlation (DIC) . . . 18
  - 2.4.7 Scanning Electron Microscopy (SEM) . . . 19
  - 2.4.8 Thermogravimetric Analysis (TGA) . . . 20

3 Experimental Testing **21**
- 3.1 Sample preparations . . . 21
  - 3.1.1 Dogbone samples . . . 22
  - 3.1.2 Aluminium pan (TGA, DSC) . . . 24
  - 3.1.3 Conductive Coating (SEM) . . . 24
- 3.2 Exposure of Products . . . 25
- 3.3 Product Uptake . . . 26
- 3.4 Thickness Measurement . . . 27
- 3.5 Wide Angle X-ray Scattering (WAXS) . . . 28
- 3.6 Differential Scanning Calorimetry (DSC) . . . 29
- 3.7 Tensile testing . . . 30
- 3.8 Digital Image Correlation (DIC) . . . 31
- 3.9 Scanning Electron Microscopy (SEM) . . . 32
- 3.10 Thermogravimetric Analysis (TGA) . . . 33

4 Results **34**
4.1 Product Uptake 34
4.2 Thickness measurement 38
4.3 Wide Angle X-ray Scattering (WAXS) 42
4.4 Differential Scanning Calorimetry (DSC) 45
4.5 Tensile testing 49
4.6 Digital Image Correlation (DIC) 54
4.7 Scanning Electron Microscopy (SEM) 57
4.8 Thermogravimetric Analysis (TGA) 63

5 Discussion **64**
5.1 Impact on Product Uptake 64
5.2 Thickness 65
5.3 Mechanical Properties 67
5.4 Impact on crystallinity 71
5.5 SEM on Deformed Samples 72

6 Conclusions **73**

7 Future Work **74**

Chapter 1

Introduction

1.1 Background and motivation

The packaging industry is a huge and growing sector but is facing increased pressure from manufactures, logistics, retailers and customers to look good, prevent damage, reduce cost and energy use. Therefore, the needs for a good product requires a good knowledge of how the packaging materials reacts to everyday uses and interactions with today products. The packaging material could consist of several material layers, such as polymers, aluminium foil and paperboard as shown in Figure 1.1. Polymers and especially polyethylene (PE) films have many applications and thanks to its favourable properties play an essential part in products used in everyday life and very notably in the packaging industry. Semi- crystalline polyethylene films have been widely researched since the middle of 20th century and it is still the most common polymer to this day. Injection moulding and blow moulding are the two most popular ways to produce high-quality polyethylene and the polymers properties and characteristics are different depending on the processing techniques. Low-density polyethylene (LDPE) films have been in use by Tetra Pak® for more than 50 years. The reason for this is polymeric materials offer many

Figure 1.1: *The packaging material for Tetra Pak® paperboard package consist of several material layers of polyethylene, aluminium-foil and paperboard.Pak (2014)*

excellent properties such as very good moisture barrier, tough and good resistance against chemicals and pressure, making it ideal for the packaging industry. As development of plastic films leads to lighter and thinner films to save materials, polymer films are expected to maintain their reliability at all time. Therefore, it is of interest to find a good experiment method strategy to examine the impact of polymer on different products to save on working time and money. Conclusively, it would be of interest for Tetra Pak® and other industries to obtain a better understanding on package performance during and after exposure to different filling products and also how to implement and utilise experimental method strategy in the future.

1.2 Objective and vision

The aim of this thesis is to obtain an increased knowledge on how packaging material and especially in this research how blown low-density polyethylene (LDPE) films react to different products at different time intervals. The objectives can be summarised as follows:

- Study thermal and mechanical mechanism of thin polymer films.
- Study chemical properties of thin polymer films.
- Perform experimental test procedures on thin blown LDPE films in an experimental environment.
- Collect all analysed data and develop an experimental method strategy.

First, a combination of thermal, mechanical mechanisms and chemical properties of polymers are studied, analysed and quantified. Afterwards, with the obtained knowledge conduct experimental test procedures of the variables of polymers such as mechanical loading and product interactions of thin LDPE films in an experimental environment as close to industrial process as possible. Finally, collecting all the analysed data to develop a possible experimental method strategy.

1.3 Experimental Methods

The methods used in this thesis consist of many different techniques that are interlinked with each other and the techniques are following:

- Product uptake measurement
- Thickness measurement
- Wide Angle X-ray Scattering (WAXS)
- Differential Scanning Calorimetry (DSC)
- Scanning Electron Microscopy (SEM)
- Tensile test
- Digital Image Correlation (DIC)
- Thermogravimetric Analysis (TGA)

First, to study and model product behaviours with polymers, a simple technique of product uptake measurement is first performed. Product uptake is used to try to study and explain the macroscopic behaviours, whilst WAXS is used to understand the nanoscopic behaviours of product interaction. To gain further knowledge and understanding TGA and DSC are performed to understand the changes in crystallinity after exposure with products. Thereafter, to properly model damage behaviour and fracture mechanisms in real life, tensile tests are conducted. DIC is also used in combination with tensile testing to study how the whole test sample reacts to mechanical loading. SEM are then used to visually observe fractures from tensile tests in nanoscopic scale. Lastly, thickness measurement is performed to study the thickness consistency of the supplied polymer sheets.

1.4 Limitations

At Tetra Pak®, a large number of different polymers are used in their packages. However, in this dissertation only one of them is used and the polymer is in pure form without additives. In addition, the commercial polymers are exposed to different temperature ranges, but in this thesis most experiments are performed at room temperature. The experiments are also limited and configured in such a way that it is possible to perform them in a laboratory environment with available test equipment. As there was no available SAXS instrument, this study could not perform SAXS measurements. Test samples are exposed to product on both side, although in reality they are only exposed to one side. The reason is that it is practically difficult to only expose one side with product.

Chapter 2

Theory

2.1 Hierarchical Length Scales in Polymer Films

To study and fully understand the polymer and its process requires an overview of the macroscopic to nanoscopic scales. A macroscopic illustration of the hierarchical structure from process to experimental tests is displayed in Figure 2.1. First, the polymer is produced and for this dissertation a blown film extrusion process is used to obtain large rolls of low density polyethylene. A smaller sheet is obtained from the polymer roll and test samples are punched or cut out of this sheet. These dogbone shaped test samples are then used in various experimental techniques, such as tensile testing, DSC and SEM.

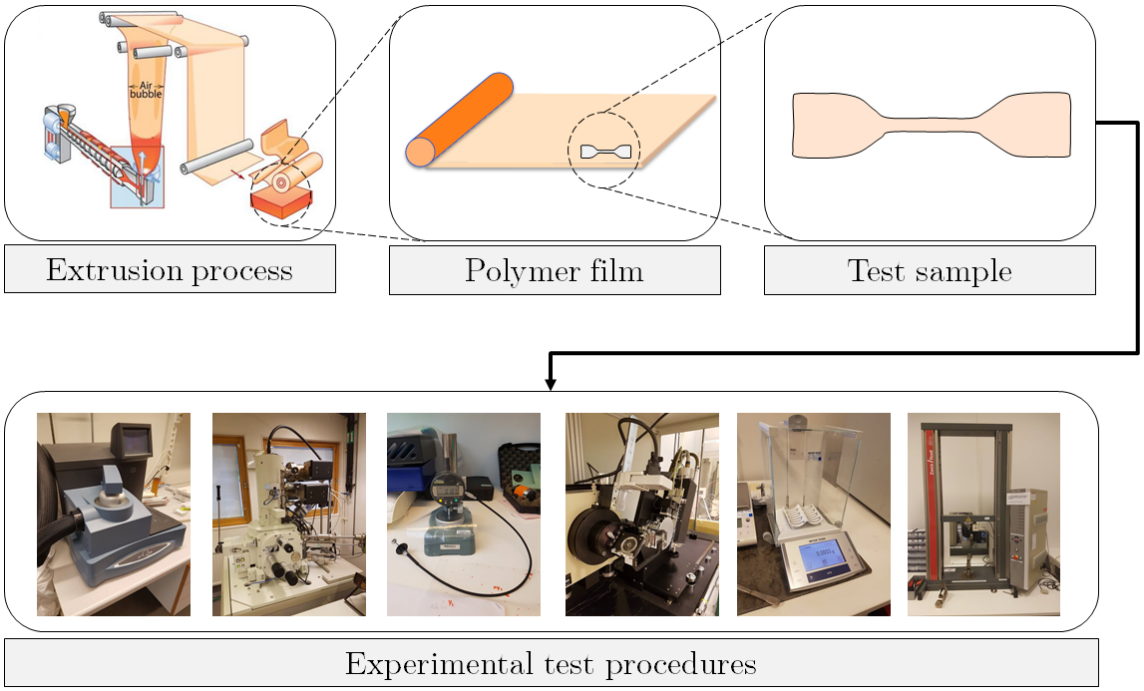

Figure 2.1: *The hierarchical structure from process to experimental tests. Vu (2019)*

In order to further investigate and gain knowledge and understanding of polymer mechanism and properties, the tested polymer internal structure is studied in both microscopic and nanoscopic scales as observed in Figure 2.2. The reason is to hopefully link and explain the macroscopic behaviour of the polymer. The morphological hierarchy begins first from a test sample and then to spherulites at between 10 μm and 100 nm. However, for this dissertation, the interest area is at lower length scales starting with the semi-crystalline domains on the scale between 100-1 nm. Lastly, also at the lowest scale with unit cells and crystal lattice on the scale between 1 nm and 1 Å. Experimental techniques such as SAXS and WAXS are used to investigate at nanoscopic lenght scales. Xu et al. (2004)

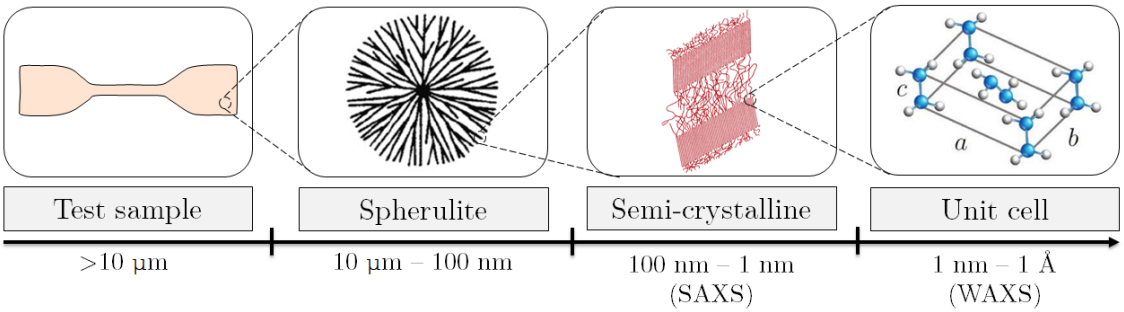

Figure 2.2: *Hierarchical of length scales of a polymer crystal.Vu (2019)*

2.2 Polymers

Polymers are molecules composed of many repeating subunits called monomers and are mainly based on carbon and hydrogen. The most common polymer to this day is polyethylene, which is also chemically one of the simplest synthetic polymers with the repeating unit of ethylene $-(-CH_2-CH_2-)_n-$. The polyethylene is a semi-crystalline polymer, which means that it consists of two phases, a crystalline phase and an amorphous phase. The polymer properties change depending on the amount of chain branch which in turn affects the amount of crystalline phases of the polymer. Polyethylene is divided into three different grades depending on the amount of chain branch and they are high density polyethylene (HDPE), linear low density polyethylene (LLDPE) and low density polyethylene (LDPE). The structural differences in each grade are displayed in Figure 2.3. This research will focus solely on low density polyethylene produced by Tetra Pak®. Grant & Arrighi (2007)

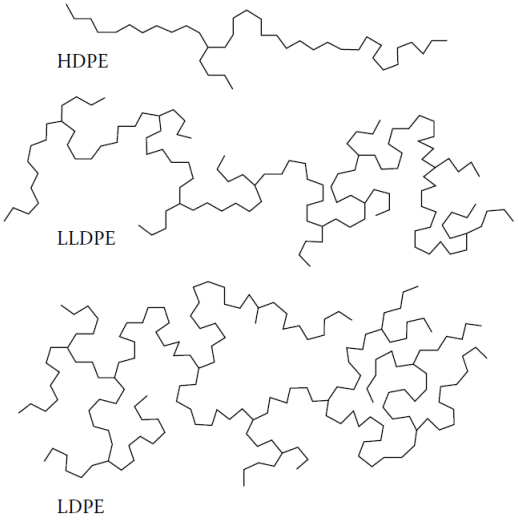

Figure 2.3: *Comparison of the three different grades of polyethylene and the difference in chain branching. Grant & Arrighi (2007)*

2.2.1 Blown film process

The project is mainly focused on polymer processed from extrusion of blown film. It is the most common method of creating polymer sheets and an important process in the packaging industry.

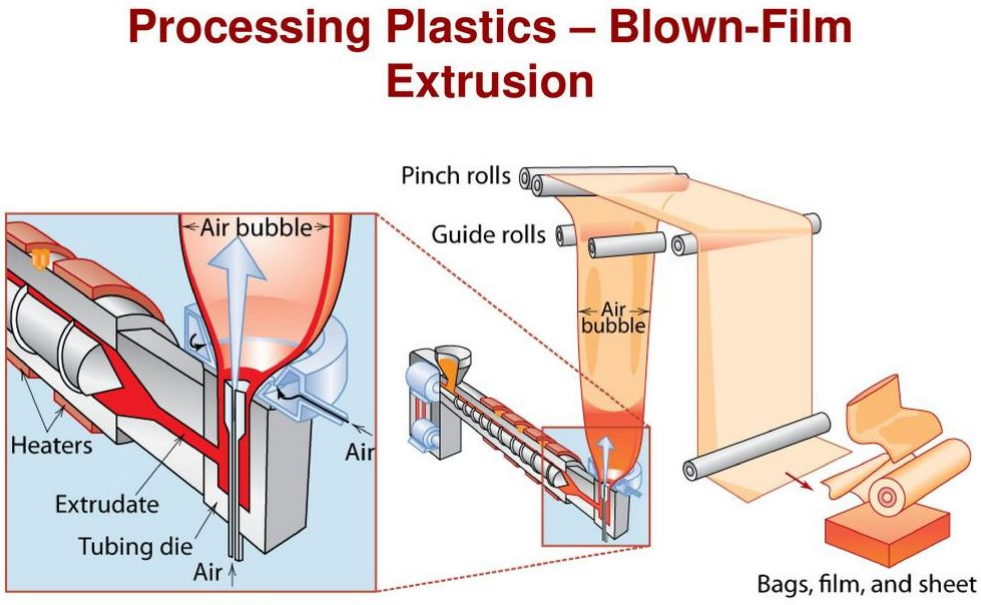

Figure 2.4: *The plastic forming process of blown film extrusion. Callister & Rethwisch (2011)*

As observed in Figure 2.4 the blown film extrusion process starts on the left with polymer pellets supplied into a rotating spiral screw. The pellets are melted by the electrical heaters and viscous shearing by the rotation of the screw. This molten melt is extruded into a tubing die. Inside this tube, air is blown into the melt. This step expands the melt and quickly cooled down to a bubble of thin polymer film. After crystallisation, the polymer film moves through rolls to collapse the bubble and then rolled up to a rolls of polymer sheets. Kim et al. (2016)

2.3 Product Interactions

The polymer is exposed to three different products in this thesis because they have different properties and are expected to affect the polymer differently. The greater the similarity of the chemical structure between the absorbed product and the polymer, the more likely is it that diffusion of product into the polymer will occur. The chemical structure of the polyethylene is shown in Figure 2.5.

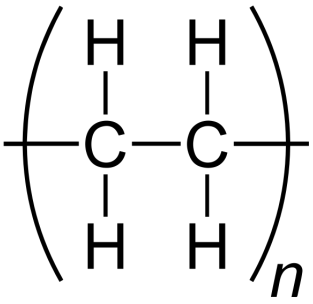

Figure 2.5: *Chemical structure of polyethylene. Magmar452 (2014)*

The three different products used in the thesis are following:

- **Water**

Water has the chemical formula H_2O, in which two hydrogen atoms are covalently bonded to one atom of oxygen.

- **Sunflower oil**

The chemical composition for sunflower oil consist of triglyceride derived from combining glycerol (left), which consist of hydroxyl groups and three fatty acids molecules (right), which consist mainly of hydrocarbon groups as shown in Figure 2.6

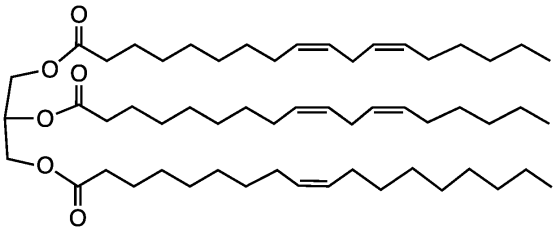

Figure 2.6: *Chemical composition of triglycerides in sunflower oil. Smokefoot (2011)*

- **Orange juice**

Unlike the previous products, Orange Juice is a solution and contains many different substances. Orange juice contain to a large extent of water, many different sugars, carbohydrates and a high concentration of Vitamin C. Figure 2.7 shows the chemical structure of Vitamin C. Nast (2012)

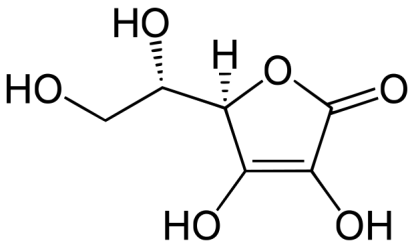

Figure 2.7: *Chemical composition of Vitamin C. Yikrazuul (2009)*

Observed from the chemical structures, both polyethylene and sunflower oil contain chains of hydrocarbons, which is an organic compound consisting of carbon and hydrogen and are therefore similar to each other. On the other hand are water and orange juice, which contains mostly of hydroxyl groups and are more chemically similar to each other than to polyethylene.

2.3.1 Mass transport processes

Polymer materials experience deterioration by environment interaction. Polymer degradation is physiochemical, which means that it is affected by both physical and chemical interactions such as swelling, dissolution, chemical reactions and radiation. When polymers are exposed to liquids, they may be affected by swelling. Swelling is usually referred to the interactions or mass transport processes for adsorption, absorption and permeation of product. This research will investigate effect of adsorption and absorption on polymer films. The mass transport through the polymer film is often a multi-step process described in Figure 2.8. Callister & Rethwisch (2011)

First, adsorption is described in that the dissolved molecules in the bulk collide with the polymer surface (1). In which they adsorb to the surface of the polymeric film (2). Adsorption is maintained by weak Van der Waals forces and the

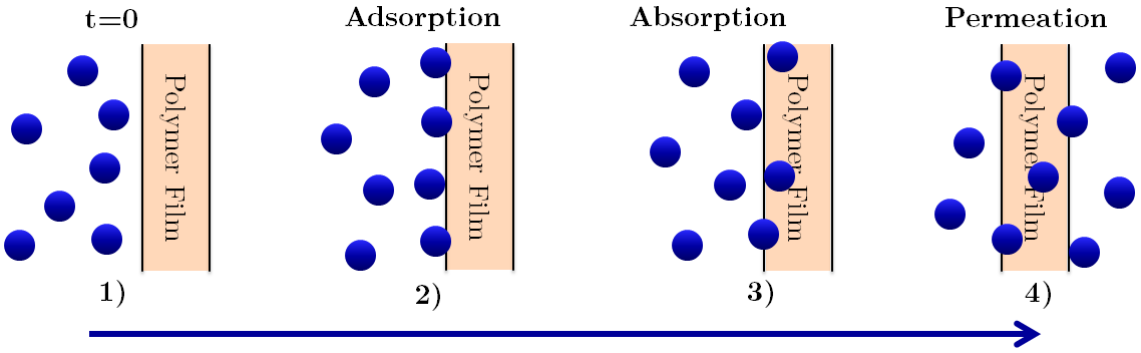

Figure 2.8: *Mass transport of product molecules through a polymer film.Jasuja et al. (2018) Vu (2019)*

dissolved molecules are easily removed from the surface. Encyclopædia Britannica (2013)

Thereafter, the product molecules may diffuse and absorb into the polymeric mass (3), the small dissolved molecules fit into and occupy vacant sites or "holes" in the polymer created from the motion of the crystalline region and polymer chains of the polymer. The availability of these vacancies determines the rate of diffusion and the amount of product absorbed by the polymer. Consequently, the different polymer regions and polymer chains are forced apart and the sample expands or swells. Furthermore, the separation results in a weaker Van der Waals bond through the polymer and results in a softer and more ductile material. Jasuja et al. (2018)

Absorption greatly affects the percentage of crystallinity in the sample. The cause is observed in Figure 2.9. Semi-crystalline polymer, such as LDPE, partially contains a crystalline region, where polymer chains are aligned and ordered. The rest of the space in a polymer consists of amorphous regions, where the polymer chains can move more freely. The crystalline phase is much denser than the amorphous phase, making it almost impervious to most product molecules. Therefore, diffusion mainly occurs on vacancies or empty spaces in the amorphous regions. Grasmeder (2017)

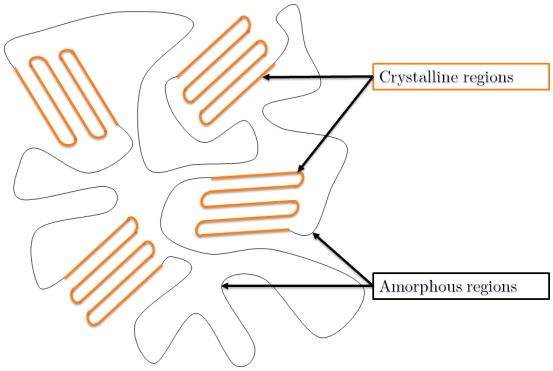

(a) Crystallites in semi-crystalline polymers. Vu (2019)

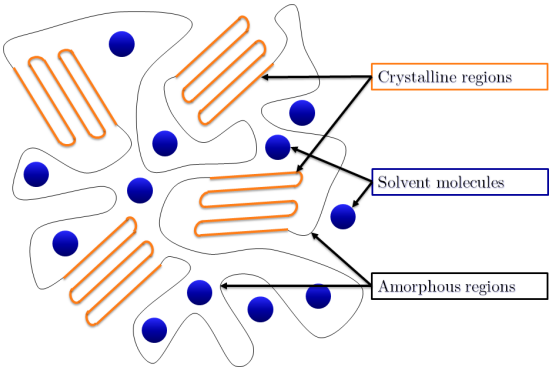

(b) Crystallites with product molecules in semi-crystalline polymers.

Figure 2.9: *A semi-crystalline polymer with amorphous regions (diffusion permeable) and crystalline regions (diffusion impermeable). Grasmeder (2017) Vu (2019)*

2.4 Theoretical Framework

2.4.1 Product uptake

Product uptake or weight measurement is an easy and very useful part of the experimental process because the difference in weight before and after exposure to different products is easy to measure and provides quick information if the polymer has adsorb or absorb any amount of product. In addition, the investigation also looks into the effect of exposure over time. This technique will investigate both direct and long-term effects on dry and swollen LDPE samples.

In order to understand the amount of product absorbed on the tested polymer sample, Equation 2.1 is used to calculate the percentage of product content w_s. The equation is defined as the total weight increase between the same dry sample m_0 and swollen sample m_1 and divided with the initial dry weight. The result gives a value on the percentage weight increase of the product relative to the sample.

$$w_s = \frac{m_1 - m_0}{m_0}, \quad [\%] \tag{2.1}$$

2.4.2 Thickness Measurement

Thickness measurement is crucial for controlling the quality of the test procedures and validating other techniques used in this research. Since this study is performed on dogbone shaped uni-axial specimens it is important that the accompanying blown LDPE film is homogeneous thick and all samples are as equal thick to each other as possible.

2.4.3 Wide Angle X-ray Scattering (WAXS)

Wide angle x-ray radiation is a beneficial tool for examining the shape, size and crystalline structure of polymers. The advantage of X-ray diffraction is the ability to obtain information about the position of the particles in relation to each other. Especially, densely and highly ordered systems such as crystalline phases are able to develop into pronounced peak. These peaks, commonly called Bragg's peak are depicted in Figure 2.10. This figure shows an example for where every Bragg's peaks relative to 2θ should be for a semi-crystalline LDPE and the crystal lattice every peak represent. Analysing the diffraction peaks or Bragg's peaks scattered at different angles and with Bragg's law it is possible to obtain information about the structure of the polymers. Schnablegger & Singh (2013)

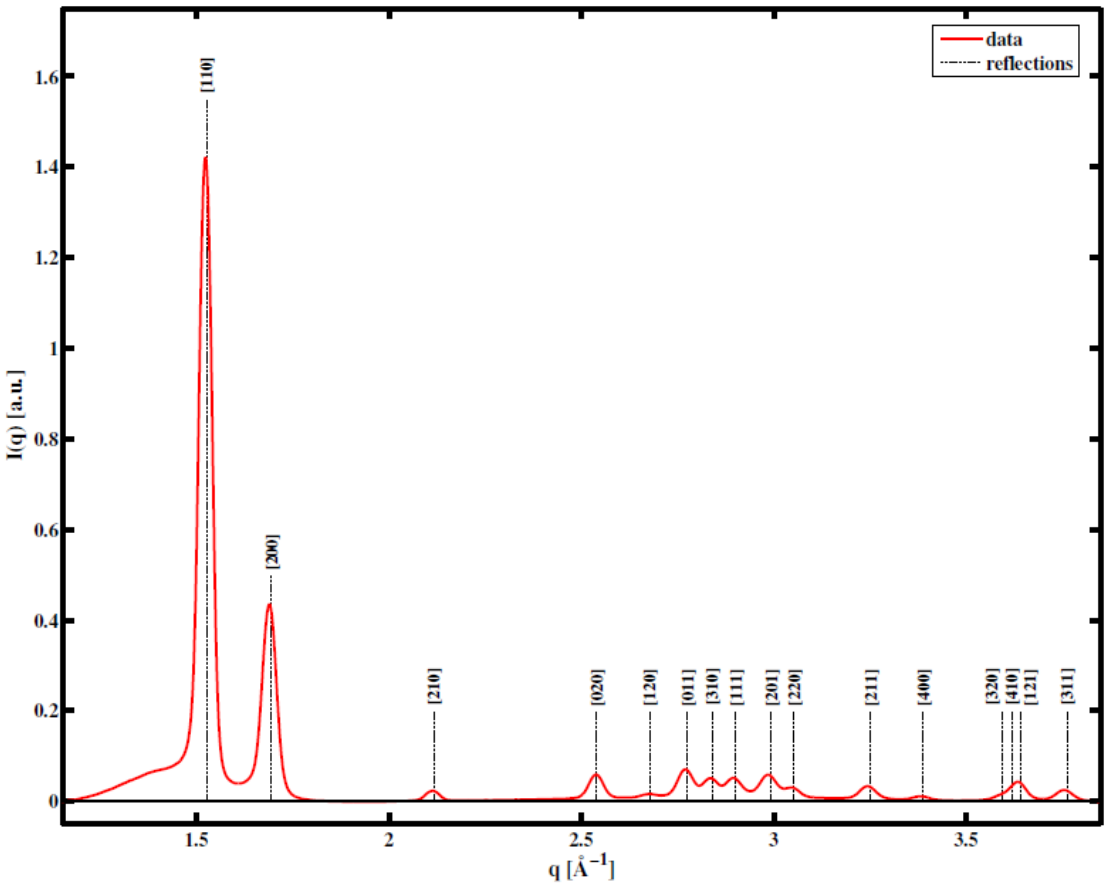

Figure 2.10: *Possible Bragg's peak and responding crystal lattice of LDPE. Schmacke (2010)*

Diffraction phenomena occurs when a monochromatic X-ray beam is transmitted through the sample. Most of the beam will pass through the sample but a fraction will be absorbed and another fraction will be scattered into all directions. Detecting and measuring the amount of X-ray scattered at different angles will produce different scattering intensity and spectrum and in turn provides structural information about the sample. WAXS is capable to obtain structural information

on the atomic distances with a diffraction spectra at angles between around 2- 90°. World (2017)

Figure 2.11a shows the basic principle of the diffraction phenomena. X-ray radiation beams with a wavelength of 0.07- 0.2 nm from source X, which hit the sample S and scatter a small fraction of the beam. The scattered beam deviate with an angle θ on the direction of the beam as seen on the right figure Figure 2.11b. The scattered beams are recorded with the help of detector D and depending on the scattering angle θ the scattering intensities varies accordingly. Alexander (2018)

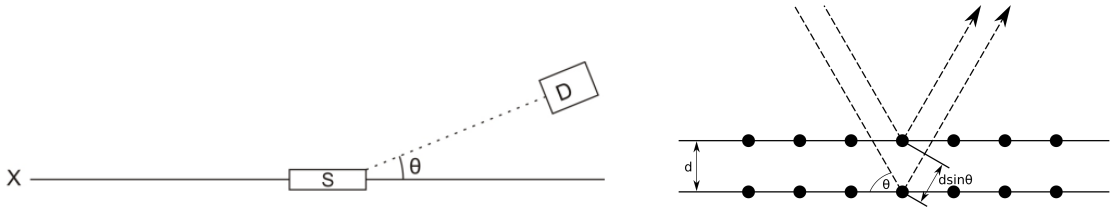

(a) *X-ray beam scattering on a test sample. Boldon et al. (2015)*

(b) *Bragg's diffraction. Furiouslettuce (2009)*

Figure 2.11: *The basic principle of diffraction phenomena.*

The results will be displayed in graphs similar to Figure 2.12 with the amorphous regions shown as very wide peak, where the crystalline peaks will appear as long and sharp peaks on top of the amorphous peaks. The reason is that the atoms for the crystalline regions are periodically arranged and structural aligned in the space as described in subsection 2.3.1. But on the other hand the amorphous regions do not possess that periodicity and atoms are randomly distributed in the space. The scattering of X-rays from periodic arrangement of atoms will be scattered only in certain directions when they hit the unit cells. This will cause high intensity peaks. Whilst, for amorphous phase the X-rays will be scattered in many directions leading to a large bump distributed in a wide range instead of high intensity narrower peaks. Therefore, calculating Bragg's equation will be useful to find the percentage of crystalline region compared to the amorphous region in the tested samples. Podorov et al. (2006)

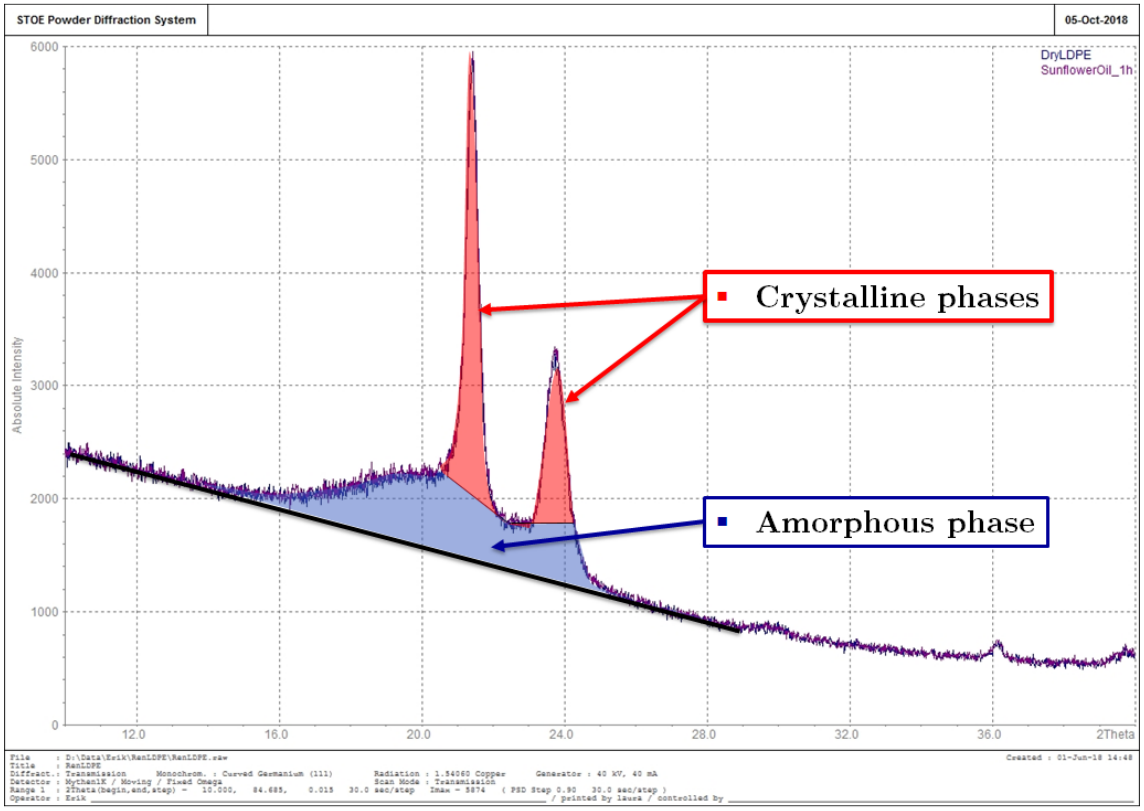

Figure 2.12: *The crystalline and amorphous areas from a WAXS measurement. Lund University & Synthesis (2019a)Vu (2019)*

Both SAXS and WAXS are used for nanoscale. However, SAXS is used for structures larger than 1 nm, while WAXS is used for smaller structures like the unit cells. The unit cells are depicted in Figure 2.13 for an orthorhombic polyethylene. These cells are the basic building blocks and represent the symmetry of the crystal structure, which in turn builds up the entire polymer. Wahlström (2018)

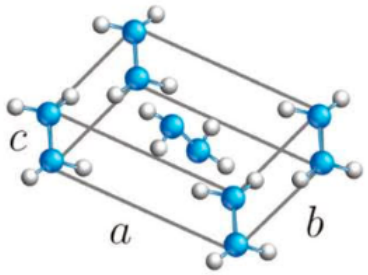

Figure 2.13: *Arrangement of polymer chains in a unit cell of an orthorhombic polyethylene. Callister & Rethwisch (2011)*

The Bragg's peaks depicted in Figure 2.12 are predicted and calculated with Bragg's law from Equation 2.2. In which θ is the scattering angle of the beam, n is the positive integer and λ is the wavelength of the X-ray beam. The distance d represent the interplanar distance between atomic planes as shown in Figure 2.11b. Schmacke (2010)

$$\boxed{2dsin\theta = n\lambda} \tag{2.2}$$

Assuming that the areas under the peaks are proportional to the scattering intensity of the sample amorphous and crystalline regions. Therefore, the percentage of the polymer that is crystalline is determined by using Equation 2.3. Integrating the area under every crystalline peaks and divide that area with the total area of all peaks, a percentage of crystallinity X_{WAXS} is obtained.

$$\boxed{X_{WAXS} = \frac{A_{crystalline}}{A_{crystalline} + A_{amorphous}} * 100, \quad [\%]} \tag{2.3}$$

2.4.4 Differential scanning calorimetry (DSC)

Differential Scanning Calorimetry (DSC) is a technique measuring the heat or enthalpy required for a polymer to melt or crystallise. The measurement is composed of two pans that are heated in a chamber. One pan contains the investigated test polymer specimen and the second pan is empty used as a reference. The DSC for this research enclose both the aluminium pans from the specimen and the reference to a single heat source. The specimen is first heated to a certain temperature and analysed to then cooled or crystallised to room temperature to clear the process history of the specimen. The specimen is then reheated and analysed a second and last time. The energy or heat changes during the increase or decrease of temperature is then used as a measure for enthalpy or heat flow changes in the sample relative to the reference. Universitat (2018)

The reason for using DSC is to study the difference in phase change and percentage of crystalline X_{WAXS} in the sample and to investigate the difference in enthalpy between dry LDPE and LDPE exposed to products. Bhadeshia et al. (2018)

Melting & crystallisation peaks

When increasing the temperature above the peak melting temperature T_m, polymer chains will undergo a transition from ordered arrangement to an arrangement in which they are able to move more freely. This process requires absorption of heat, which means that melting is an endothermic process. This is observed in the melting cycles in Figure 2.14 and Figure 2.15. Integrating the area under these peaks will provide values for the melting enthalpy δH_m. From the same peak it is also possible to identify a maximum peak melting temperature T_m, which is useful to confirm the validity of the method as T_m should have the same value for

all heating cycles. Bhadeshia et al. (2018)

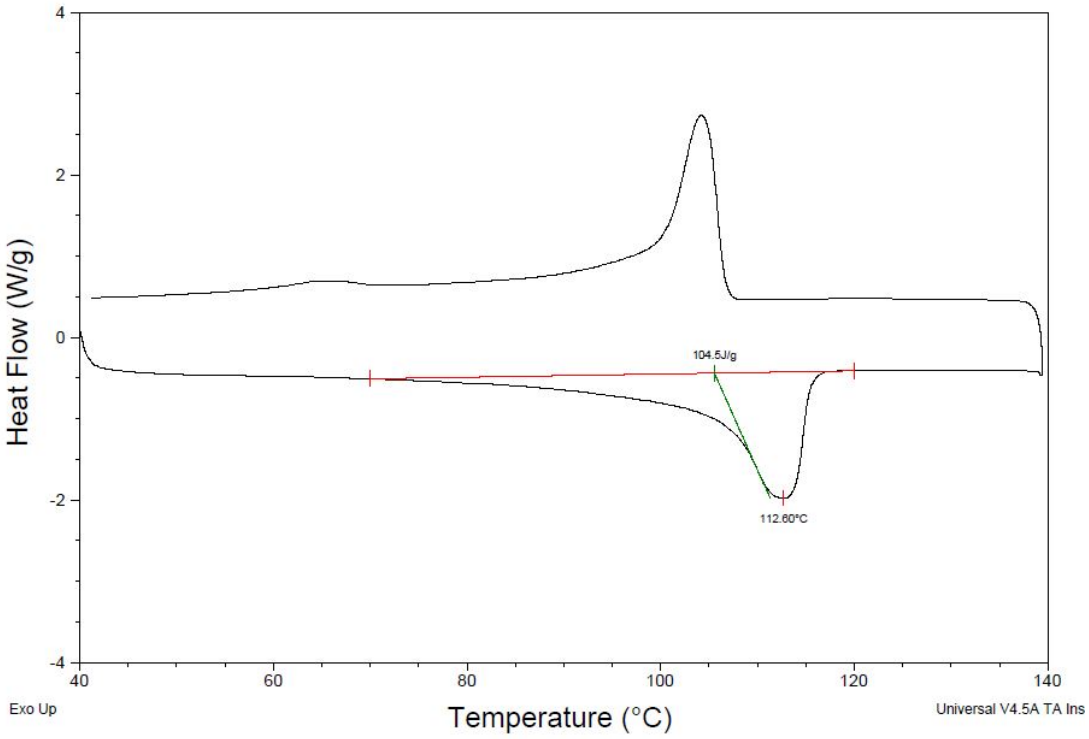

Figure 2.14: *First melting cycle for a dry LDPE sample.Lund University & Synthesis (2019b)*

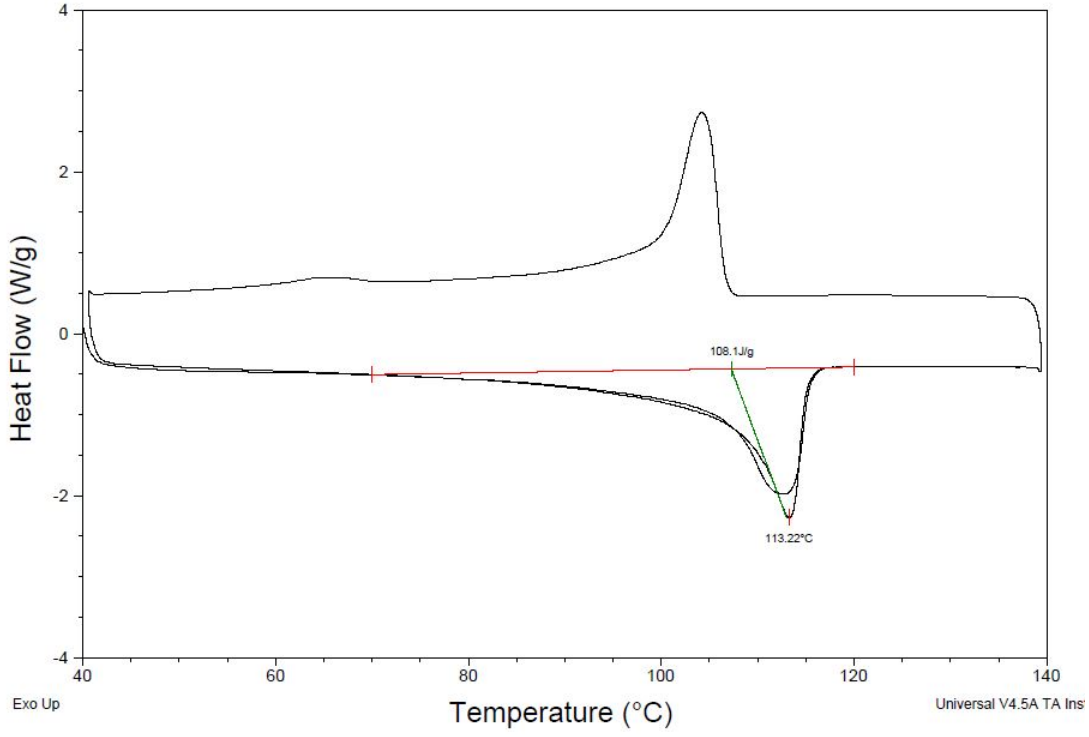

Figure 2.15: *Second melting cycle for a dry LDPE sample.Lund University & Synthesis (2019b)*

It is also possible to calculate the crystallisation enthalpy, where the polymer starts to crystallise by integrating the area of the top peak instead as depicted in Figure 2.16.

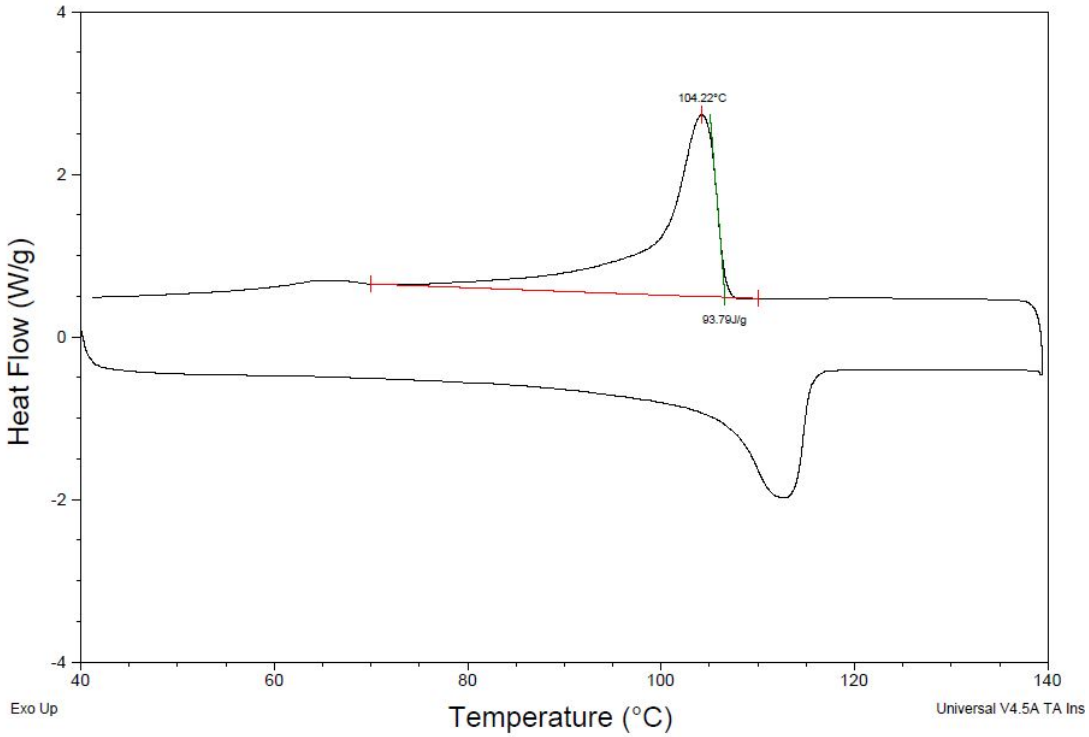

Figure 2.16: *Crystallisation cycle for a dry LDPE sample. Lund University & Synthesis (2019b)*

The first Equation 2.4, describes the heat flow or the heat that are supplied per unit of time, which will be plotted versus temperature to obtain plot as seen in Figure 2.14 and Figure 2.15. Universitat (2018)

$$\boxed{Heatflow = \frac{Heat}{Time} = \frac{q}{t}, \quad [W, J/s]} \tag{2.4}$$

Equation 2.5 below depicts the calculation for percentage crystalline. In which the melting enthalpy δH_m and cold crystallisation enthalpy δH_{cc} are determined by integrating the area under respectively peaks. $\delta H_{m100\%}$ is a reference value and represents the melting enthalpy if the samples would be 100% crystalline. According to PerkinElmer Instruments the reference melting enthalpy for LDPE is 293,6 J/g. PerkinElmer also cite that δH_{cc} may not be observed in blown film experiment due to its thermal history and will therefore be disregarded in the calculations. Sichina et al. (2000)

$$X_{DSC} = \frac{\delta H_m - \delta H_{cc}}{\delta H_{m100\%}} * 100 = \frac{\delta H_m}{\delta H_{m100\%}} * 100, \quad [\%] \tag{2.5}$$

2.4.5 Tensile testing

In order to evaluate changes in the polymers mechanical properties tensile tests are performed on both dry and product exposed test sample, in which stress and strain data are obtained and compared. A test specimen is mounted on the tensile testing machine by its end and the instrument will continuously apply load, which elongate the specimen at a constant rate until fracture. Uni-axial tensile tests with dogbones shaped test samples are presented in the stress and strain curve shown in Figure 2.17. An knowledge of the deformation mechanism during tensile testing is important to understand if the product has an effect on the mechanical properties of the polymers. Wahlström (2018)

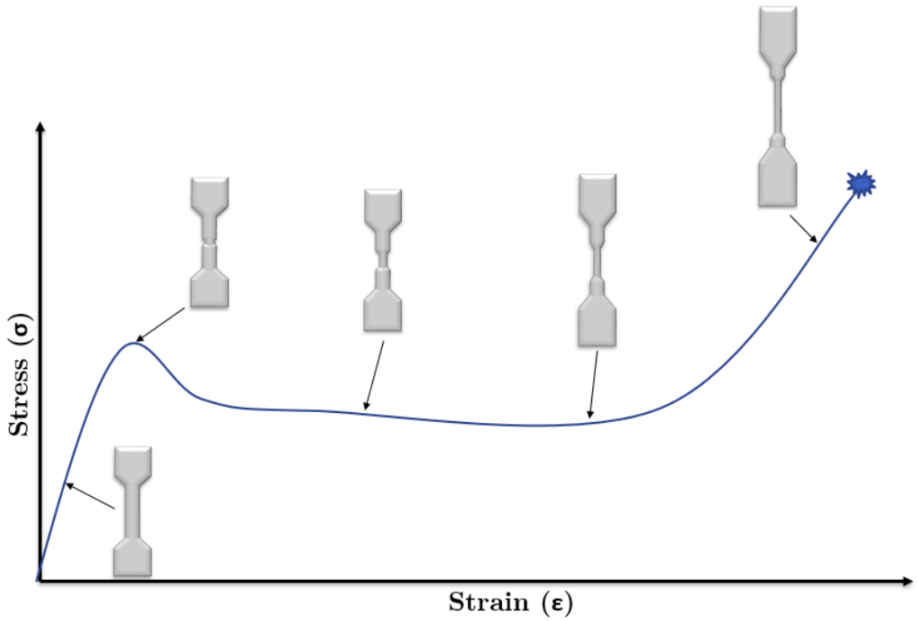

Figure 2.17: *Typical stress and strain graph for a tensile tested LDPE in MD and the shaping of necking strip. Wahlström (2018) Vu (2019)*

From the stress and strain data measured load versus elongation are recorded. These values are dependent on the geometrical factors of the test specimens. Therefore, the relationship of load versus elongation is summarised to respective parameters of engineering stress versus engineering strain. Xiong (2014)

Engineered stress σ is calculated as shown in Equation 2.6. In which F is the applied force and A_0 is the initial area. Schümann et al. (2016)

$$\boxed{\sigma = \frac{F}{A_0}, \quad [N]} \tag{2.6}$$

The engineered strain ϵ is defined according to equation Equation 2.7, where l_0 is the initial length and Δl is the difference or elongated distance from the initial length. Schümann et al. (2016)

$$\boxed{\epsilon = \frac{\Delta l}{l_0}, \quad [\%]} \tag{2.7}$$

2.4.6 Digital Image Correlation (DIC)

Digital Image Correlation, DIC is an optical measurement technique which measure and record with a camera the deformation and displacement of a test specimen through a speckle pattern as depicted in Figure 2.18. The results are images throughout the tensile tests and these are utilised in an image analysis. From this data it is then possible to calculate the local strain and displacement in all directions of the specimen by using a cross-correlation algorithm that tracks the speckle patterns through all images. Nilsson (2017)

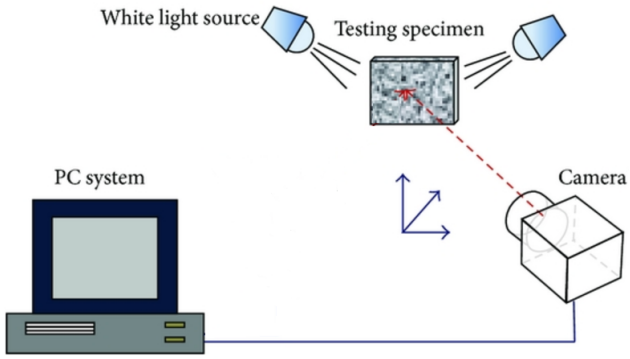

Figure 2.18: *Typical set-up for a DIC measurement. Liao et al. (2014)*

One feature with tensile tests is the necking phenomena in which a section of the test sample cross-sectional area decreases by a greater proportion compare to the surrounding when applied with stress. Necking is able to occur at different places and sometimes at two or several places. The necking phenomena is depicted in the red area in the rightmost Figure 2.19 of a tested polymer sample. As observed from the DIC figure most of the applied stress occur at the necking area and it is assumed that the rest of the localised area has a homogeneous strain distribution. Therefore, the objective with DIC is to be used in conjunction with tensile test to further investigate how the entire test sample reacts to load. Sguazzo & Hartmann (2018)

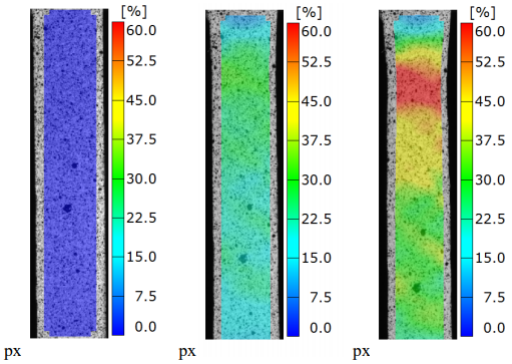

Figure 2.19: *Evolution of necking for an test sample measured with DIC at a displacement rate of 50 mm/min. Sguazzo & Hartmann (2018)*

2.4.7 Scanning Electron Microscopy (SEM)

The scanning electron microscope (SEM) used in this project uses a focused beam of electrons to interact with atoms in the sample and produce various signals with information. One such signal is the secondary electron, which will be used to obtain topographical information on the LDPE samples. Depicted in Figure 2.20 is the mechanism of emission of secondary electrons (SE) from a electron beam source. The electron beam interact with the investigated specimen surface and secondary electrons are ejected from the specimen. These interactions occurs just within a few nanometers from the specimen surface. Collecting the signal of these secondary electrons beamed in an area, two dimensional digital video and images are captured. Swapp (2017)

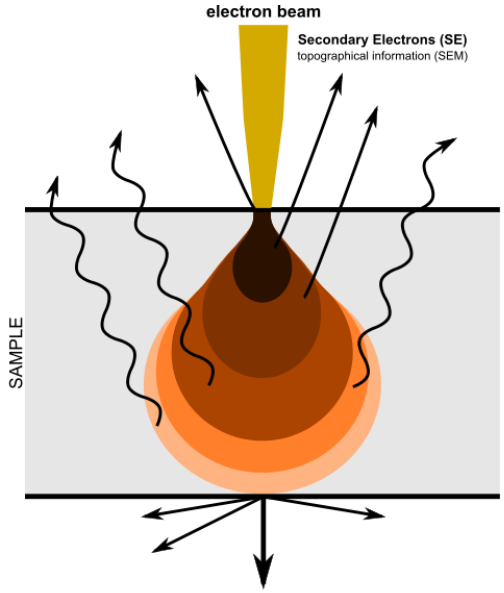

Figure 2.20: *Mechanism of scattering of electrons from a SEM. Claudionico (2015)*

2.4.8 Thermogravimetric Analysis (TGA)

Thermogravimetric analysis (TGA) is used to evaluate the thermal degradation of the polymer used in this research. It is important to know the thermal stability of the specimen for uses in DSC as that technique only works in thermally stable ranges. TGA is a technique to monitor the mass increase or decrease of a sample specimen as a function of temperature. An aluminium pan with specimens of the investigated LDPE samples are subjected to very high temperature. According to an article from Eduard Piiroja and Helle Lippmaa, thermal degradation for LDPE was obtained between 450 - 525°C and that should be well above the thermal ranges for this research. However, as the thermal degradation can vary greatly, it is important to test all the polymer used in this thesis. Piiroja & Lippmaa (1989)

Chapter 3

Experimental Testing

3.1 Sample preparations

In this thesis polymer rolls of blown film sheet of LDPE are supplied from Tetra Pak®. From these sheets, test specimens are punched out of and the geometry of these polymer sheets are presented in figure 3.1. Two material directions, the machine direction (MD) and cross direction (CD) are marked on the polymer sheet. MD is in the the direction of the extrusion, whilst CD is in the perpendicular direction. The CD width of the supplied polymer is 170 mm.

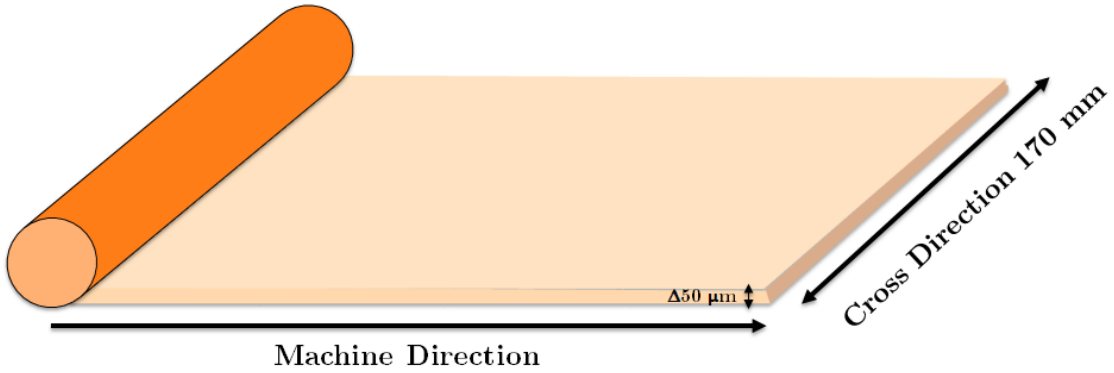

Figure 3.1: *Geometry of a blown film polymer sheet.Vu (2019)*

Two batches of the same blown film LDPE sheets are supplied from Tetra Pak® at two different occasions. The two films have a density of 46 g/m^2 and an average thickness of 50 μm. Most experimental procedures were used with the first batch of polymer film. The second batch is used for thickness measurement and some parts of the tensile tests.

3.1.1 Dogbone samples

Figure 3.2a shows the pneumatic cutting press used for preparation of test samples. The pneumatic cutting press belonged to the Material Analysis Laboratory at Tetra Pak®. The instrument version is EP 02 and is manufactured from the company Elastocon AB. Elastocon (2018)

Presented in Figure 3.2b is the geometry of the test samples used in this thesis, these dogbone shaped samples are punched out from the supplied blown film sheet according to EN ISO 527-3 standard. This 120 mm long dogbone shape consist of two 25 mm wide shoulders at each end and a 33 mm long and 6 mm wide gauge section between them. This is to ensure that the sample will fracture within the gauge section in the tensile tests and to acquire more manageable samples to work with. TestResources.net (2013)

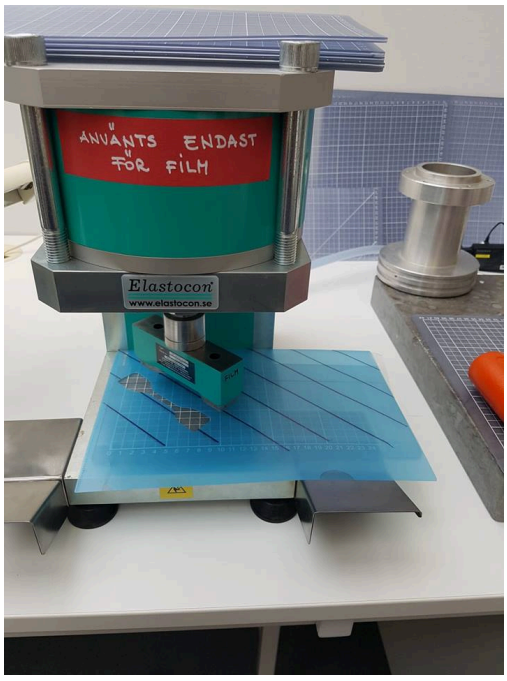

(a) *The pneumatic cutting press with samples cut at 45°.*

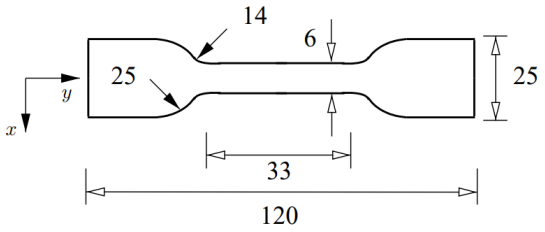

(b) *Geometry of dogbone shaped test specimen according to EN ISO 527-3 measures. Sguazzo & Hartmann (2018)*

Figure 3.2: *The experimental setup for punching dogbone samples.*

Figure 3.3 shows the geometry of a section of the polymer sheet used for thickness measurement. The dotted section is 165 mm wide and 220 mm long and the distance between two dots in MD direction is 20 mm and for CD direction it is instead 15 mm in between.

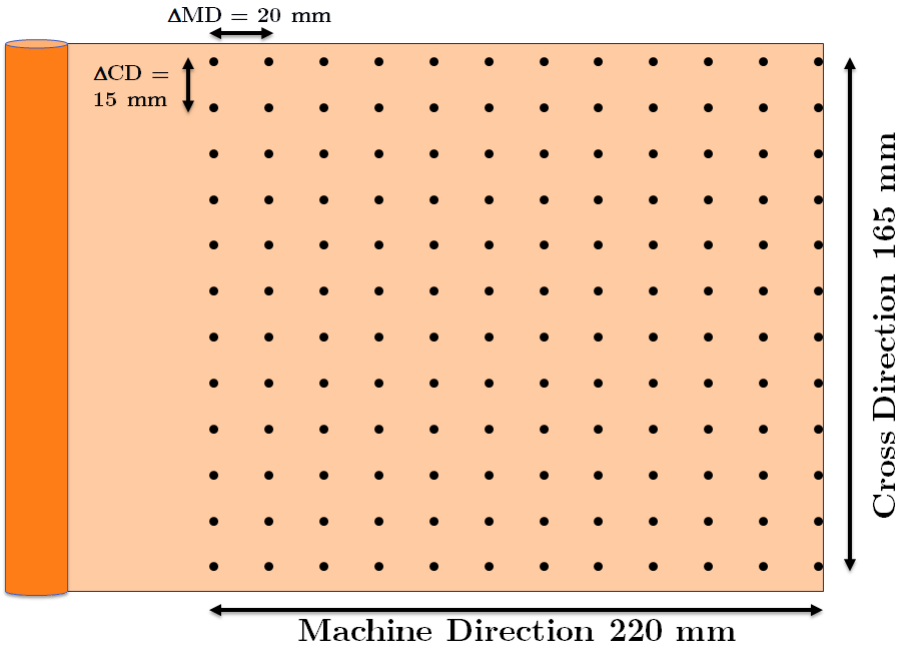

Figure 3.3: *Blown film polymer sheet with geometry of tested section. Vu (2019)*

Figure 3.4 display how the dogbone samples are punched out in both MD and CD directions. They are also portrayed in the same scale as the polymer sheet. Every column of samples cut in MD are able to fit five specimens within the available space but only one sample is able to fit in one column in the CD direction. The cut samples in the same direction are collected mixed and stored until the experimental procedures.

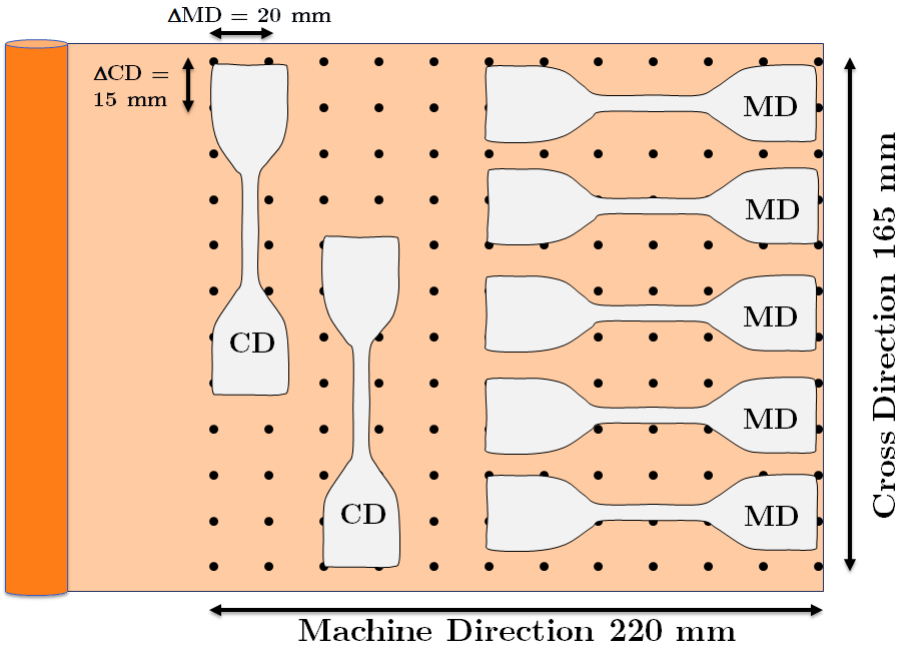

Figure 3.4: *Examples of cut test samples positions on the polymer sheet. Vu (2019)*

3.1.2 Aluminium pan (TGA, DSC)

Both the thermogravimetric analysis (TGA) and differential scanning calorimetry (DSC) requires cut specimens of the samples to be sealed into aluminium pans and weighted. The sealing process is described in Figure 3.5. First, observed in Figure 3.5a, a small specimen is cut, put into an aluminium pan and weighted. Afterwards, both the aluminium pan and lid are sealed together with the specimen using the instrument seen in Figure 3.5b to produce the final product in Figure 3.5c. Commonly, a pin hole is punched on the aluminium lid if volatile materials are analysed, but because none of the tested samples are volatile, punching pin holes are not needed in this thesis.

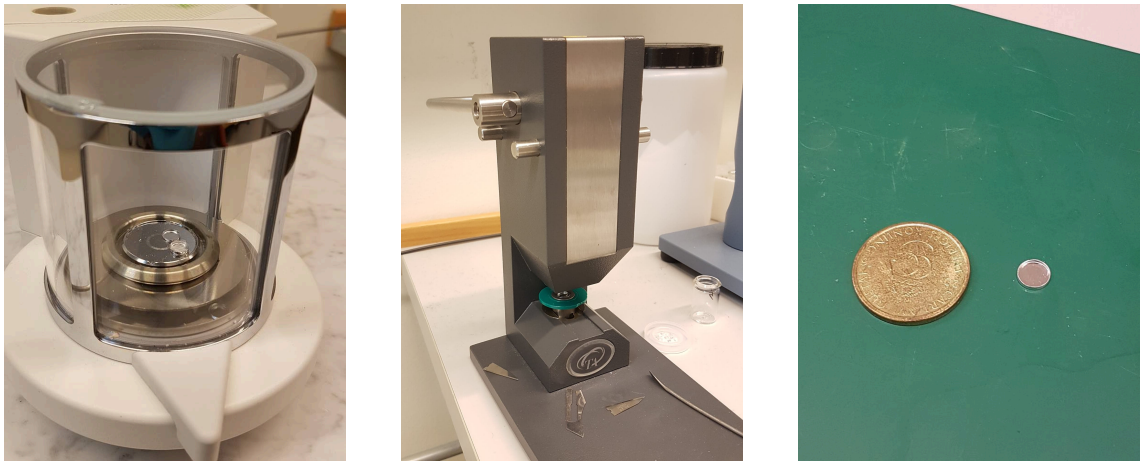

(a) Weight measurement before sealing.

(b) The instrument used for sealing pans.

(c) Close-up on a sealed aluminium pan.

Figure 3.5: *The process of sealing an aluminium pan with LDPE specimen and lid.*

3.1.3 Conductive Coating (SEM)

First, to be able to obtain visual images of polymers in SEM, the samples needs to be prepared with a conductive coating as polymers are non-conductive. The coating is also used to ensure that the samples is able to withstand vacuum conditions and reduce thermal damages as LDPE samples are beam-sensitive. Three dry LDPE samples are investigated, the first one is a non-tensile tested specimen that is used as a reference sample. The other two samples are punched in machine direction and cross direction and tensile tested. These test samples are cut at the fracture point into small specimens and mounted on specimen holder with conductive adhesive. For coating a gold/palladium sputter coater Balzers SCD 04 from the division of food science at LTH as shown in Figure 3.6a are used to apply a thin uniform conductive layer throughout the specimens. The coated samples with an extra reference sample is observed in Figure 3.6b.

(a) The coater used for applying a conductive surface layer.

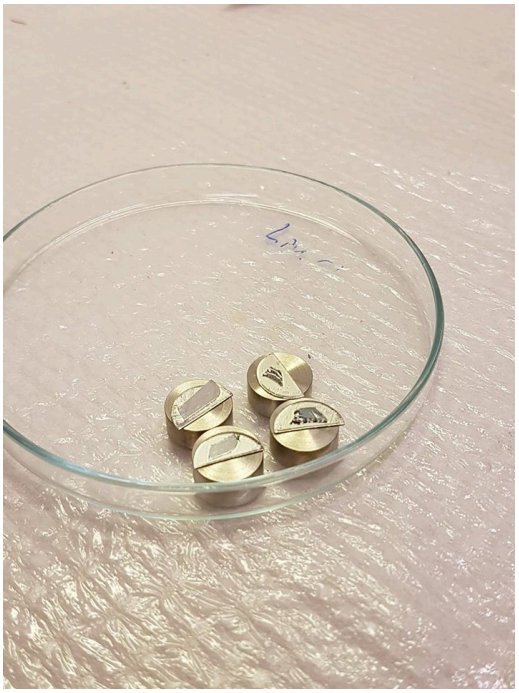

(b) Mounted and gold/palladium coated LDPE samples.

Figure 3.6: *The equipment and resources used for conducting a SEM analysis on dry polymer samples.*

3.2 Exposure of Products

The experimental setup for product exposure are conducted in enclosed containers with minimal exposure to the environment. For tensile tests the ends of every set of test samples are taped over as depicted in Figure 3.7a and thereafter taped on the containers. Afterwards, the containers are filled with product so that it covers the entire narrow gauge section on all test samples. The reason to avoid exposing the ends is to reduce error values such as friction during tensile measurements. After exposure the ends of the samples are taped over again but firmly deeper so that the narrow gauge section test samples only stretches to 50 mm. Finally, they are then cut into individual pieces and stored. The containers used in this thesis are food storage containers made of glass from IKEA with dimensions of 21 x 15 x 7 cm and every container are able to fit five tensile test samples as shown in Figure 3.7.

(a) Set of prepared polymer samples before exposure.

(b) Set of polymers in a container exposed with sunflower oil.

Figure 3.7: *Experimental setup for exposure of product.*

3.3 Product Uptake

Product uptake measurements are performed on punched LDPE samples that are subjected to different products such as sunflower oil, water and orange juice at different time intervals. Five different time intervals are tested which are 10 seconds, 5, 10, 60 minutes and 10 days. The weight measurements are performed using an instrument called Mettler Toledo XS204 balance and belongs to the package laboratory at Tetra Pak®. The instrument is able to measure with an accuracy in milligrams with up to three significant digits. Initially, before exposure four dry LDPE reference samples are marked with a small cut and weighted. These same four samples are then placed in a container with the tested product throughout the experimented time frame. After exposure, the exposed samples quickly wiped clean from residual liquid with dust-free tissues and weighted.

Figure 3.8: *Product uptake measurement instrument with three significant digits.*

3.4 Thickness Measurement

The reason to conduct thickness measurement is to examine if the blown films supplied from Tetra Pak® have a homogeneous and predictable thickness throughout the film or otherwise it is possible that it could affect the results on several techniques in this report such as the tensile measurements.

The thickness technique is conducted using a Mitutoyo thickness instrument as seen in Figure 3.9b with three significant digits belonging to the package laboratory at Tetra Pak®. First, the tested LDPE polymer film is measured and cut to a length of at least 30 cm. Afterwards, depicted in Figure 3.9a 12 x 12 sample points are marked on the film for a total of 144 sample points. The space between two neighbouring points in MD direction is 2 cm for a total length of 22 cm and for CD direction the space is 1,5 cm for a total length of 16,5 cm. The thickness experiment is conducted on the second batch supplied from Tetra Pak® and on three different parts on the same LDPE roll .

(a) The thickness measurement instrument.

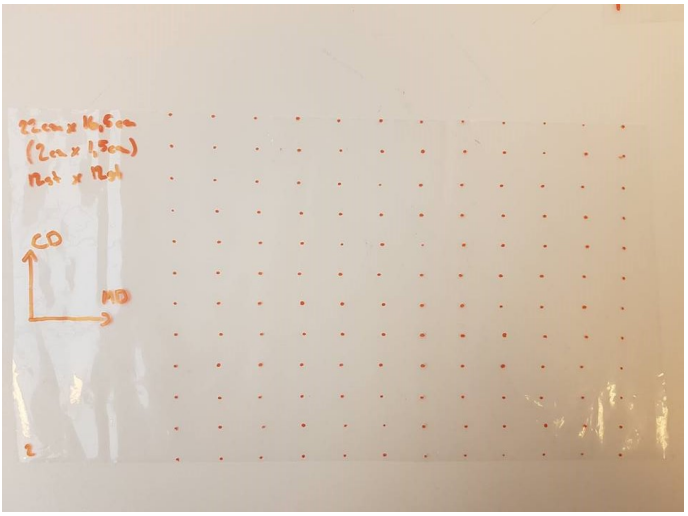

(b) One of the blown LDPE film used for thickness measurement with 144 sample points.

Figure 3.9: *The equipment and resources used for conducting a SEM analysis for dry polymers.*

3.5 Wide Angle X-ray Scattering (WAXS)

The experimental instrument used for Wide Angle X-ray Diffraction (WAXS) experiments are called ”STOE STADI-MP”. The radiation used in this experiment is transmitted from a copper anode with a wavelength (λ) of 1.54060 Å. The diffraction instrument is shown in both Figure 3.10a and Figure 3.10b. Small specimens of LDPE test samples, both dry and exposed to different products at different time intervals are cut into a rectangular shape with dimensions of around 20 x 6 mm and inserted into the holder as seen in Figure 3.10c. Thereafter, the holder is inserted into the instrument and the specimen is radiated with X-ray beams and detected on the other side, this method is called transmission mode. The specimens tested in WAXS are dry LDPE sample and swollen LDPE samples which are exposed to oil in an enclosed container for 1 hour and 10 days.

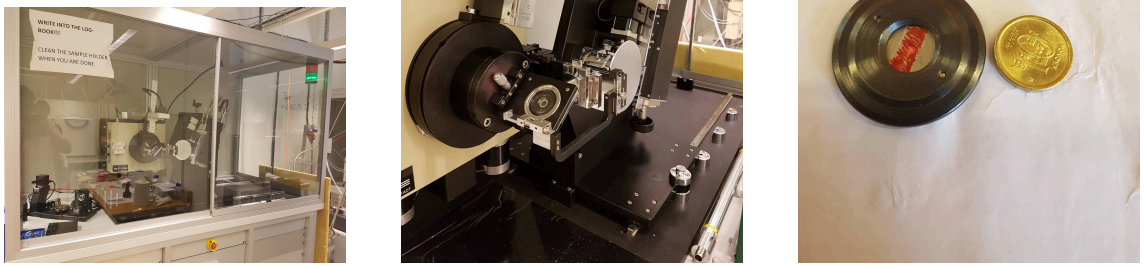

(a) *The Wide Angle X-ray Diffraction (WAXS).*

(b) *A close-up look into the WAXS instrument.*

(c) *Sample holder with a LDPE specimen.*

Figure 3.10: *The resources used for WAXS measurement.*

The material department at LTH was not familiar with using WAXS to calculate the crystallinity and therefore, we were unable to calculate the crystallinity from the software associated to the WAXS instrument. A free software called Origin® 2018 was used instead to predict and integrate the area under the peaks and then inserted in the equations in subsection 2.4.3 to obtain the percentage crystallinity. However, it is not the most accurate method as both the crystalline and amorph regions overlap each other.

3.6 Differential Scanning Calorimetry (DSC)

The DSC measurements are conducted using a TA Instruments DSC Q2000 at the material department at LTH as shown in Figure 3.11a. The DSC experiment are performed on four dry punched LDPE test samples and eight punched LDPE test samples exposed to sunflower oil, water and orange juice at two different time intervals. The first four samples are exposed to product for 60 minutes and the last four samples are exposed to product for 10 days. The test samples are cut into small specimens and inserted into aluminium pan and weighted to up to 2 - 3 mg. In Figure 3.11b the investigated sample pan is inserted in the same heater next to an empty reference pan.

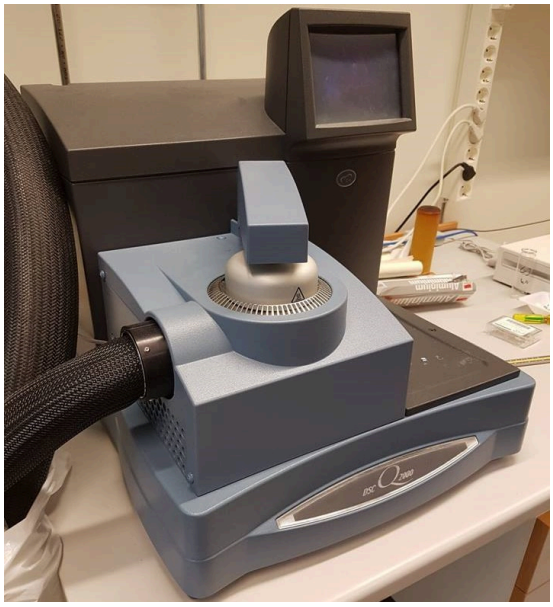

(a) *The differential scanning calorimetry instrument.*

(b) *The reference pan(upper left) and the sample pan(bottom right).*

Figure 3.11: *The DSC measurement instrument and the orientating of the pans.*

For this thesis, the DSC tests are conducted with three temperature cycles on all samples and all three cycles have an heating or cooling rate of $10°C$/min as seen in Table 3.1. First a heating cycle is performed from room temperature to $140°C$ to observe the effect of exposure to products. Next a cooling cycle cooled the sample to $40°C$ to recrystallise the sample and erase the previous thermal and processing history of the sample. Lastly, a heating cycle is performed to confirm the validity of all samples.

	Initial temperature	Target temperature
Cycle 1 (heating)	Room temperature	140°C
Cycle 2 (cooling)	140°C	40°C
Cycle 3 (heating)	40°C	140°C

Table 3.1: *Temperature changes on all three cycles.*

3.7 Tensile testing

Punched polymer test samples cut to dogbones shapes are used in tensile testing. Both dry reference LDPE samples and LDPE samples exposed to different products are tested. Samples are cut in machine direction, cross direction and at 45° degrees. Figure 3.12 shows the instrument used, it is a Zwick/Roell Z010(Static Materials Testing Machine) at Tetra Pak® in a climate chamber with controlled temperature of around 23°. Included with the equipment is the software TestExpert II that is used to evaluate the results. The Zwick/Roell machine is equipped with a load cell of 10kN. The test rate is performed at a displacement rate of 500 mm/min and 50 mm/min until fracture. Nilsson (2017)

Figure 3.12: *The Zwick/Roell Z010 tensile testing apparatus.*

Images on Figure 3.13 shows tensile test of a dry LDPE test specimen, how it is mounted on the holders and the elongation when load is applied. The top part is mounted first and carefully oriented so that it align as straight down as possible to minimise orientation errors. After the polymer samples are mounted, it is stretched with a load between 0 - 0.1 N so that the specimen is not slacking but also not in tension.

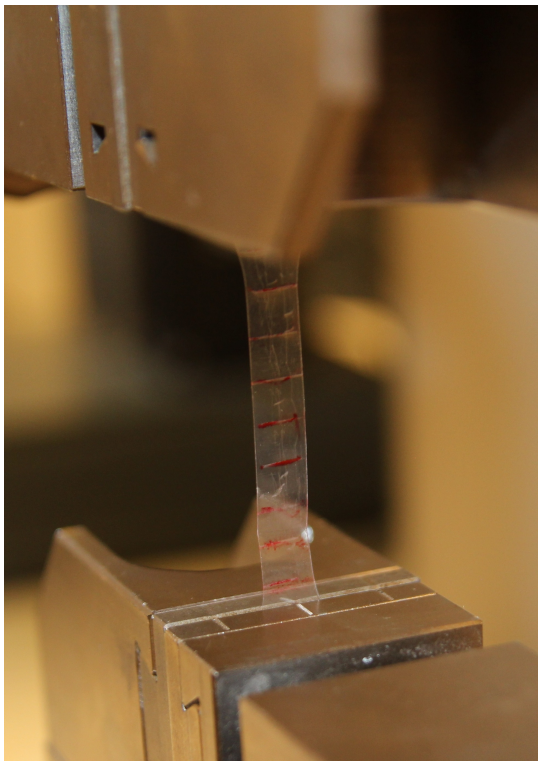

(a) *An unloaded polymer specimen installed on tensile test holders.*

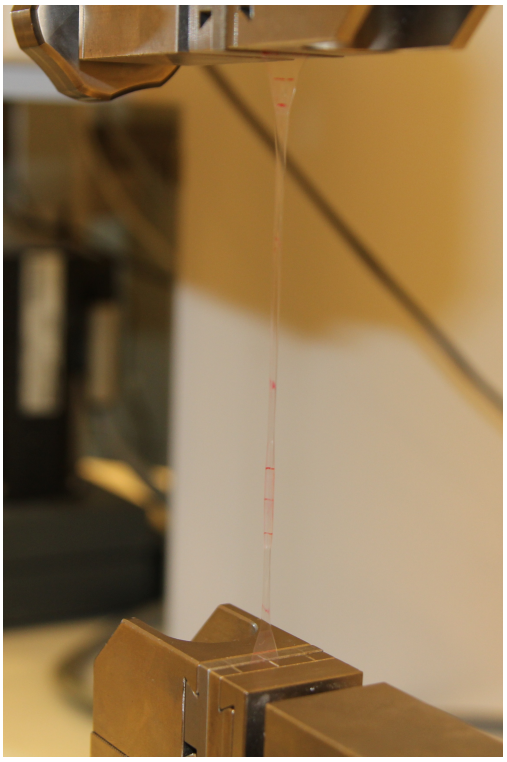

(b) *A loaded and elongated polymer sample on a tensile test.*

Figure 3.13: *Images of tensile test of a polymer sample.*

3.8 Digital Image Correlation (DIC)

DIC consist of several steps, first a speckle pattern are applied on the tested samples. The point with the powder is to increase the accuracy and precision of the DIC measurement and not affecting the tensile properties of the material. In this thesis a special chalk spray paint is used. It is made of coloured chalk powder that does not bond to the surface but hardens after contact with the polymer as shown in Figure 3.14. A camera with manual focus is used to capture images with a delay of one second until fracture. A slower displacement rate of 50 mm/min was used for DIC, to allow the camera to capture the images.

Figure 3.14: *A LDPE test specimen that has been prepared with chalk paint.*

GOM Correlate

The images recorded during tensile testings are imported and analysed in a free software program, GOM Correlate software. A surface component is defined and a standard mesh is created from the software. Creating the surface component requires input on facet size and point distance. Facet size is needed for the software to track points between different images. Due to large deformation of the test samples, a big facet size intervals of 30 - 40 pixels are used. The point distance decides the overlap of the facets and a value of 16 pixels is used in this thesis. Metrology (2019)

3.9 Scanning Electron Microscopy (SEM)

The application and objective with using SEM in this project is to obtain and analyse high-resolution images of tensile tested polymer samples in both machine direction and cross direction. The shapes at the fracture point from both directions are investigated and compared to non-tensile tested dry LDPE polymer samples to study if there are any visible difference. The SEM experiments are conducted and displayed using the Field Emission SEM JSM-6700F as shown in Figure 3.15 at the division of food science at LTH. The electron detector are detecting lower secondary electrons (LEI). The investigated samples are two dry LDPE polymer samples that have been punched and tensile tested in machine and cross direction respectively. Magnification of 90x, 400x and 1500x are used.

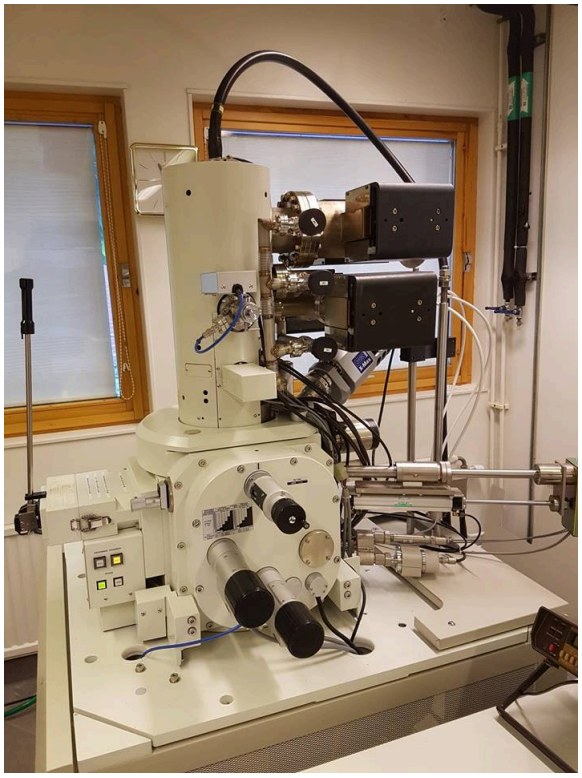

Figure 3.15: *The scanning electron microscopy instrument used in this research.*

3.10 Thermogravimetric Analysis (TGA)

The thermogravimetric analysis are performed using a TA Instruments TGA Q500 as shown in Figure 3.16. A small specimen of around 1 mg of cut LDPE sample is sealed into an aluminium pan container and inserted into the instrument. The sample is then heated from room temperature to 600°C.

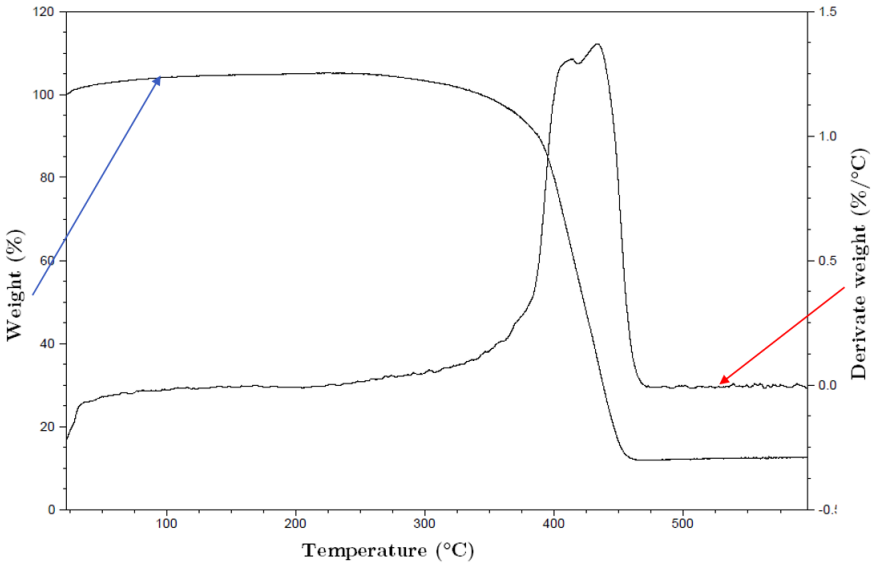

Figure 3.16: *The thermogravimetric analysis instrument used in this research.*

Chapter 4

Results

4.1 Product Uptake

The results from the initial product uptake measurement were first documented and then compared to the results after exposure to produce graphs like Figure 4.1. The grey peaks are dry reference samples measured before exposure and the red peaks next to them are after exposures. All tests, both dry reference and product exposed samples ended up at a weight of around 90 - 98 mg.

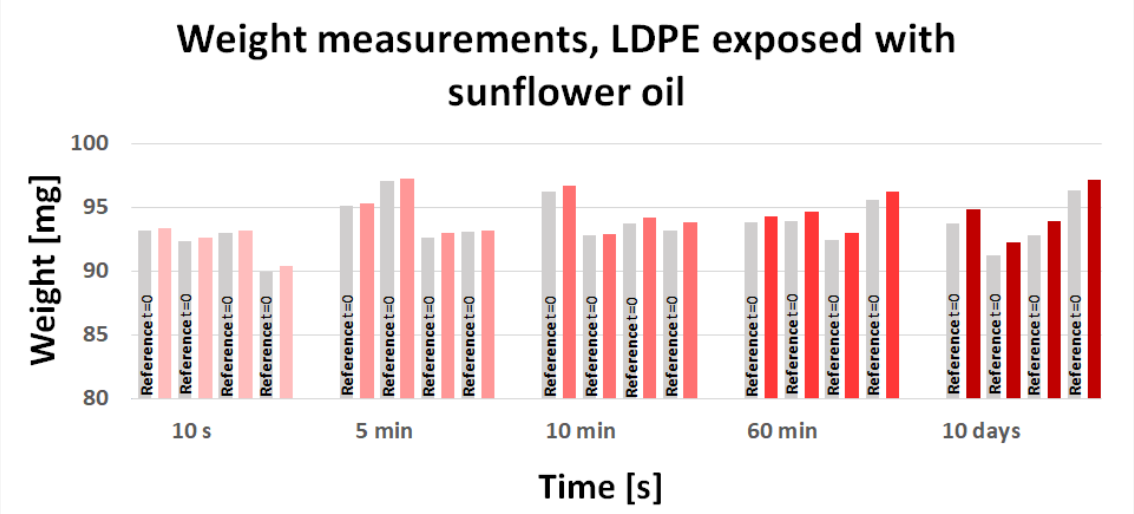

Figure 4.1: *The difference in weight from dry sample to exposure with sunflower oil.*

The same experiment were performed with water as products to observe the polymer moisture resistance and in turn the absorption of water. The results are depicted in Figure 4.2, in which the grey peaks represent the dry reference samples and the blue peaks next to them are after exposure. Hardly any weight difference is observed between the dry reference and exposed samples and the weight interval was the same as the previous test with weights between 90 - 98 mg.

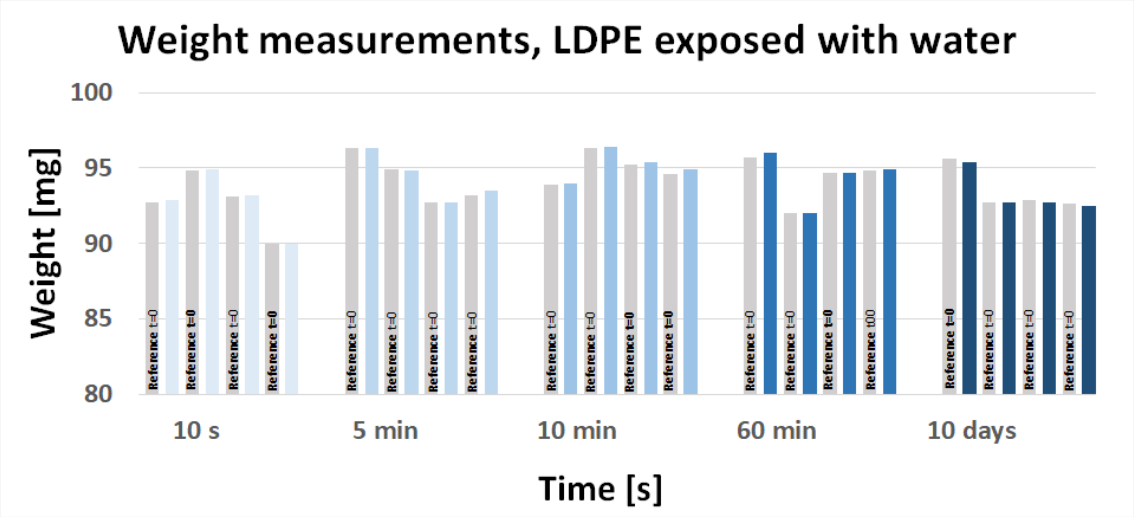

Figure 4.2: *The difference in weight from dry sample to exposure with water.*

The last experimented product was with orange juice and the results are observed in figure Figure 4.3. The reference samples are depicted as grey peaks and next to them are the same samples after exposure to orange juice displayed as yellow peaks. A small increase is seen on every yellow peak compare to their respective grey peak. However, compare to the previous weight tests, weight measurements this time gave a lower weight interval with values between 84 - 94 mg. The reason may be because a new batch of LDPE was used for this experiment which should be identical but may have different thicknesses.

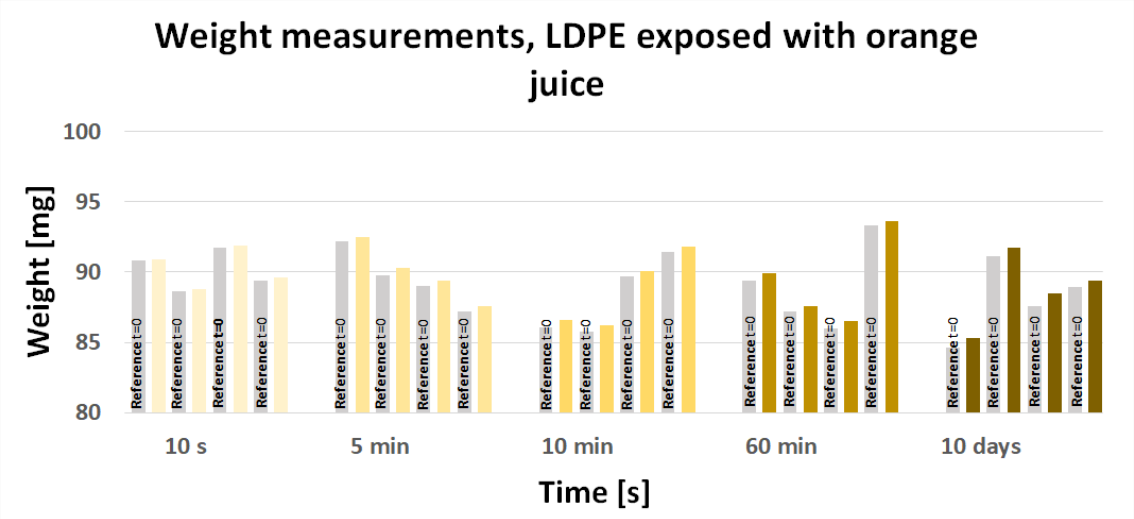

Figure 4.3: *The difference in weight from dry sample to exposure with orange juice.*

Average Weight Difference

Collected in Table 3 in the appendix shows the data for the average percentage weight difference for the three different products at different exposure times and the respective standard deviation. To further visualise the results from the table, each product is plotted on the weight difference against exposure time.

First, depicted in Figure 4.4 is the average percentage difference of LDPE test samples exposed to sunflower oil. Observable from the figure is the weights of LDPE with exposure to sunflower oil, which are steadily increasing with time for up to 1.07% after 10 days of exposure. Every individual data points also display a two standard deviation (2σ) error bar, which represent a confidence level of 95%. Galarnyk (2018)

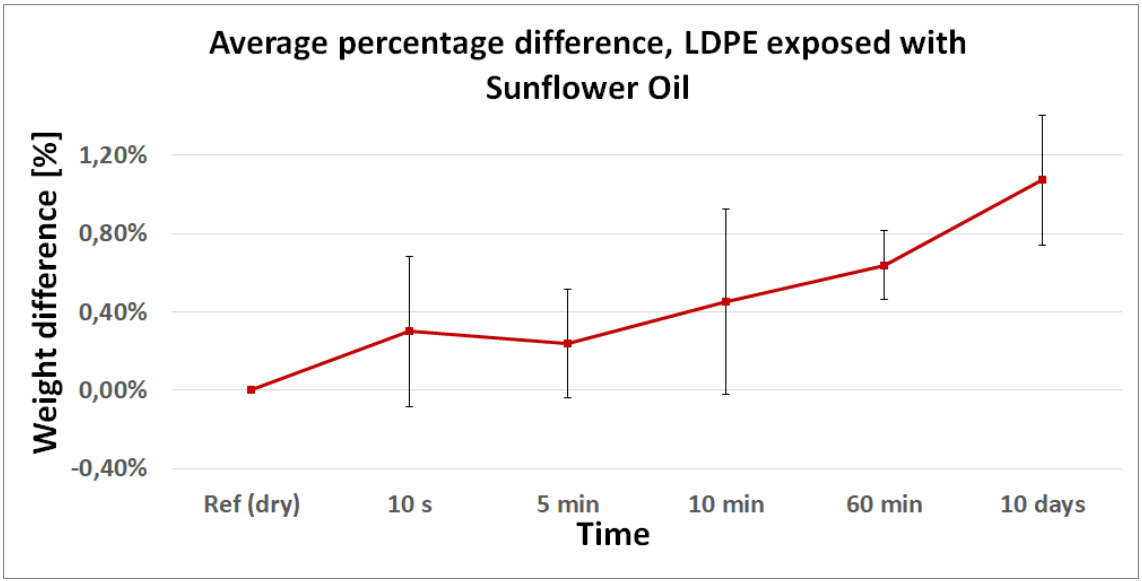

Figure 4.4: *Average weight of sunflower oil at different exposure time.*

Figure 4.5 shows the average percentage weight for exposure to water at different time with two standard deviation error bars. Water stays at a steady 0.11 % weight increase throughout the first 60 min of experiment and then decreases to -0.13 % compared to initial average weight after 10 days of exposure.

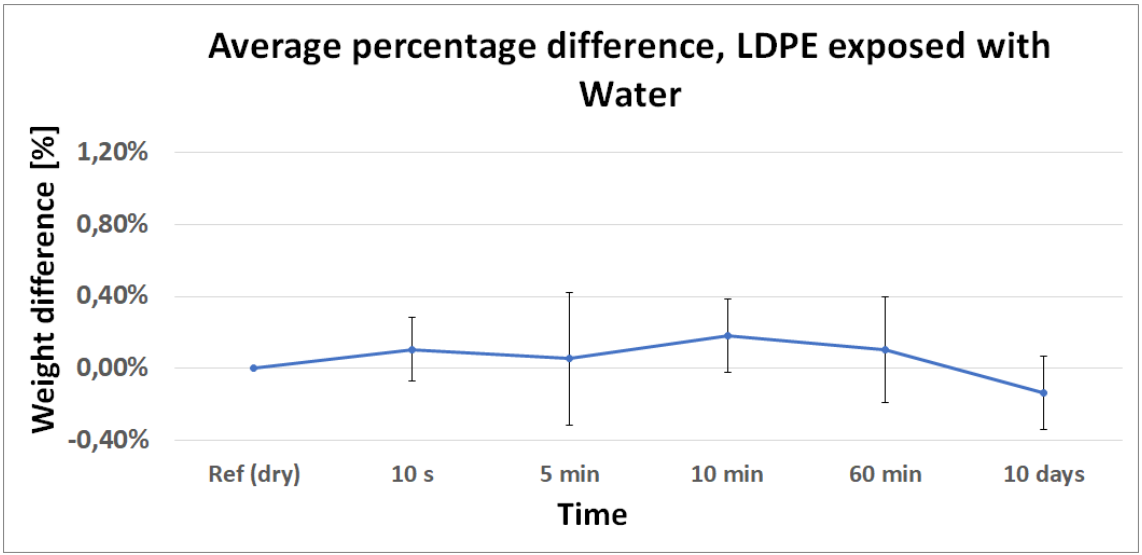

Figure 4.5: *Average weight of water at different exposure time.*

Orange juice gain a weight increase as illustrated in Figure 4.6 for the first 5 minutes of exposure and maintain a steady percentage weight difference of around 0.48% for at least 60 minutes. However, after 10 days of exposure the average percentage weight difference had increase up to 0.77%.

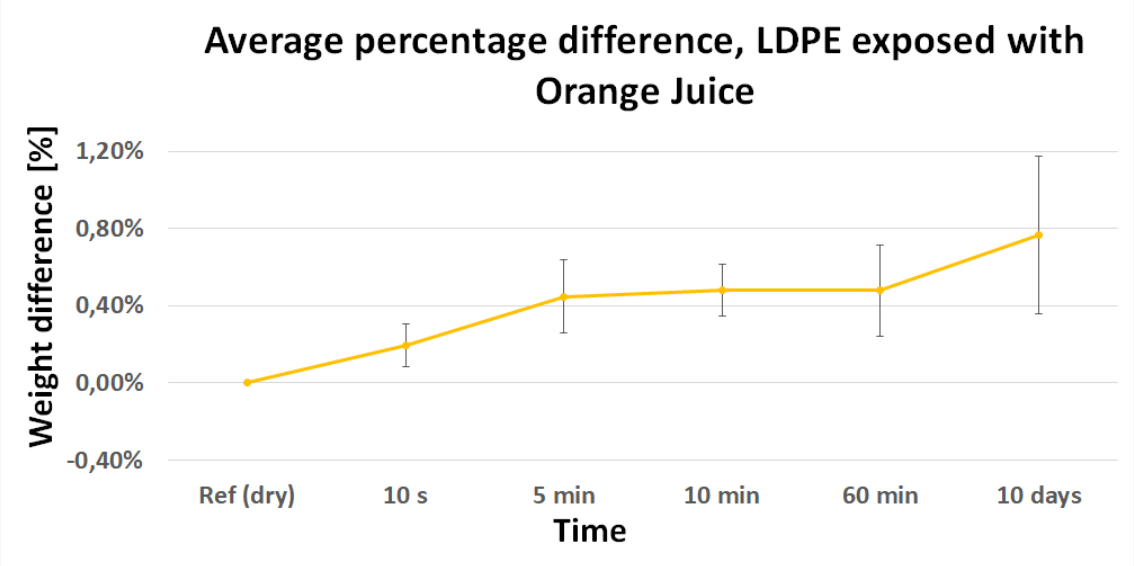

Figure 4.6: *Average weight of Orange juice at different exposure time.*

4.2 Thickness measurement

Thickness Intensity Map

In this section some of the thickness measurement are shown, figures with more detailed information is found in appendixes Table 7. In Figure 4.7 a calculated thickness map of the studied dry LDPE film in dimension of 22 x 16.5 cm is seen. A three-colour gradient are representing the thickness of the polymer film. The thickness of the polymer film varies between 54 - 46 μm. The thickest part of the polymer film will show red, the thinnest as green and yellow when the thickness is exactly 50 μm. From the result of the map, it is almost possible to split the polymer film into two thickness segments with a thinner upper body and a much thicker lower body.

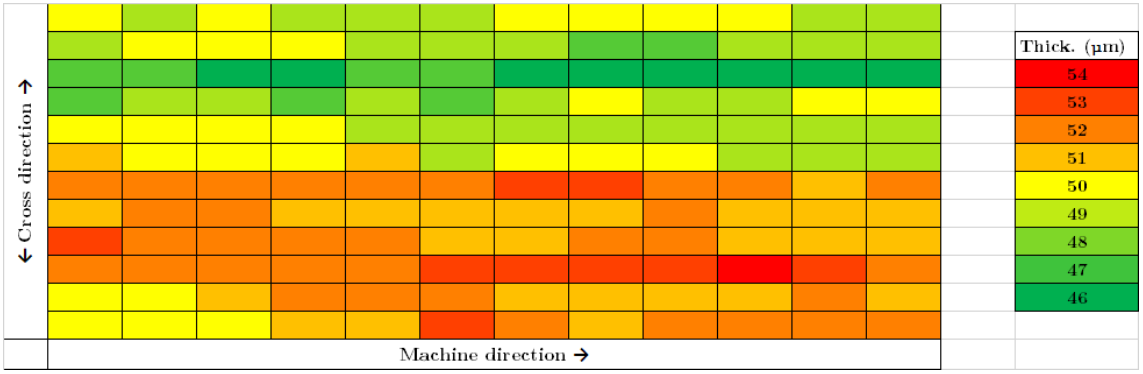

Figure 4.7: *Thickness map of one segment of polymer film.(A)*

The second figure Figure 4.8 was taken from another part of the polymer film but with the same dimensions as the first figure. The big thickness difference does not display as clearly as in the first figure, but the difference is still visible with a thinner upper part and thicker bottom part.

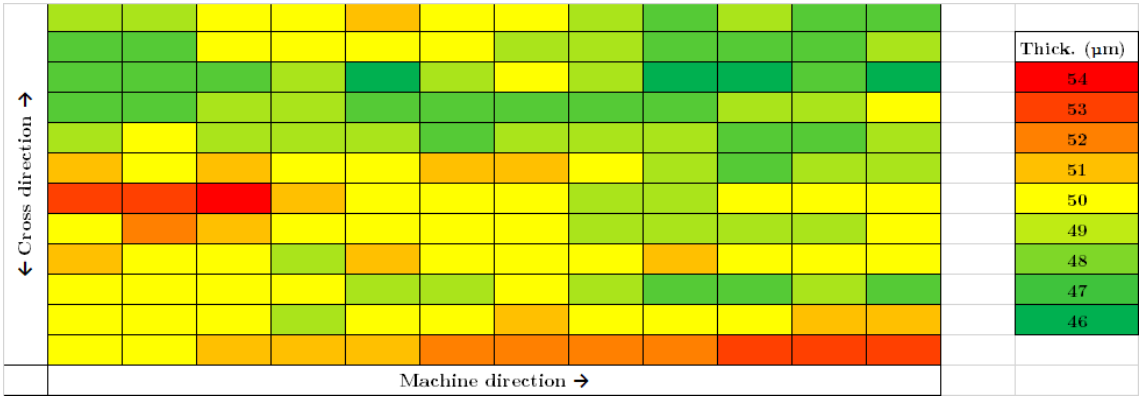

Figure 4.8: *Thickness map of one segment of polymer film.(B)*

One final thickness measurement was made on another position on the polymer film as seen in Figure 4.9. The thickness difference is clearly visible here, in which almost the whole upper segment are green. It appear to exist a bigger thinner cavity in the green upper middle part of the examined film.

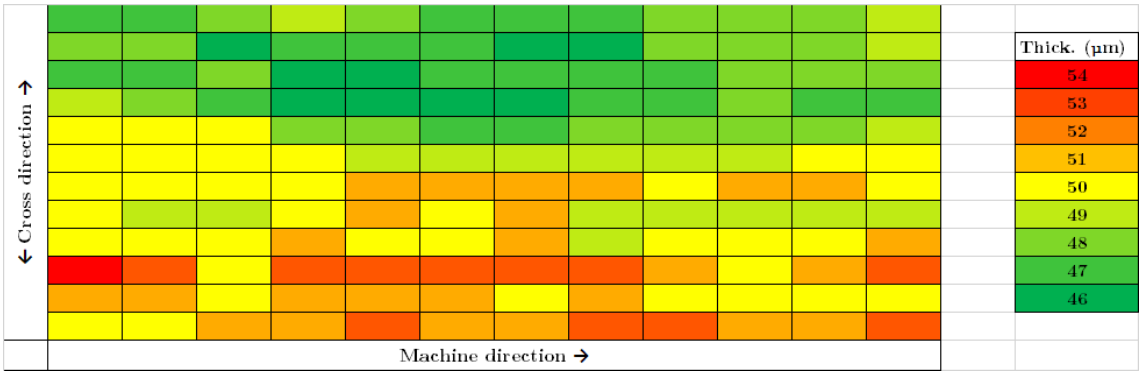

Figure 4.9: *Thickness map of one segment of polymer film.(C)*

3D - Thickness Intensity topography

Below are simulated 3D topography figures of thickness difference of the three tested polymer films. In Figure 4.10 the split in thickness is clearly seen between the upper-right and lower-left segments. The red elevated parts are the thickest parts of the tested polymer film and the green parts are the thinnest.

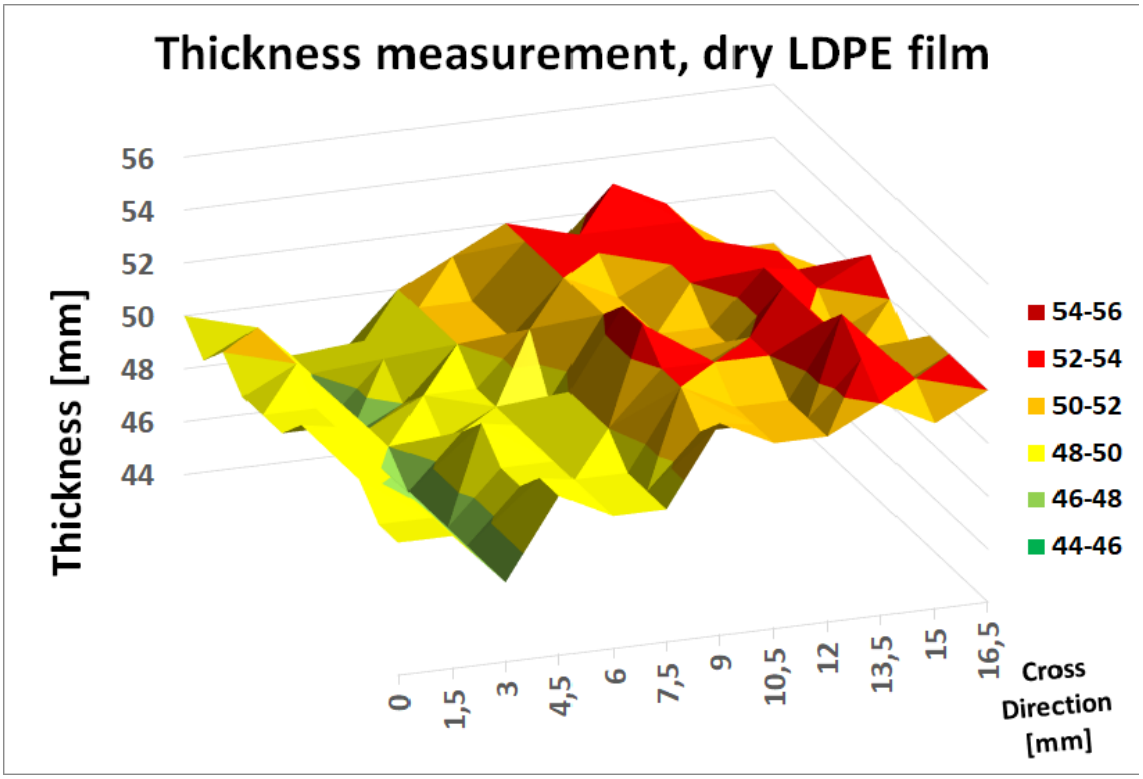

Figure 4.10: *3D-thickness topography of one segment of polymer film.(A)*

The thickness measurement of the second polymer film is displayed in Figure 4.11. However, this image do not show the difference in thickness as clearly as in the previous figure. The plane is much more smooth and uniform throughout the film.

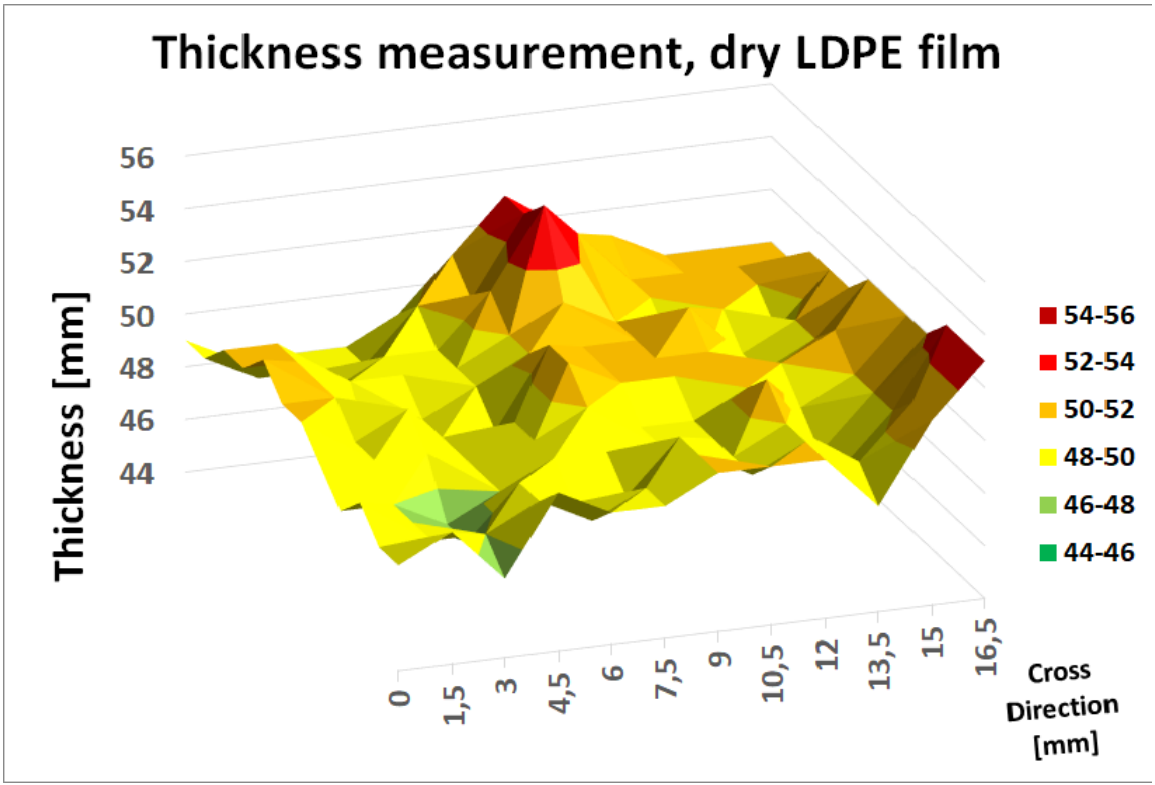

Figure 4.11: *3D-thickness topography of one segment of polymer film.(B)*

The last measured polymer film depicted in Figure 4.12 is similar to the first 3D figure as the thickness difference is clearly observable. With a thicker upper-right segment and a thinner bottom-left segment.

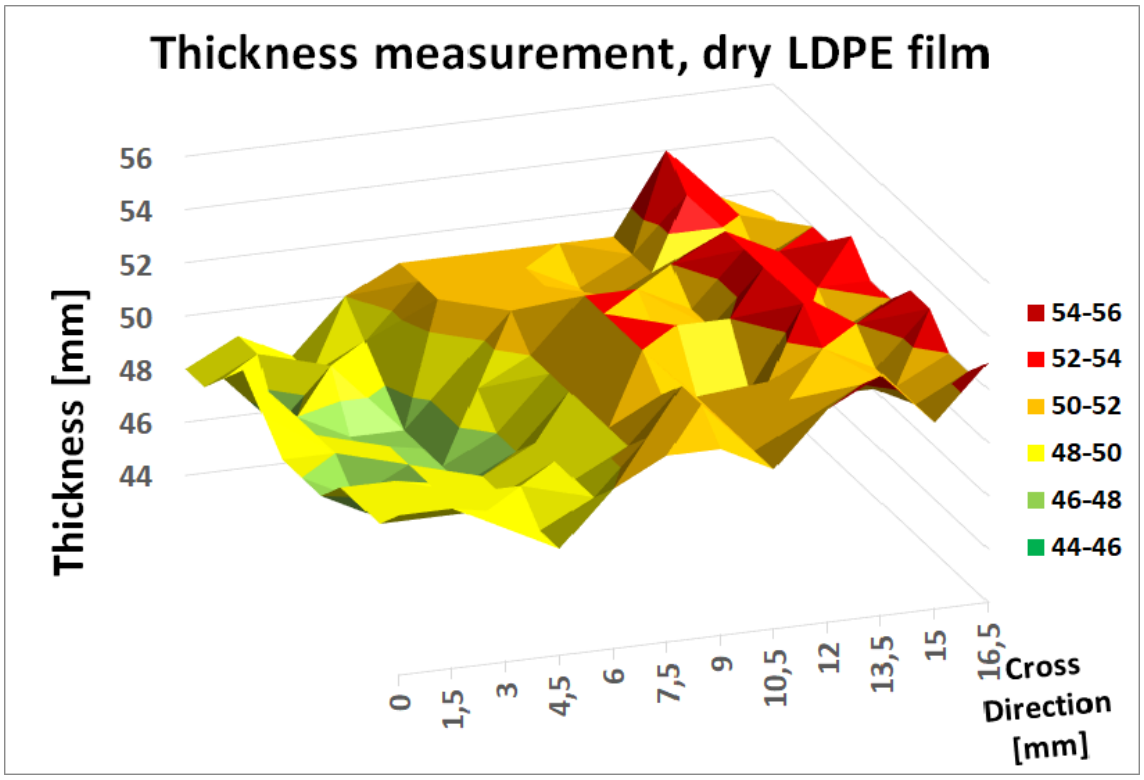

Figure 4.12: *3D-thickness topography of one segment of polymer film.(C)*

4.3 Wide Angle X-ray Scattering (WAXS)

The first measurement of WAXS was conducted on dry LDPE and the result are shown in Figure 4.13. Observed from the image, at least two sharp peaks are seen on top of a very broad amorphous peak. This confirm that the experimented sample has a semi-crystalline structure. Only the first two sharp crystalline peaks were integrated as the rest of the crystalline peaks were insignificant small and difficult to measure.

Integrating the areas under the first two peaks resulted in a crystalline area of 2390 points and a total area of all peaks of 6567 points. This resulted into a percentage crystallinity of 36.7% for a dry LDPE sample.

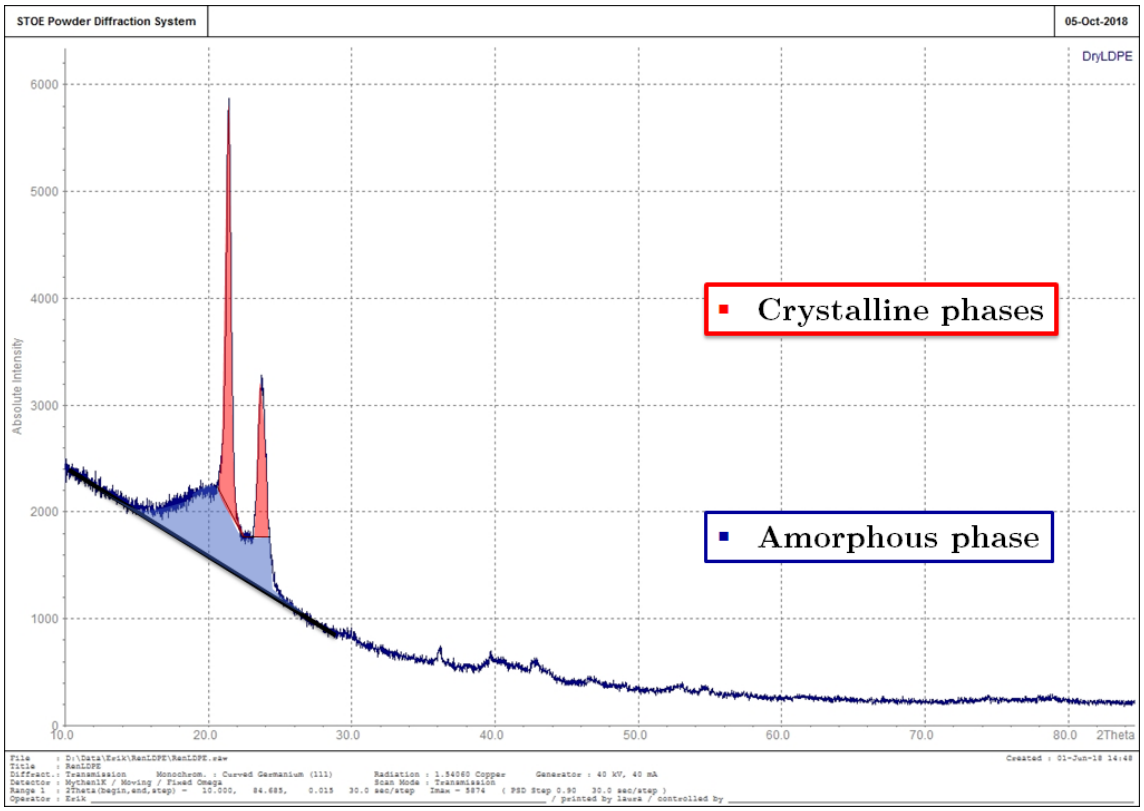

Figure 4.13: *Diffraction graph of dry LDPE.*

The second measurement with LDPE exposed to sunflower oil for an hour resulted in a very similar graph as seen in Figure 4.14. The calculations as described in section 2.4.3 showed a crystalline area of 2436 points and a total peak area of 6567 points, which results in a crystallinity of 37.1% in the exposed sample.

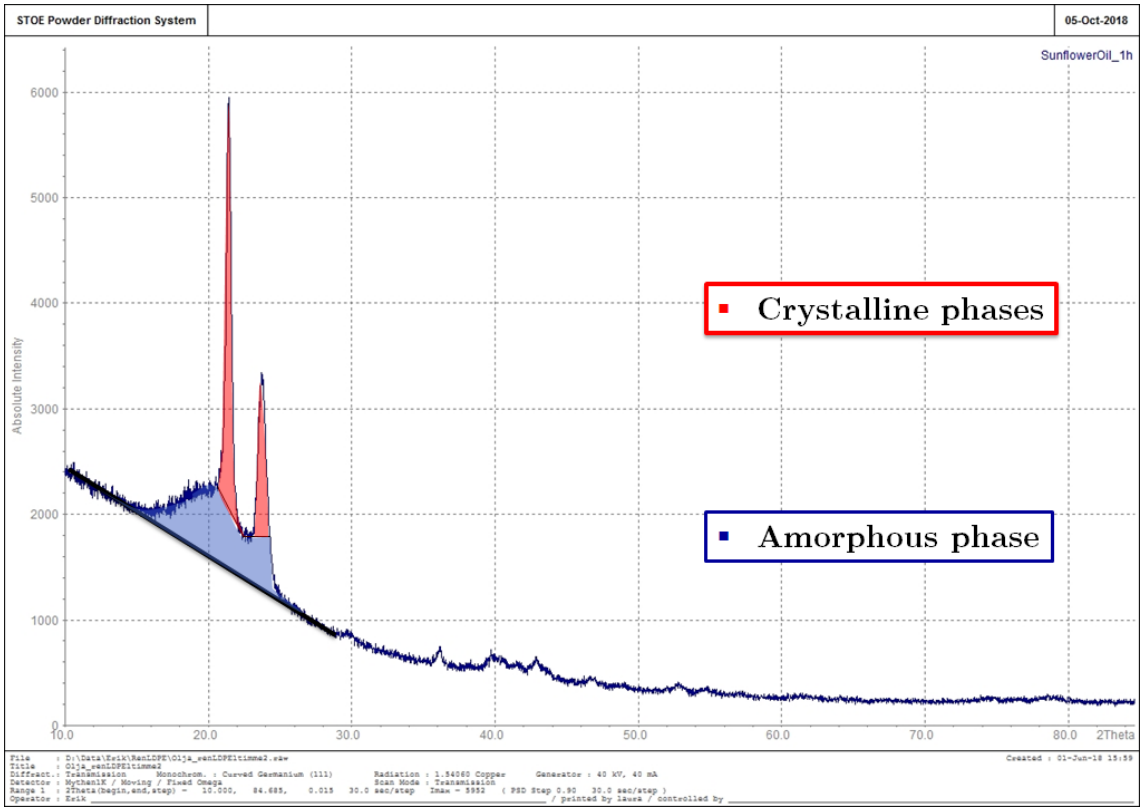

Figure 4.14: *Diffraction graph of LDPE exposed with sunflower oil for 1h.*

Very similar graph and values were also obtained as observed in Figure 4.15, which was performed with sunflower oil but exposed for a longer period of 10 days. Calculation from this graph gave results of the crystalline area of 2461 points, a total peak area of 6662 points and a crystalline percentage of 36.95 %

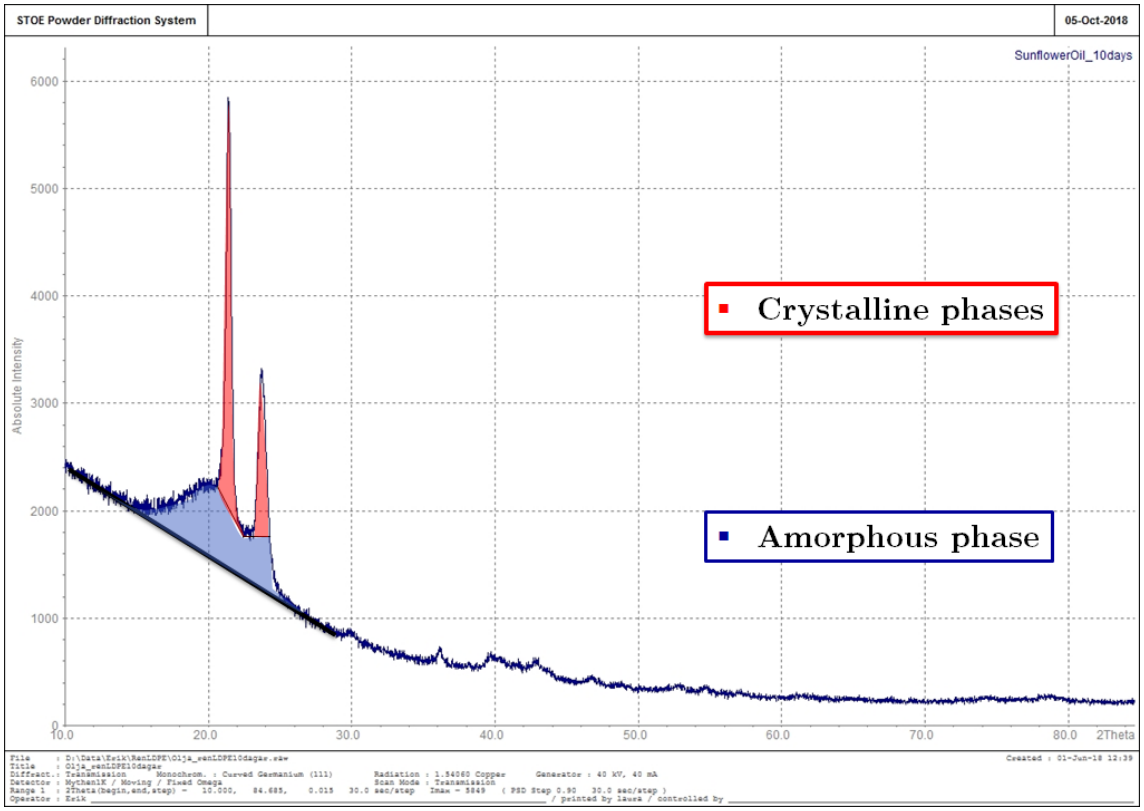

Figure 4.15: *Diffraction graph of LDPE exposed with sunflower oil for 10 days.*

Collected in Table 4.1 are the calculated crystalline peak areas, total areas and percentage crystallinity for every tested products. As observed the percentage crystallinity for every samples are very similar to each other with values around 37 %.

Solvent	Crystalline peak area	Total peak area	Crystallinity (%)
Dry LDPE	2389,7	6506,9	36,7%
Sunflower Oil 1h	2436,2	6566,6	37,1%
Sunflower Oil 10days	2461,5	6662,4	36,9%

Table 4.1: *Calculated areas and percentage crystallinity based on WAXS.*

4.4 Differential Scanning Calorimetry (DSC)

From the DSC measurement, a lot of data were obtained on the LDPE samples enthalpy values and peak temperatures. Calculated from these values the percentage crystallinity for each sample was obtained. This raw data is found in appendix Table 2.

An example of the results from the DSC measurement is depicted in Figure 4.16 for the first melting cycle for a dry LDPE specimen. A temperature ranges of 70-120 °C was picked and a melting enthalpy was obtained from DSC associated software with a value of 104,5 J/g and also a melting temperature of 112,60 °C. Figure 4.17 shows the second melting cycle for the same specimen. Here we receive a melting enthalpy of 108,1 J/g and a melting temperature of 113,22 °C.

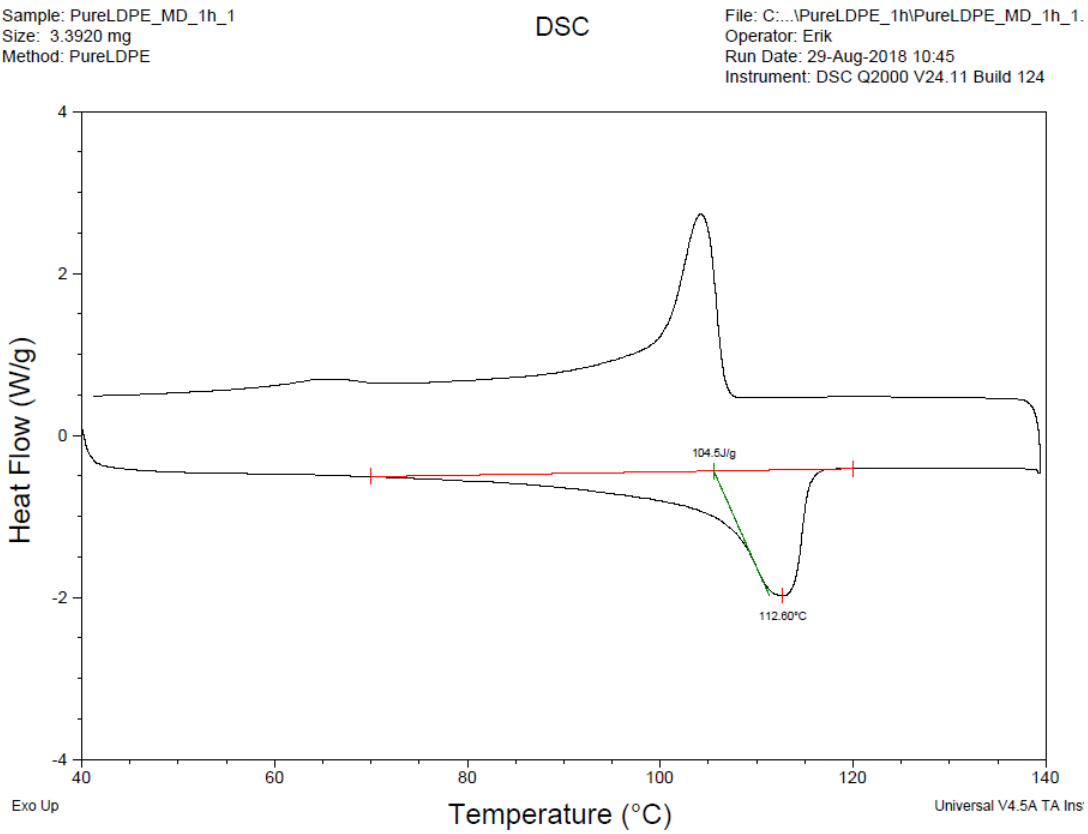

Figure 4.16: *An example of a result from the first melting cycle with dry LDPE.*

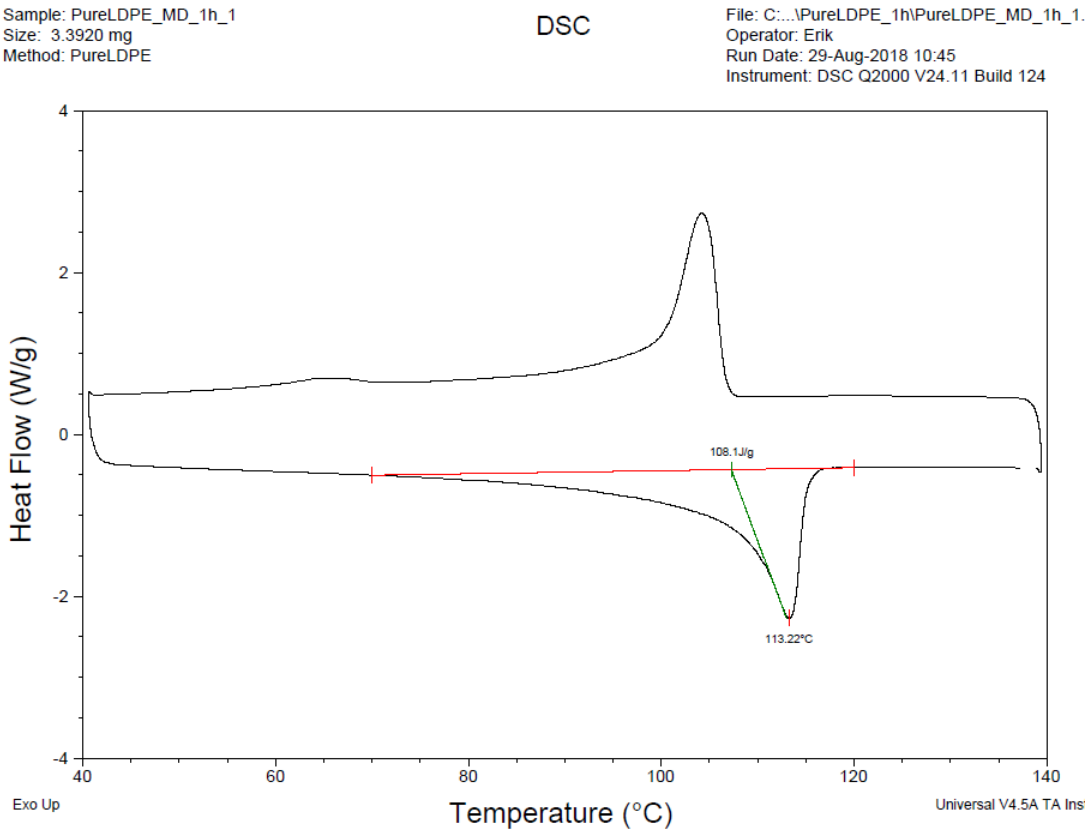

Figure 4.17: *An example of a result from the second melting cycle with dry LDPE.*

For comparison, Figure 4.18 shows an example of the first melting cycle for a LDPE specimen that was exposed to sunflower oil for 10 days which exhibited the greatest swelling. The melting enthalpy was lower than for the dry example with a value of 98,07 J/g. The melting temperature did not change much at all and stayed on a value of 112,09 °C. Figure 4.19 shows the second melting cycle for the same specimen and here we obtained a melting enthalpy of 103,8 J/g with a melting temperature of 113,24 °C.

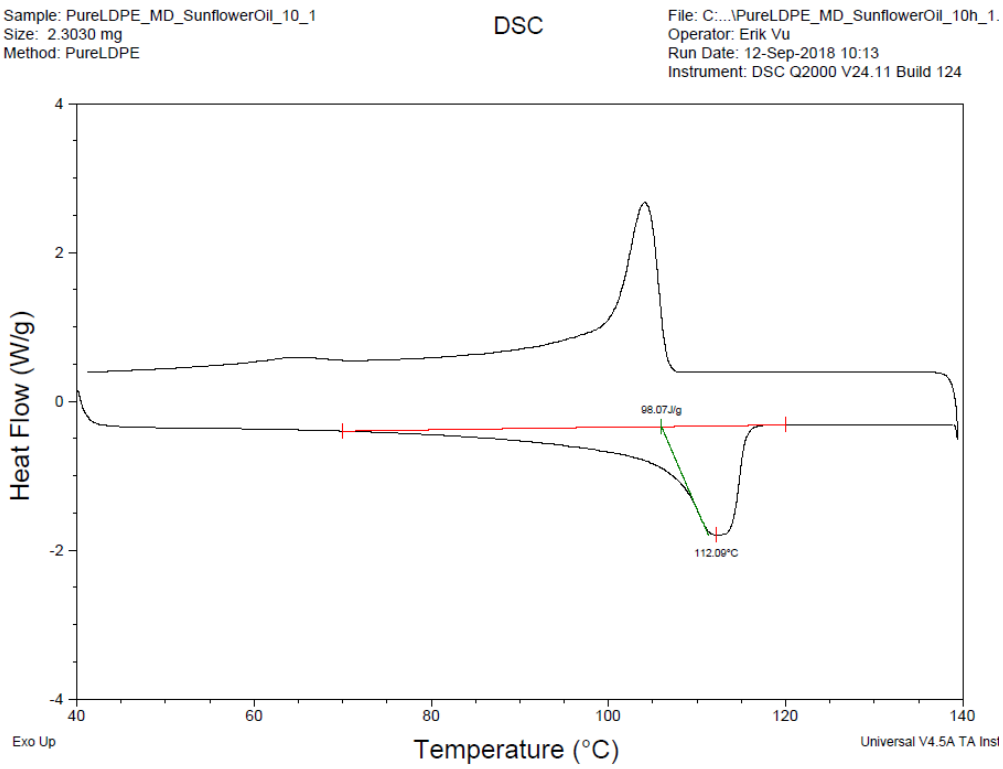

Figure 4.18: *An example of a result from the first melting cycle.*

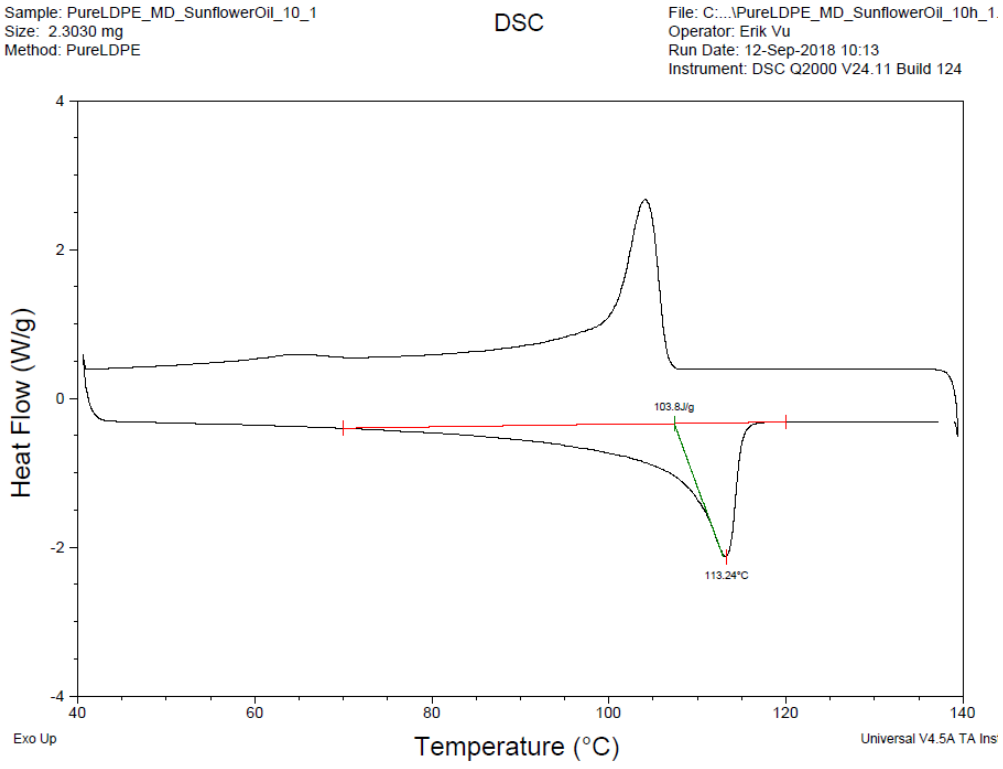

Figure 4.19: *An example of a result from the second melting cycle.*

Figure 4.20 display the crystallinity for the first heat cycle for every tested sample. Most of the tested samples showed a crystallinity between 33 - 37 % except for the polymer exposed with orange juice for 10 days, that had a crystallinity up to 40 %. The reason for this disparity is maybe because of a layer of yellow film stuck to the surface of the polymer after exposure that was difficult to remove. Water initially obtain a lower crystallinity but return to the same value as the reference sample after 10 days. Three samples, one solved in water and two solved in orange juice failed due to several factors such as failure of machine or the instrument was not cooled enough. Therefore, these were not included in the results for the first heat cycle.

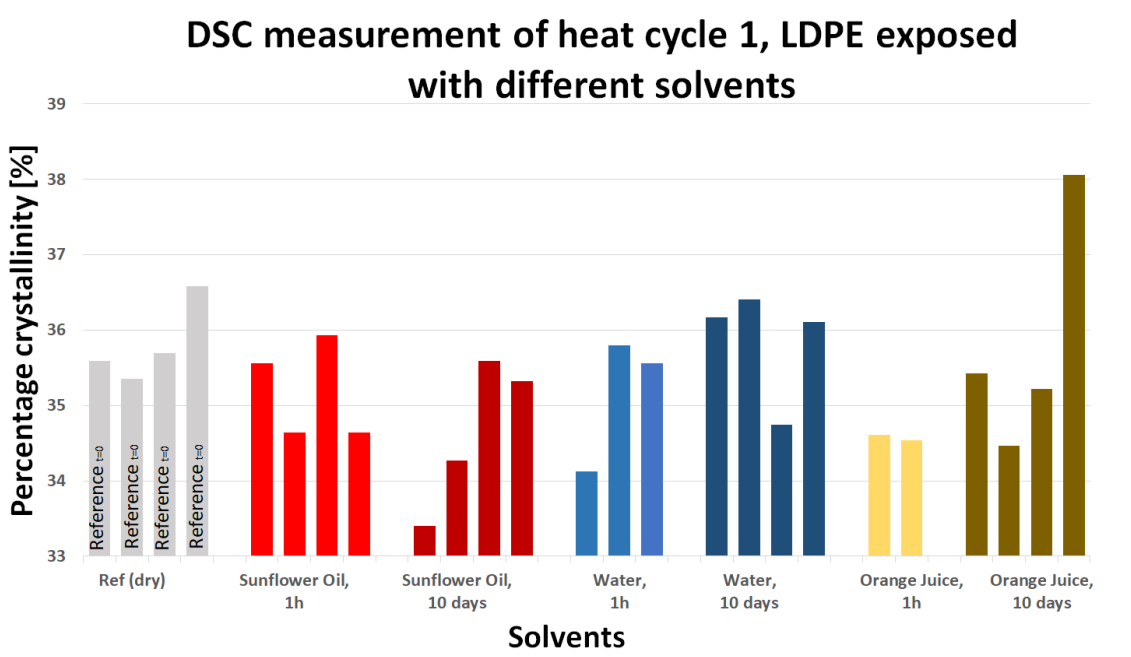

Figure 4.20: *Crystallinity of LDPE exposed to different products at first heat cycle.*

The third heat cycle erased all processing history done on the polymer film. Therefore, all samples should have similar values. This is observed in Figure 4.21 in which all samples almost have the same percentage crystallinity of around 38.5 %.

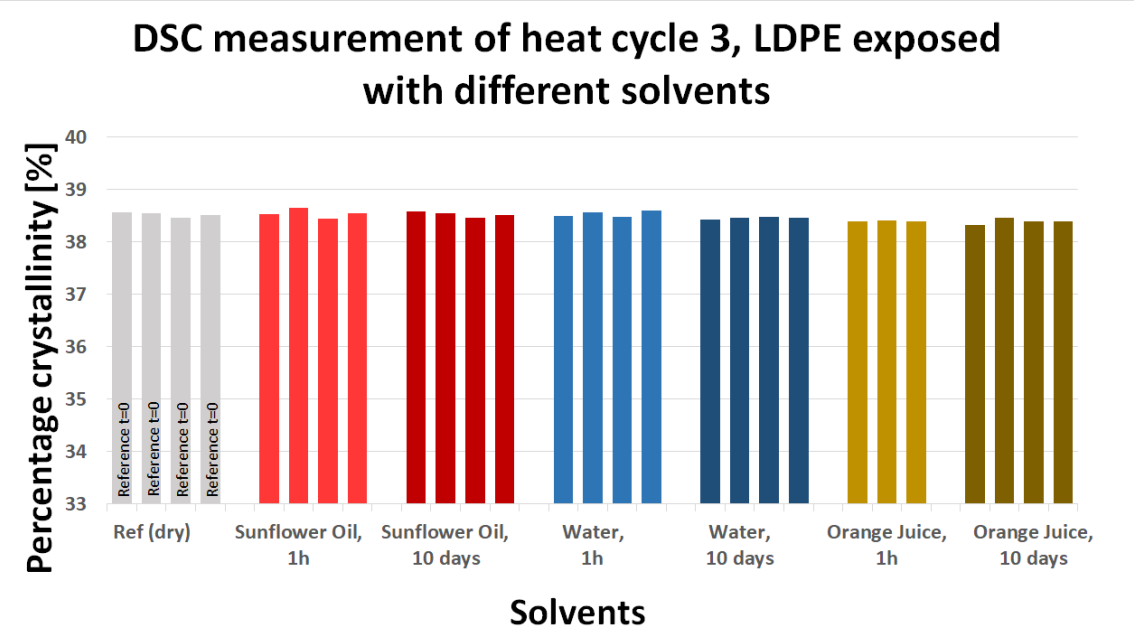

Figure 4.21: *Crystallinity of LDPE exposed to different products at third heat cycle.*

4.5 Tensile testing

Tensile measurements were performed with LDPE test samples cut in three different directions. The typical result for them is depicted in Figure 4.22, where a sample from each direction is picked. The test samples were punched LDPE without exposure of product with a displacement rate of 50 mm/min. Observed clearly from the figure are three very different curves for each direction. The curve for MD exhibited high strength but low elongation, while CD showed the opposite with a low strength but almost double the elongation distance. The curve for the specimen at 45° behaved like a mix of both MD and CD, with the properties of both a high strength and a high elongation.

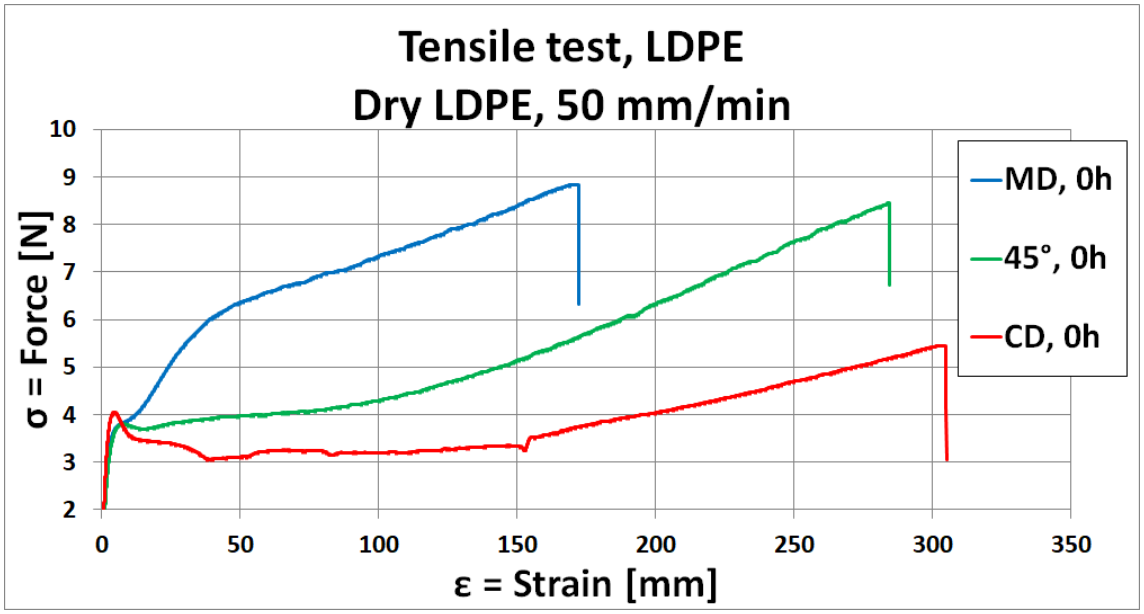

Figure 4.22: *Typical tensile test results of Dry LDPE samples cut in different directions with a displacement rate of 50 mm/min.*

Dry Reference, LDPE tests

First, tensile samples were made on the machine direction on dry LDPE samples without exposure to products as seen in Figure 4.23. 23 samples were tested, 7 pieces of the first batch polymer film and 16 pieces of the second batch polymer film. The reason the samples are divided into two batches is because the first batch polymer film went out of supply. The second polymer film may have other properties because of batch variation. For all conducted tensile tests, the first batch was run at a displacement rate of 500 mm/min and the second batch a rate of 50 mm/min. Test samples achieved a strength of around 9 N for the first batch and slightly lower for the second batch polymer with values of around 8 N. The strain had a large difference in the elongation between the two batches, with an elongation up to 320 - 340% increase of strain from the original length for the first batch and an increase of 280 - 330% for the second batch.

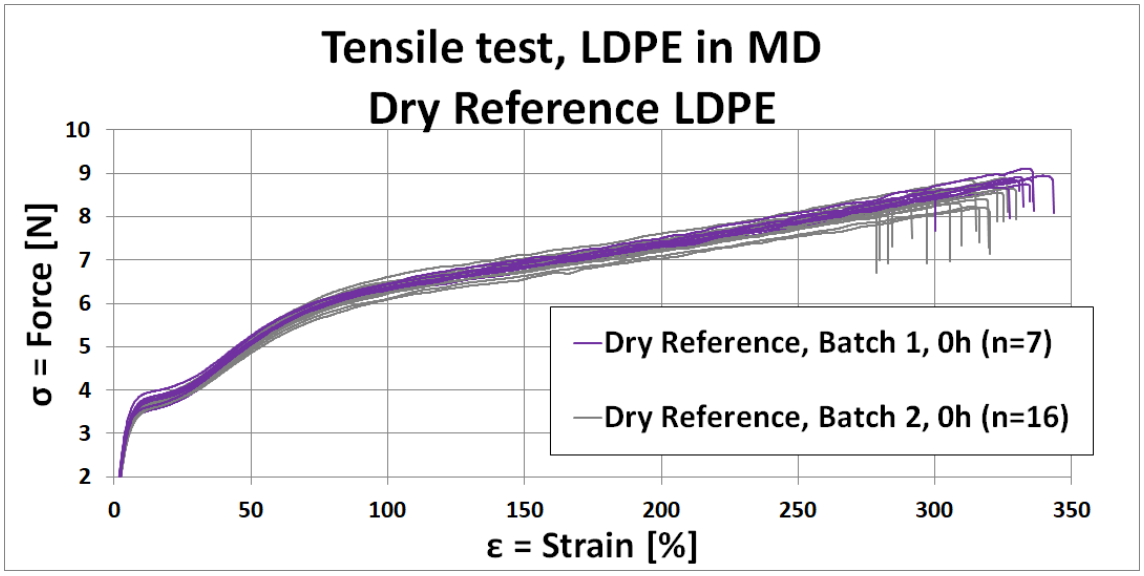

Figure 4.23: *Tensile test results of dry LDPE test samples, cut in machine direction.*

In addition, tensile samples were performed with eleven dry LDPE test samples from the first batch in cross direction as depicted in Figure 4.24. As can be seen from the figure, the test samples have a very low strength, where it initially holds a strength of 3.5 N until between 300 - 400 percent elongation where the strength increases slowly up to 6 N until fracture. Unlike MD, this direction tends to strain much longer with an elongation of around 650% from the original length. The results from CD also gave very irregular and crooked curve and during the experiment several necking could be observed, which were not present at the tests with MD. Due to the unpredictable variations, subsequent tensile tests were made mostly on LDPE exposed with products punched in the machine direction.

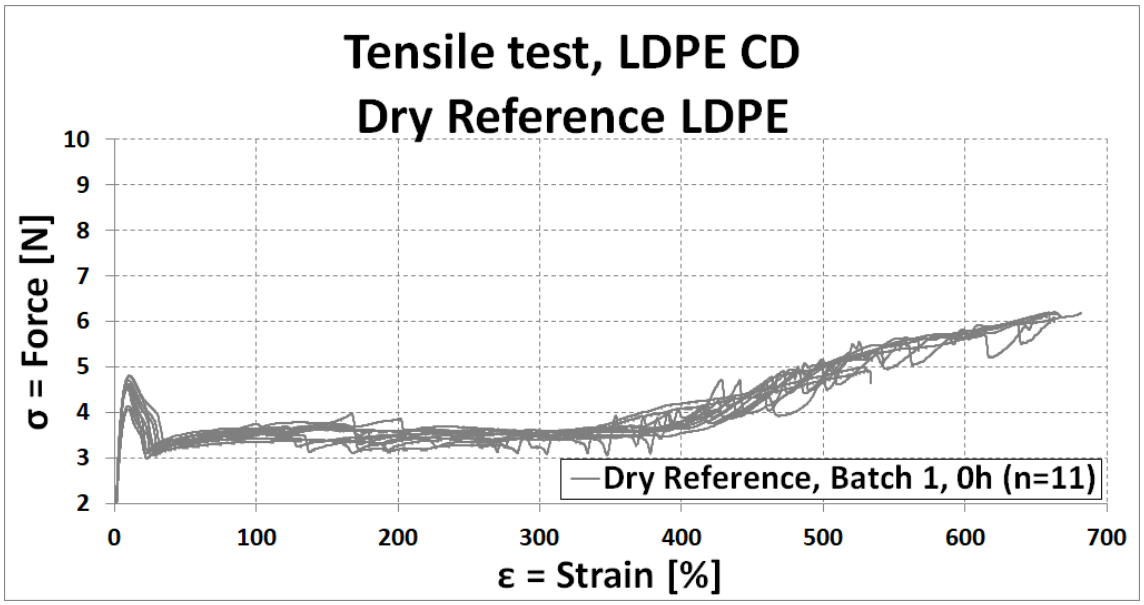

Figure 4.24: *Tensile test results of dry LDPE test samples, cut in cross direction.*

Product exposed, LDPE tests

In order to expand the result, tensile tests were performed on punched LDPE samples in MD that had been exposed to sunflower oil for 1 hour as shown in Figure 4.25. 7 samples were made from the first batch and 10 from the second batch. The first batch had a very large variation in strain, where the majority of samples were elongated to 300 - 330% in strain, but a pair of samples ended up at around 260% in elongation. The second batch was also divided into two parts where a number of samples were elongated to a range of 280% and some other between 300 - 310% elongation.

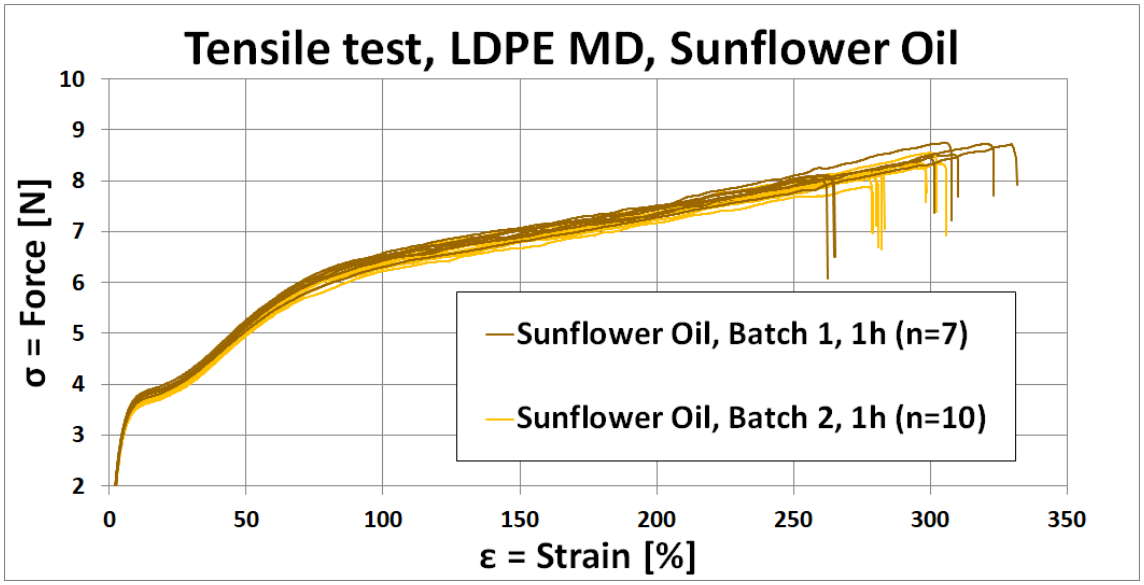

Figure 4.25: *Tensile test results of dry LDPE test samples, cut in machine direction.*

Figure 4.26 shows the results of samples exposed to water for one hour. Seven samples were made from the first batch and 12 from the second batch. The first batch is elongated to a value between 290 - 310%. The second batch had a little more variation and got a strain between 270 - 320% and it also had a large variation in strength through all samples, which was not present in previous tests. The reason may be setup error, since the variation in strength was not present in the first batch.

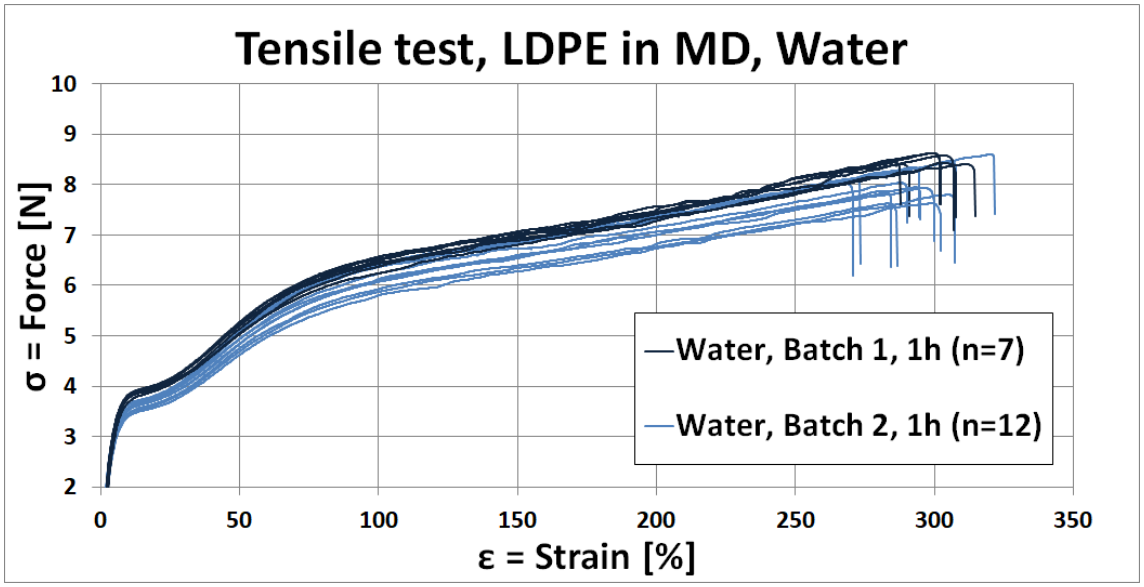

Figure 4.26: *Tensile test results of sunflower oil exposed LDPE test samples, cut in machine direction.*

Tensile tests were also conducted on samples exposed to orange juice as depicted in Figure 4.27. 6 samples were tested but they were tested only with the second batch of LDPE. The variation was large with an elongation up to 280 - 330%.

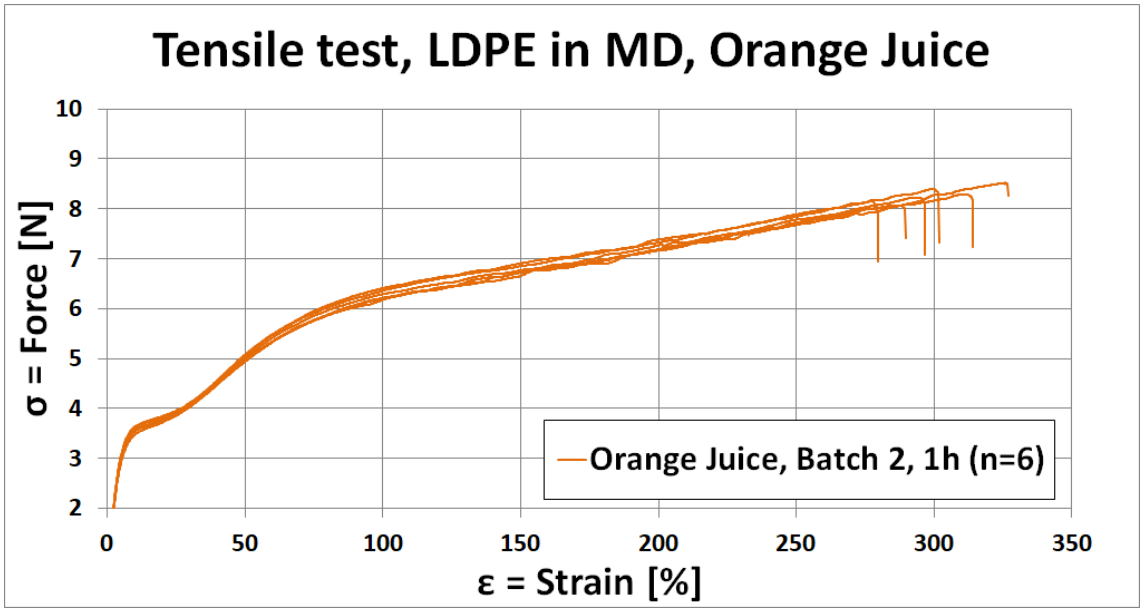

Figure 4.27: *Tensile test results of orange juice exposed LDPE test samples, cut in machine direction.*

Tensile tests were scheduled to be exposed for a longer period of up to ten days but no tests could be performed due to technical complications as the instrument on which the tensile test were conducted on, broke down and it took a long time before the instrument was repaired. In the future it would be wise to do more regular tests and better allocate the time for the tests.

4.6 Digital Image Correlation (DIC)

Digital Image Correlation (DIC) was used to visualise the strain evolution and local deformation in addition to the tensile tests. DIC were conducted on dogbone test specimens punched in machine direction, cross direction and 45°. More images are found in appendixes Figure 7 of DIC measurement with LDPE samples exposed to different products. For all tests five different time were picked to represent the strain evolution. The first four chosen time were: 0, 20, 50, 125 sec. The fifth and last image represent the last second before fracture, which differs between all conducted tests. All tests were conducted with a displacement rate of 50 mm/min.

The local strain evolution for a LDPE test sample in MD during a tensile test is visualised in Figure 4.28. The images are taken at time: 0, 20, 50, 125 and 195 seconds. As observed the strain evolution are quite uniform throughout the specimen except on the edges. There is no clear necking that is identified in any of the images.

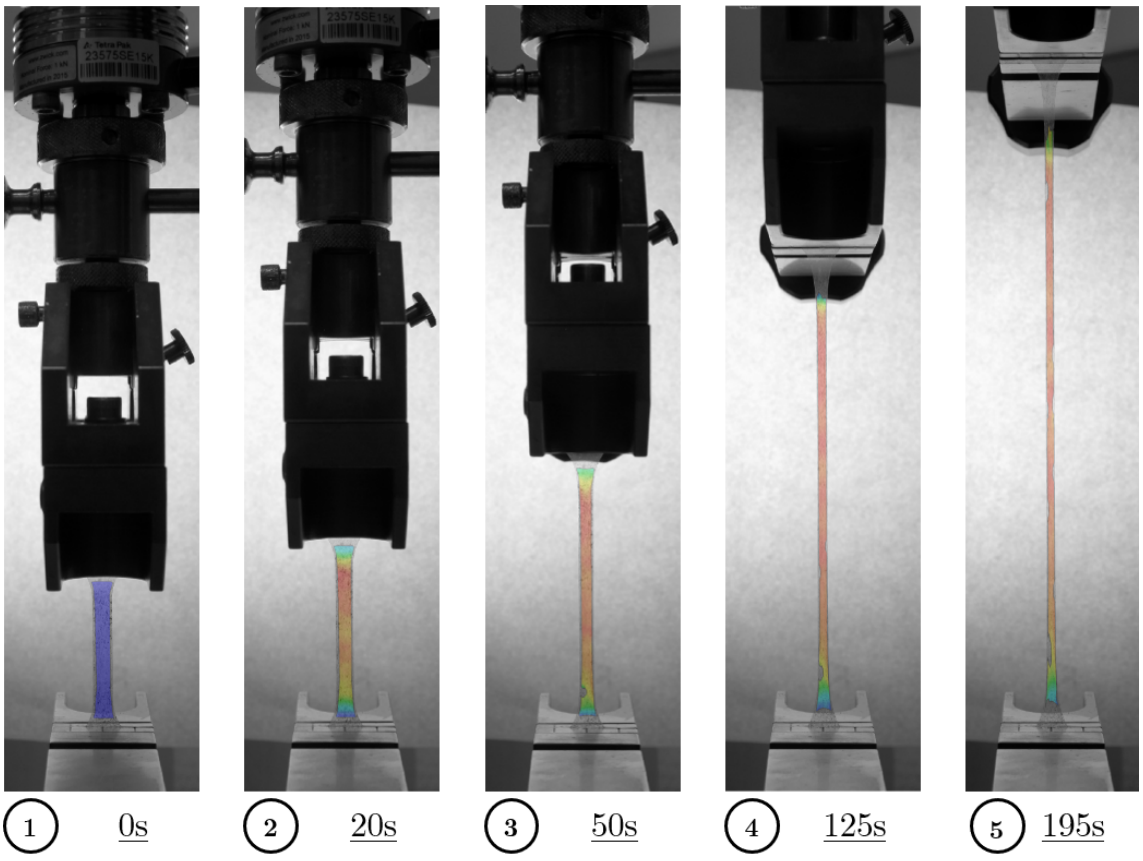

Figure 4.28: *The strain distribution of a LDPE test specimen in machine direction at 0, 20, 50, 125 and 195 sec with a displacement rate of 50 mm/min. (MD)*

Figure 4.29 shows images of DIC measurement in CD direction and the images are taken at 0, 20, 50, 125 and 373 seconds. The cross direction specimen elongated for a much longer time and strain than expected. Therefore, the entire elongated test was not included in the last image. During the tensile test the chalk powder used for DIC accuracy did not stay on the polymer but fell off and thus caused the DIC to not register for the two last images. This test clearly showed necking on the test specimen, it even occurred at several locations. At 20 seconds two necking strips were identified. One is found in the upper section as a red strip and the other in the bottom section as a green strip. After 50 seconds the specimen developed with three necking strips, the previous red strip developed into two necking strip.

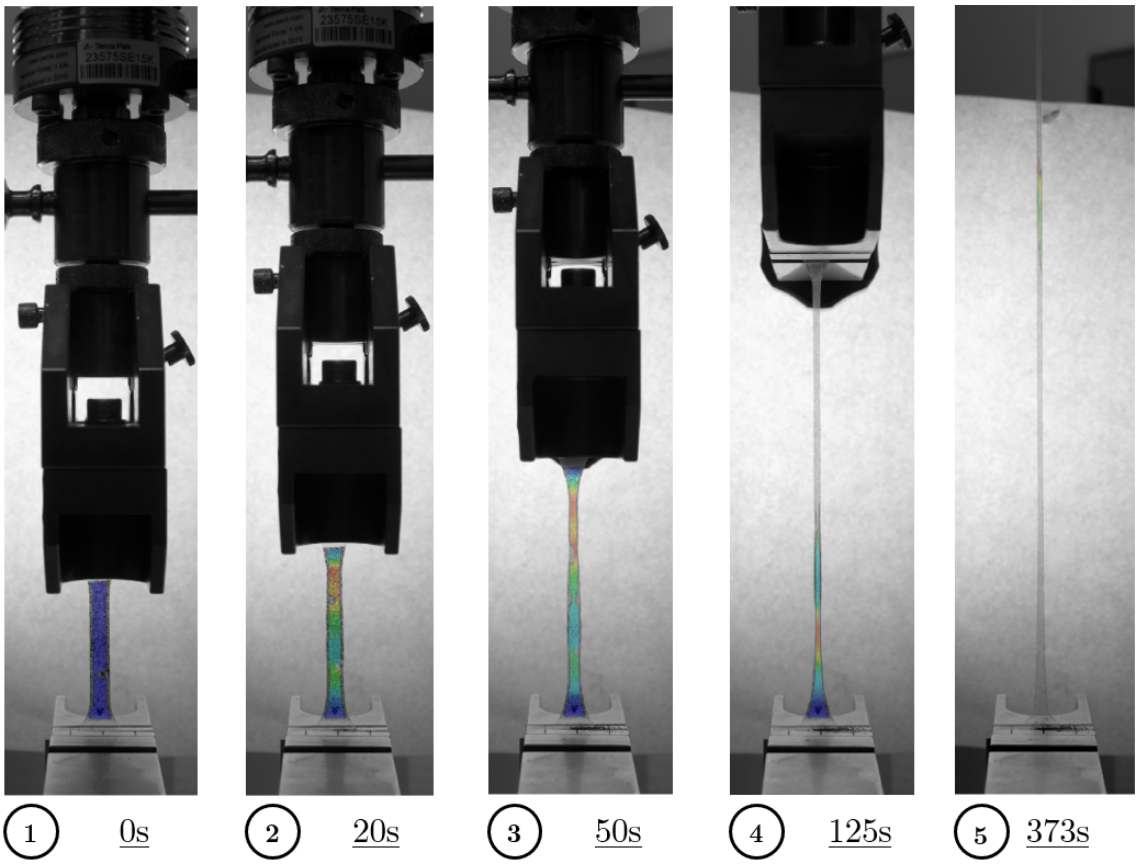

Figure 4.29: *The strain distribution of a LDPE test specimen in cross direction. The images are taken at 0, 20, 50, 125 and 373 sec with a displacement rate of 50 mm/min. (CD)*

DIC was also conducted on punched dry LDPE cut in 45 ° and the results are seen in Figure 4.30. The images are taken at 0, 20, 50, 125 and 345 seconds. This specimen also elongated to a longer strain compared to the results from machine direction but not as long as the tests from cross direction. This test also had difficulty with chalk powder and did not fully register the two last images. Observed from the results a necking strip is identified on the lower section of the test specimen at 20 and 50 seconds.

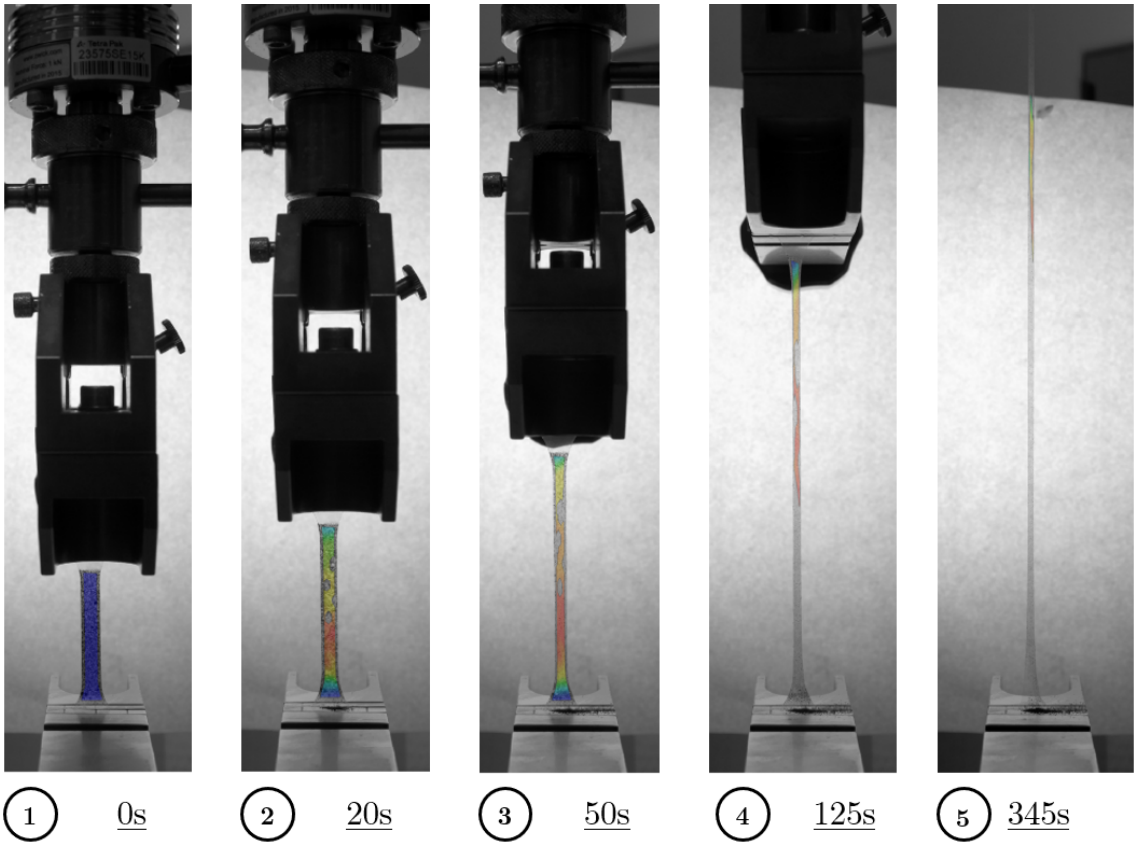

Figure 4.30: *The strain distribution of a LDPE test specimen in 45° direction. The images are taken at 0, 20, 50, 125 and 345 sec with a displacement rate of 50 mm/min. (45°)*

4.7 Scanning Electron Microscopy (SEM)

SEM images at different magnitude were taken with both dry LDPE samples and fractured tensile tested samples in MD and CD. The location where the SEM image was taken and zoomed in are also shown as red dotted circles and boxes.

Dry reference samples

First, from the SEM analysis, two images of dry MD LDPE reference sample were obtained. The first image, Figure 4.31a was captured from a magnitude of 400x and taken randomly on the edge of the sample. This reference sample had not been affected by any physical or chemical changes and therefore does not show anything unusual. An enhance image Figure 4.31b was then taken and it showed strips following the punched edge of the specimen.

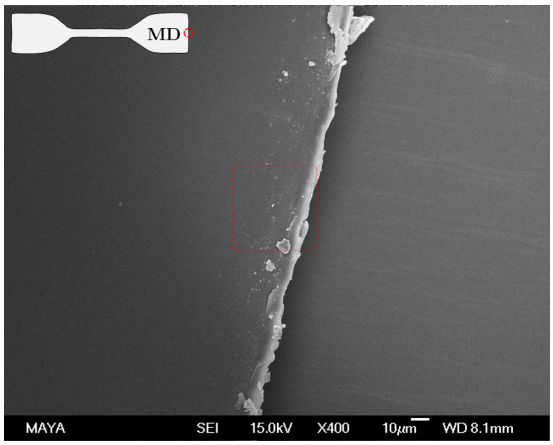

(a) SEM image of a dry reference sample at 400x magnitude.

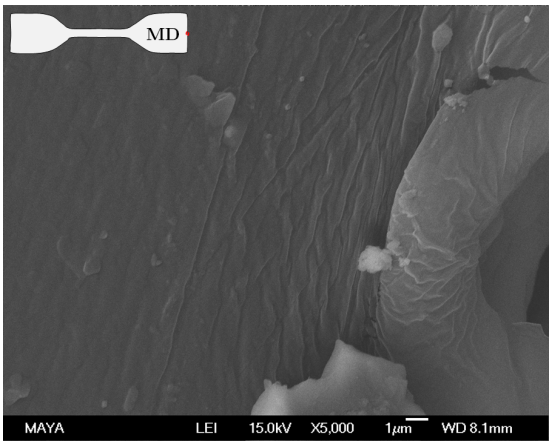

(b) SEM image of a dry reference sample at 5000x magnitude.

Figure 4.31: *SEM images of dry reference LDPE samples.*

Machine direction, tensile tested dry samples

Three SEM images were taken on a LDPE sample that was cut in machine direction and tensile tested at different magnitude levels. In the first Figure 4.32, an image was taken with a magnitude of 90x on an area where the fracture strip was broken from the tensile test. In this image we see that the strip has been broken inward twice in the machine direction.

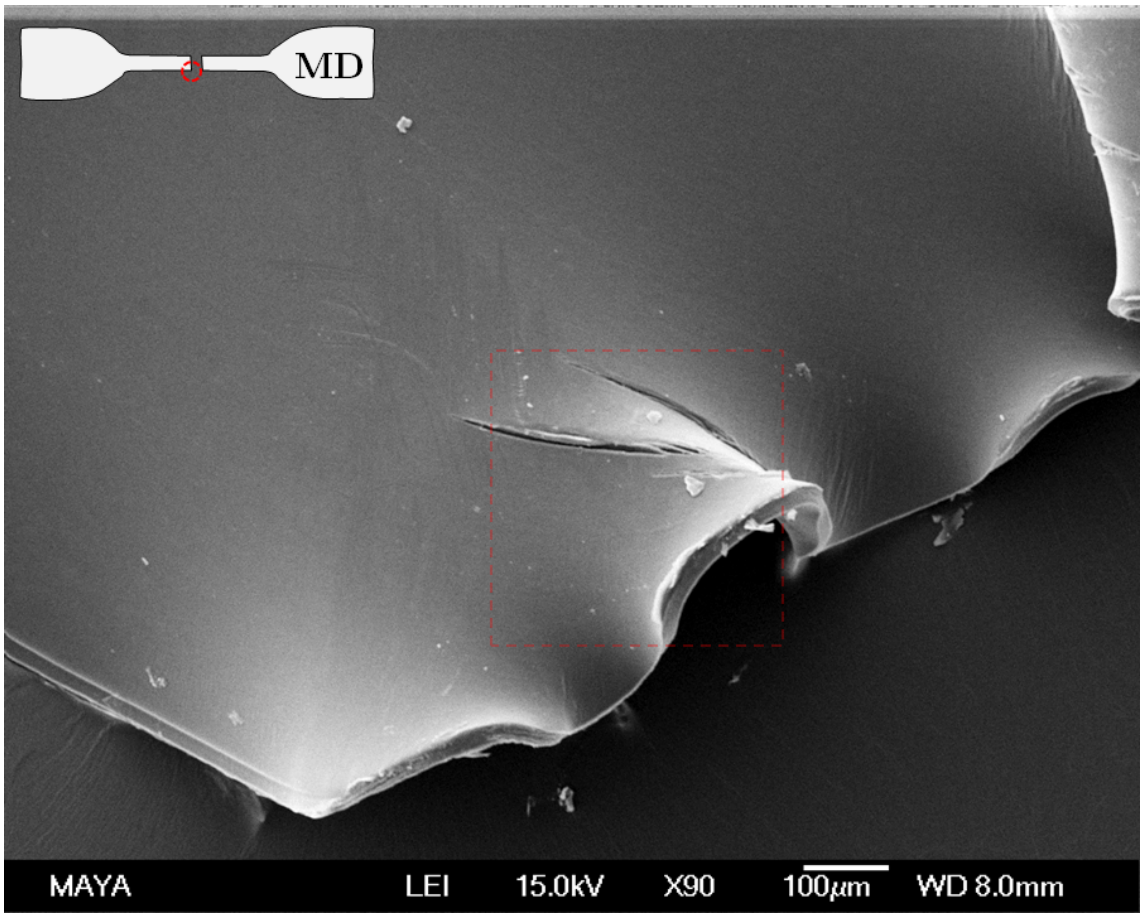

Figure 4.32: *SEM image of tensile tested MD sample at 90x magnitude.*

On the second image on Figure 4.33 we zoomed in and enhanced the area around the inward broken strip at a magnitude of 400x. Examining the broken strip revealed fibre or threadlike structure where the separation occurred.

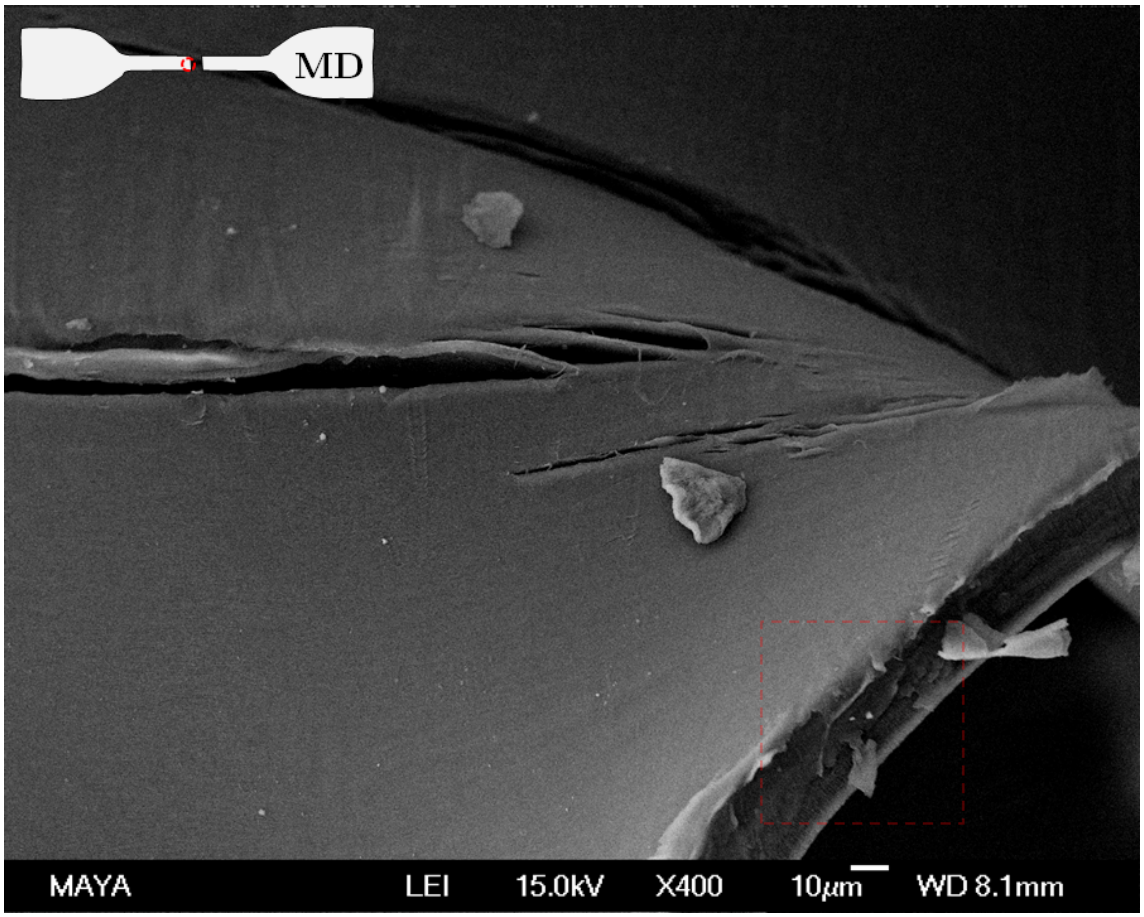

Figure 4.33: *SEM image of a tensile tested MD sample at 400x magnitude.*

One last image of the edge was also obtained as depicted in Figure 4.34 at a enhanced magnitude of 1500x. Different layers are observed as well as small hanging strip of polymer from the fracture.

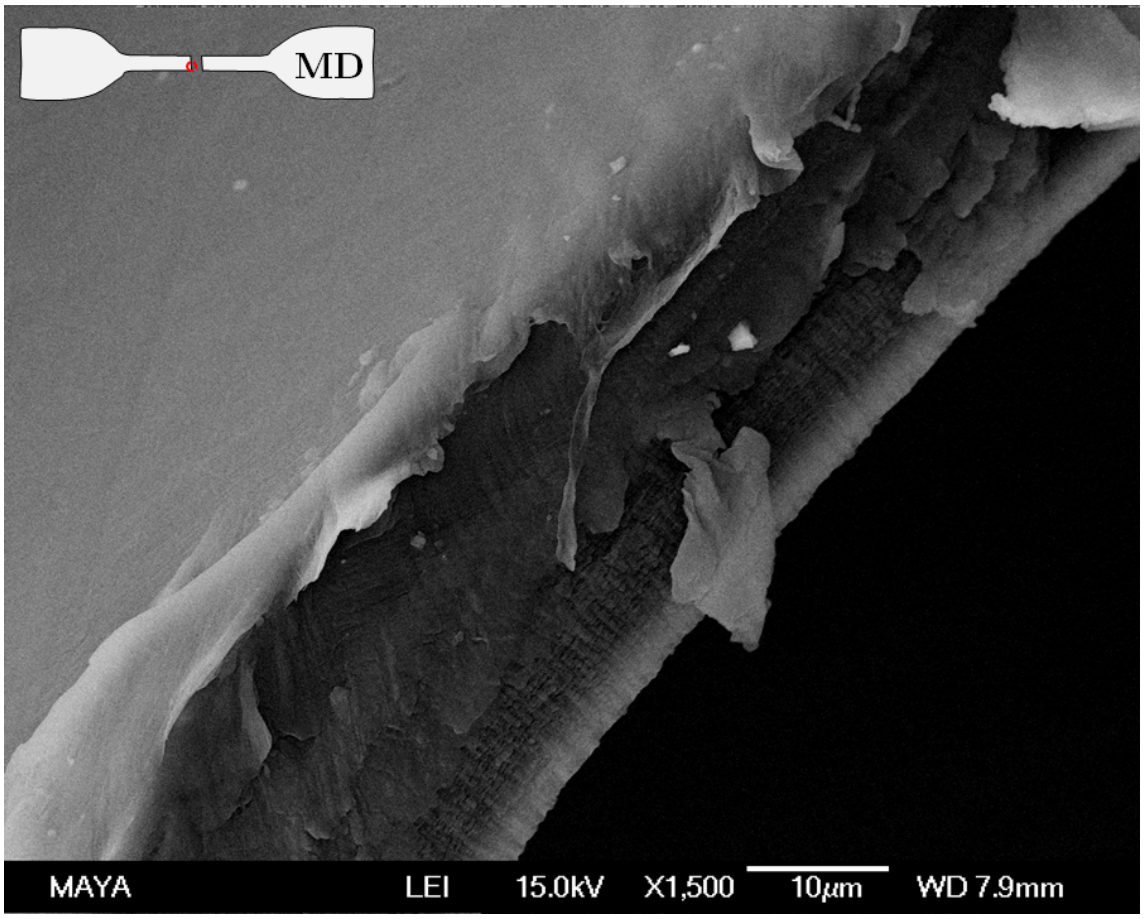

Figure 4.34: *SEM image of a tensile tested MD sample at 1500x magnitude.*

Cross direction, tensile tested dry samples

Two images were also captured on a dry LDPE sample tensile tested in cross direction. From the first Figure 4.35 we zoomed in on the fractured strip where the polymer was broken at a magnitude of 90x, it is similar to the fracture strip from MD displayed in Figure 4.32. However, the CD tensile tested specimen does not display any broken strips that appeared from the MD tensile tested sample.

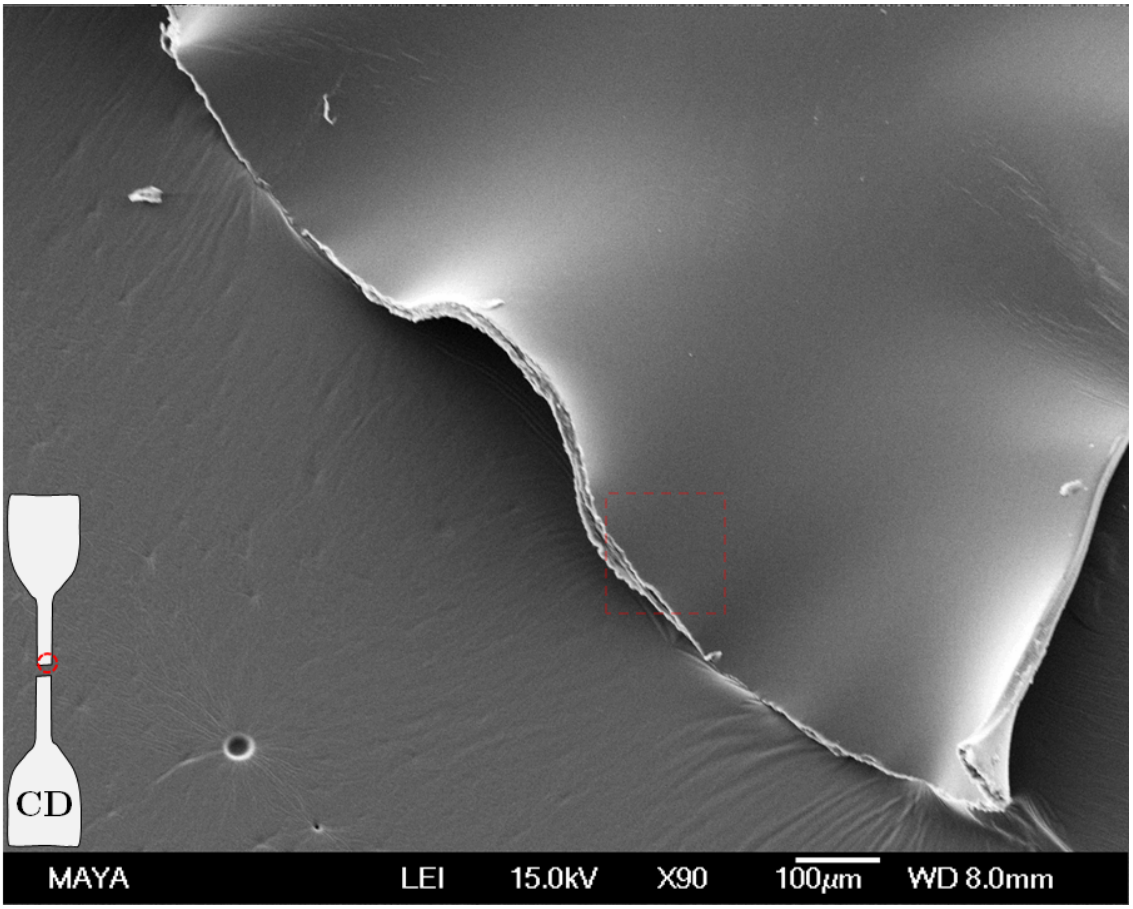

Figure 4.35: *SEM image of a tensile tested CD sample at 90x magnitude.*

One enhanced image was taken on the edge where the polymer was fractured. With a magnitude of 1500x we are able to see from figure 4.36 that the edge was not as flat and structured like the equivalent picture for MD on figure 4.34.

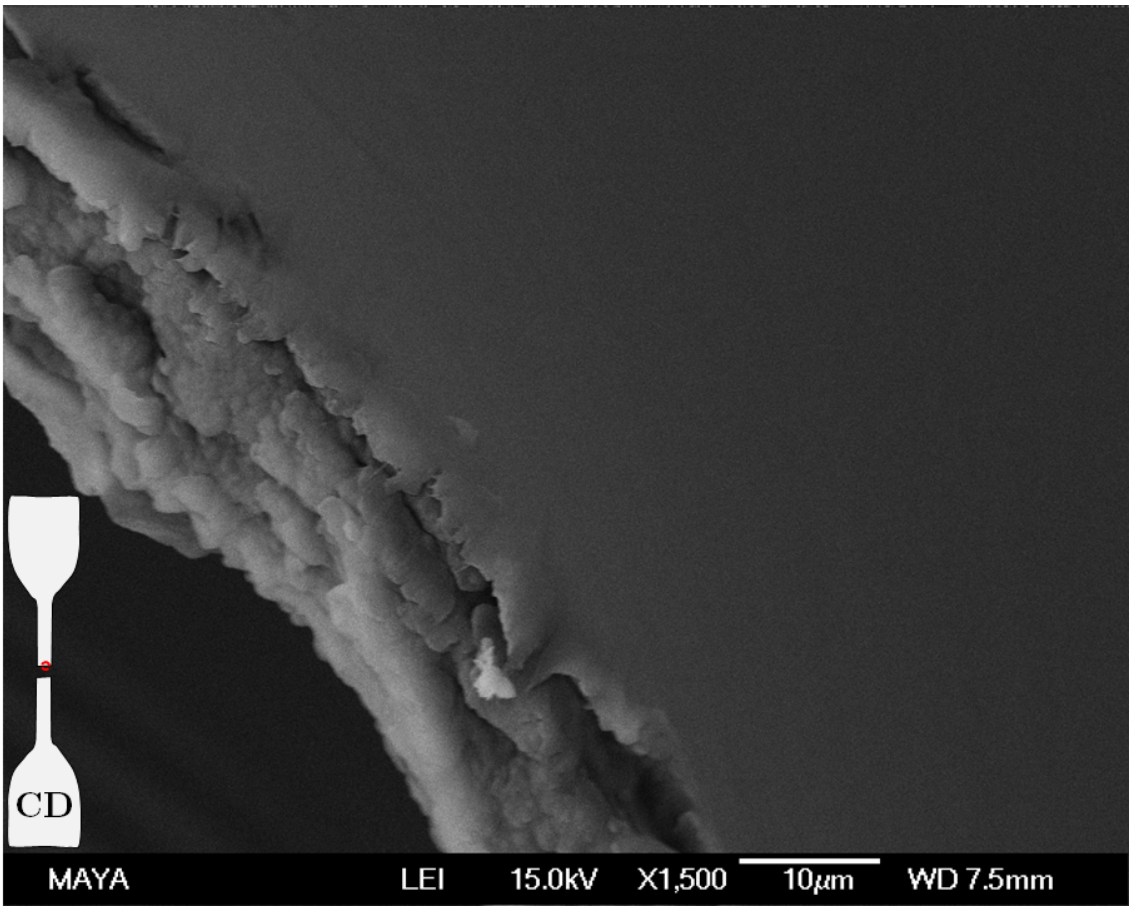

Figure 4.36: *SEM image of a tensile tested CD sample at 1500x magnitude.*

4.8 Thermogravimetric Analysis (TGA)

The reason we conducted the Thermogravimetric Analysis was to find the thermal degradation range of LDPE and it is identified in figure 4.37. On the upper left line is the percentage of polymer that is left in the aluminium pan after temperature increase. Following this line, a sharp decrease in percentage of weight is observed at around the temperature range of 400 - 450 °C. This is described as the thermal degradation range for the experimented LDPE samples and this is well above the temperature range we need for using the DSC.

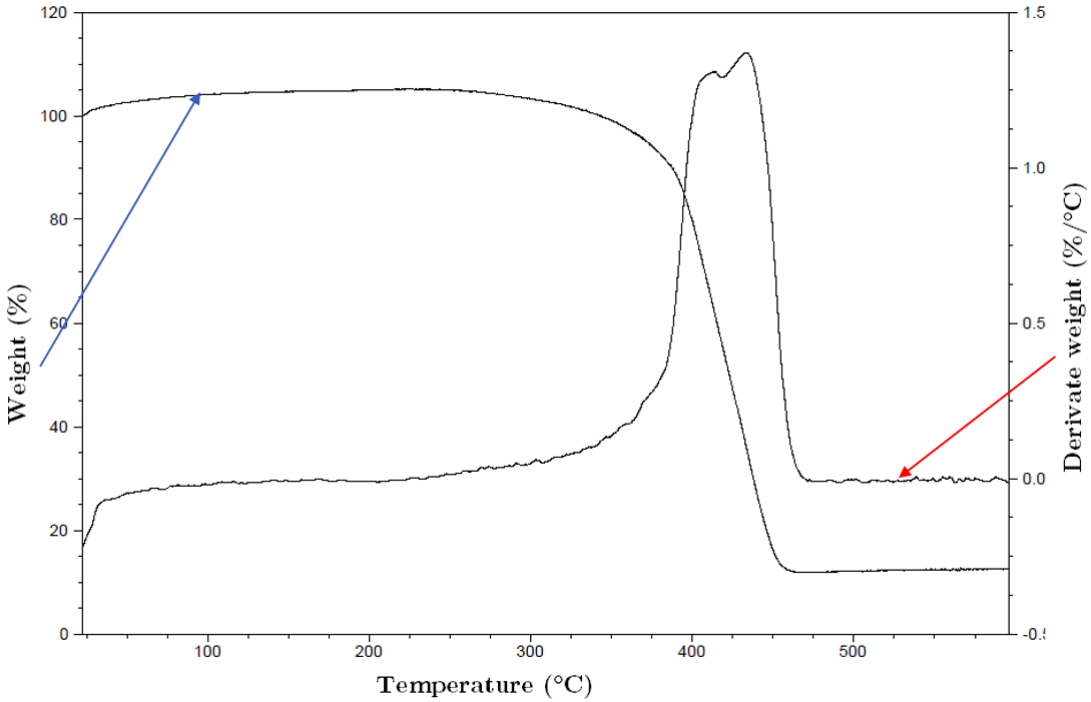

Figure 4.37: *TGA image of dry LDPE.*

Chapter 5

Discussion

This thesis uses many different techniques and in this section a discussion of the results from the different techniques are presented and how they may correlate with each other. Because of the difference in mechanical behaviour of MD, CD and 45° a conclusion at one direction must not be true in another direction.

5.1 Impact on Product Uptake

To further visualise the results on product uptake, the average weight difference from the three different products are plotted and depicted in Figure 5.1. Both sunflower oil and orange juice shows an steady increase in average weight. Sunflower oil shows a bit higher average increase at longer exposure time. This is expected as described in section 2.3, that the greater the similarity of chemical structure between the product and polymer, the more likely it is for swelling to occur and with a more observable effect. Therefore, sunflower oil as product for polymer samples should result in greater swelling than with water as sunflower oil is more chemically similar to organic materials such as polymers. The results for water seems to vary around the initial reference weight, which is expected as LDPE should have good moisture resistance and it is more chemical different than water. Orange juice is more chemical similar to water but consist of other chemicals that could affect the weight, such as the observable and difficult to remove unknown layer that was stuck to the test sample surfaces. However, the results in this time interval are not significant enough to make any concrete conclusion on the impact on product uptake. For the future it would be interesting to observe the product uptake at longer exposure time, when the product uptake has time to stabilise and saturated the whole test samples instead of steadily increasing in weight.

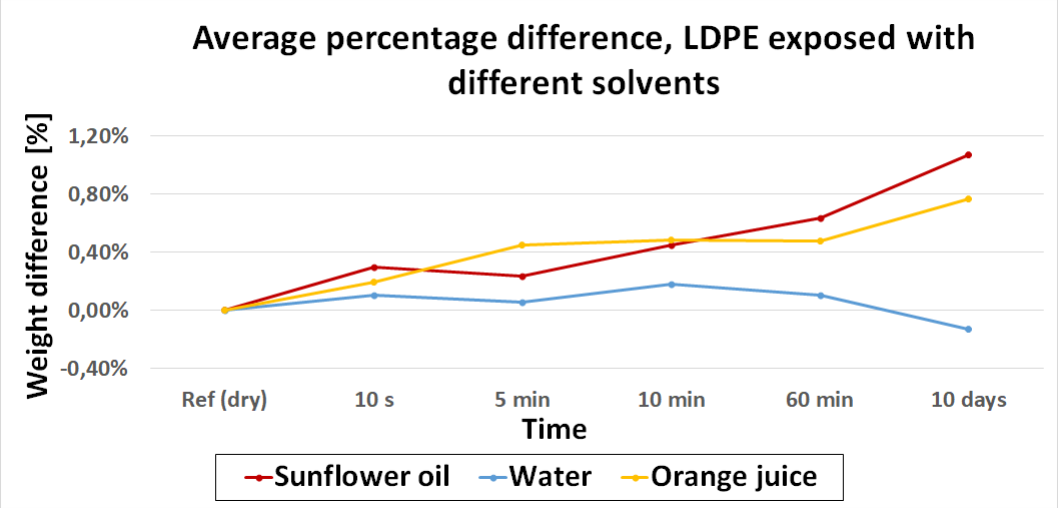

Figure 5.1: *Percentage weight difference between the three products at different exposure time.*

5.2 Thickness

Figure 5.2 shows the 3D simulation of thickness measurement at the level of the polymer film in cross direction. The split in thickness is even more clear and the thickness varies greatly between 47 and 54 mm.

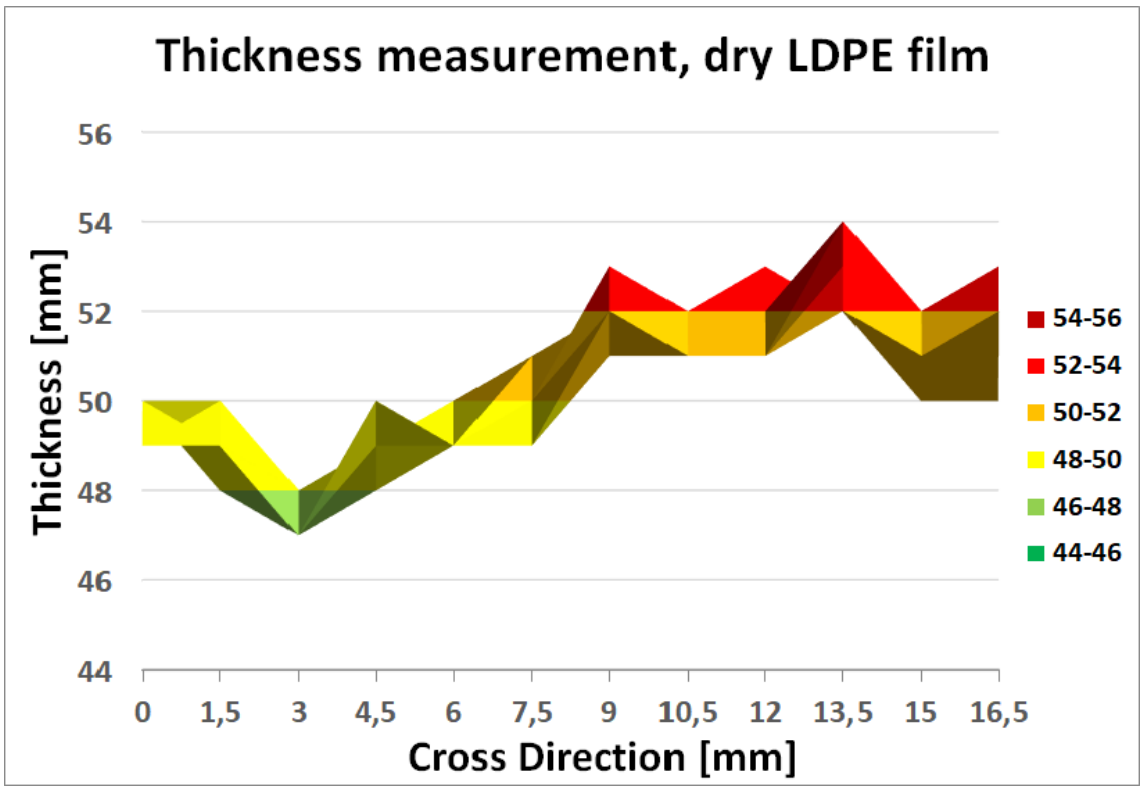

Figure 5.2: *3D-thickness map of one segment of polymer in CD at the same level as the specimen. (A)*

Figure 5.3 shows the thickness at the same level of the specimen and the thickness varies the same as previous test, between 47 - 54.

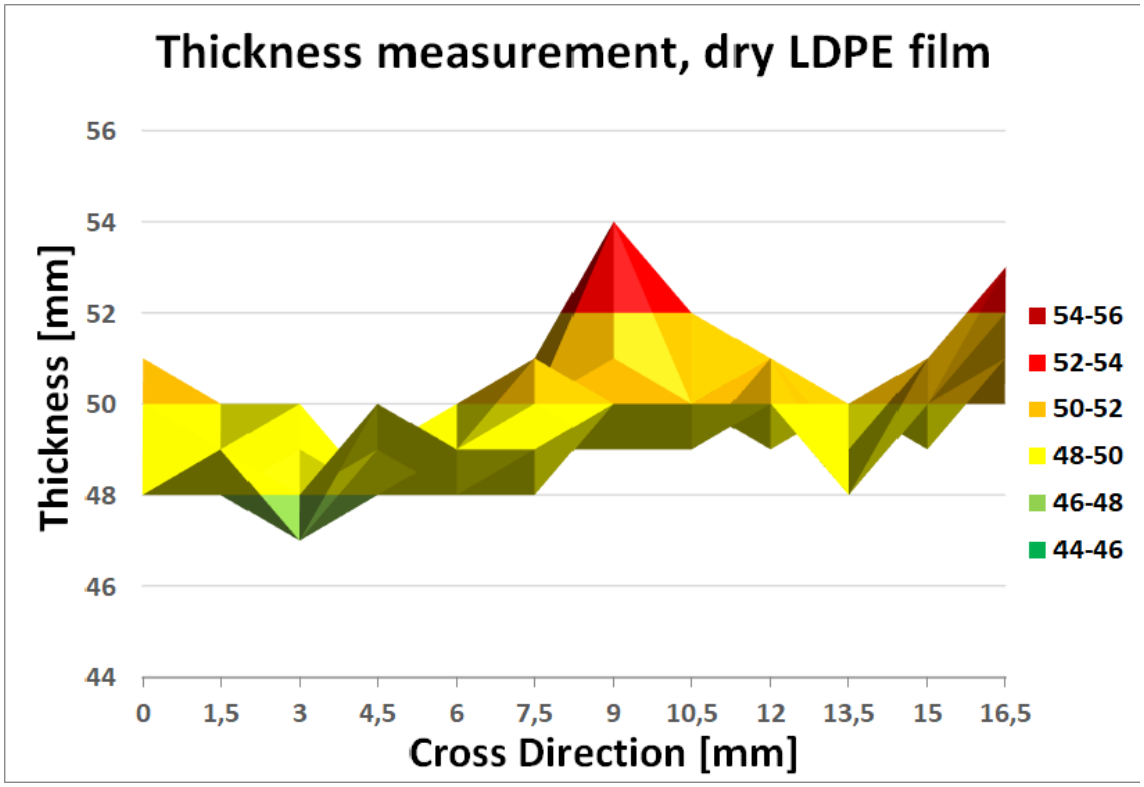

Figure 5.3: *3D-thickness map of one segment of polymer in CD at the same level as the specimen. (B)*

The thickness difference appear even more clearly in Figure 5.4. The thickness also varies between 47 - 54 mm, same as the previous tests.

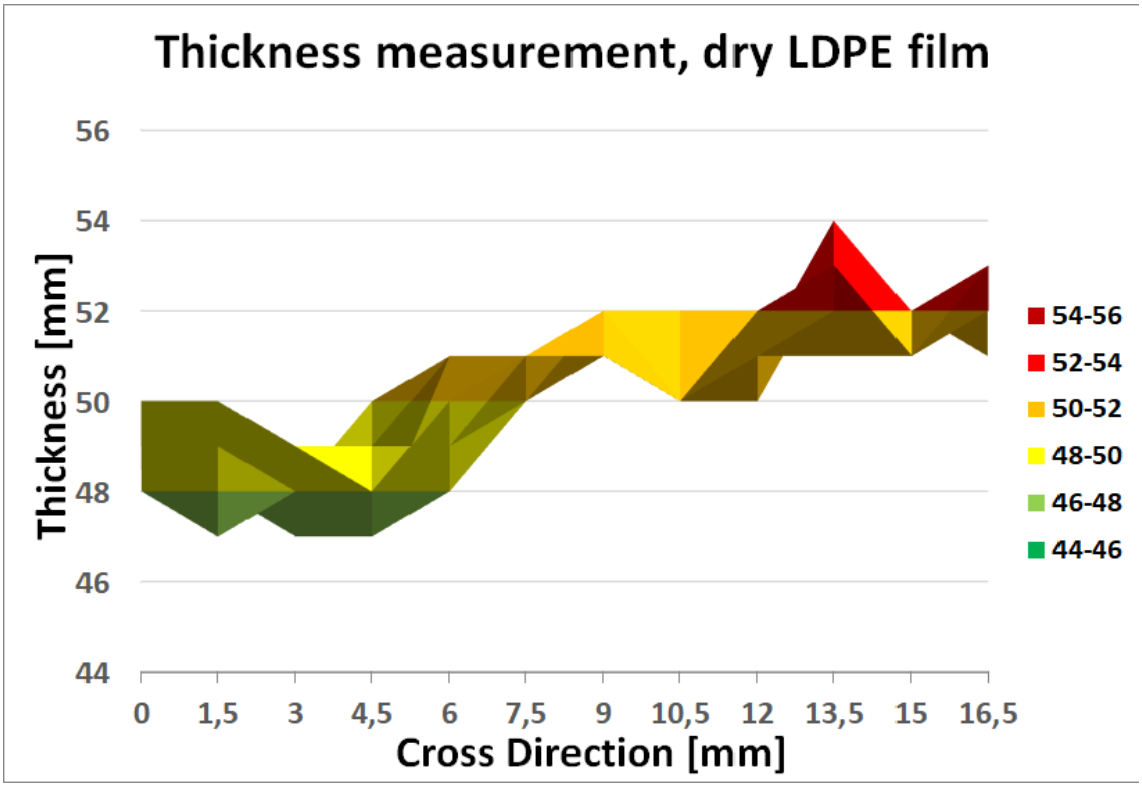

Figure 5.4: *3D-thickness map of one segment of polymer in CD at the same level as the specimen. (C)*

The thickness measurement showed interesting results, it is possible to see the difference in thickness throughout all three tested LDPE blown films. The polymer film was divided into two sections, a thinner and a thicker segment. It also appeared that the same thickness variation is maintained through all three blown films. The test samples were not punched out with the different thickness variations in mind. Therefore, several experimental methods conducted in this thesis such as the tensile test and product uptake may receive big error margins because of the thickness variations.

5.3 Mechanical Properties

The impact on mechanical properties is explained by comparing the results from tensile tests with different products and with the addition of DIC. The visual appearance, stress & strain curves and local strain deformation are compared to each other. These are presented in figures below with LDPE samples tested in MD, CD and 45°.

Average curves of dry reference and exposed to products for both the first batch and the second batch, LDPE in machine direction, is visualised in Figure 5.5. The results are not so big as most of the results elongate to around 300%. The dry reference samples generally have a longer elongation than the exposed samples, especially for the first batch of dry reference, which have a longer average elonga-

tion than the other samples with a strain at around 330%. However, it is difficult to identify any clear behaviour between the samples with the different products. Water is not expected to affect the properties of the polymer as they are chemically different as depicted in section 2.3, but in all tests with sunflower oil water and orange juice, a lower load are obtained on average compared to the reference samples. However, the difference is not large and a conclusion from the results is difficult to do within this time frame. For future testing, exposure to products should be performed for a longer time.

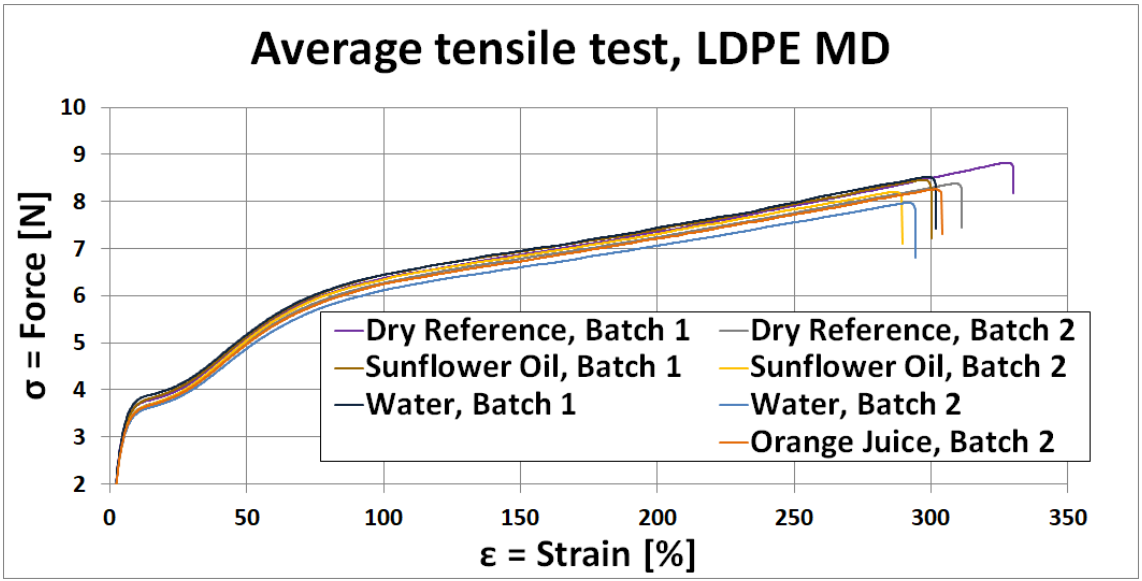

Figure 5.5: *Average tensile test results of dry reference samples and sunflower oil, water and orange juice exposed LDPE test samples exposed for 1h, punched in machine direction.*

Additionally, from Figure 5.6 we have compared the results from both tensile test and DIC in MD and here we observe that after the strong initial increase in strength and then the curve follows a stable increase in stress at increased strain until fracture. The DIC also reflect this behaviour with a homogeneous local strain on the entire test specimen throughout the experiment without any identifiable necking.

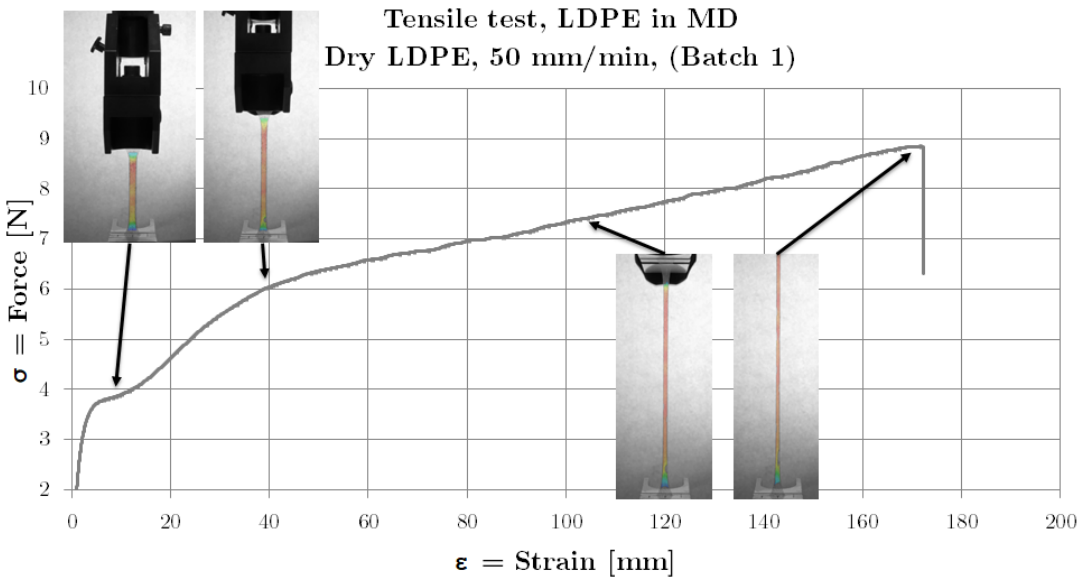

Figure 5.6: *Comparison between tensile test and DIC for a test specimen in MD.*

Figure 5.7 shows the comparison of a CD punched specimen. In the CD test after the initial increase in stress, the CD specimen follow an decrease in stress and then a slow increase in stress until fracture. The reason for the decrease in stress is possibly explained visually with the DIC measurement. Because, the specimen punched in CD develop several necking strips when stress is initially applied, whilst the specimen punched in MD does not show any necking at all. Therefore, the decrease in stress is an indicator on that necking are occurring on the test specimen. The maximum stress level for CD specimen is not as high like in the MD test and the explanation for this behaviour could be that the CD specimen is able to elongate to a much longer strain before fracture. The stress & strain curve is also more irregular and crooked than for the MD test. The reason for this is unclear but as the blown film polymer microstructures are not most align and oriented perpendicular to the process flow, it could cause the visual choppiness of the curves.

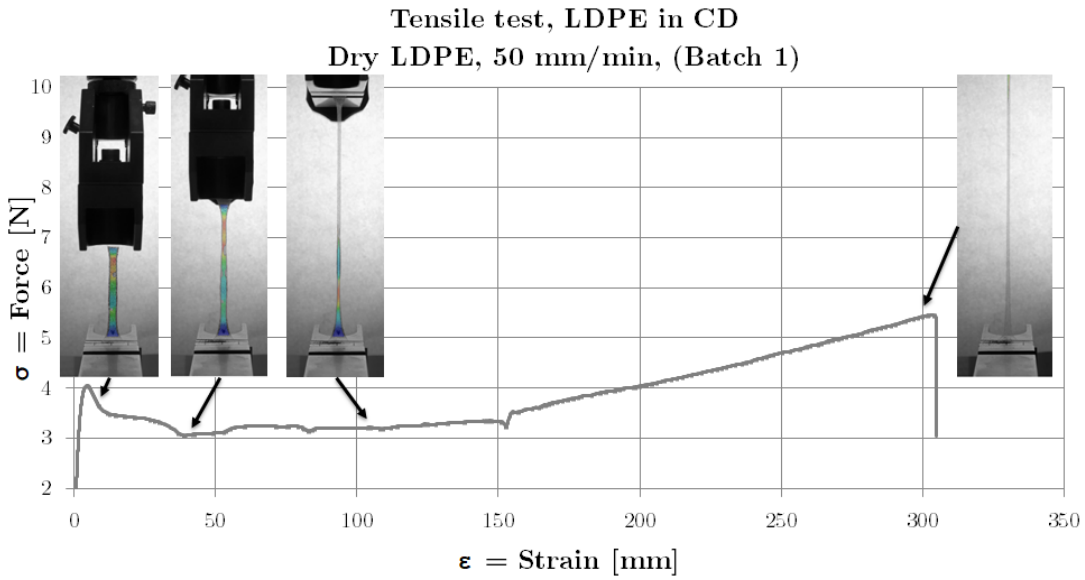

Figure 5.7: *Comparison between tensile test and DIC for a test specimen in CD.*

A comparison was also made on a test specimen in 45 ° as seen in Figure 5.8 The stress & strain curve is displayed as a mix between MD and CD. The curve exhibit high stress like in MD but it is also displaying high elongation similar to CD. This is apparent on the DIC images as only one large necking strip is identified.

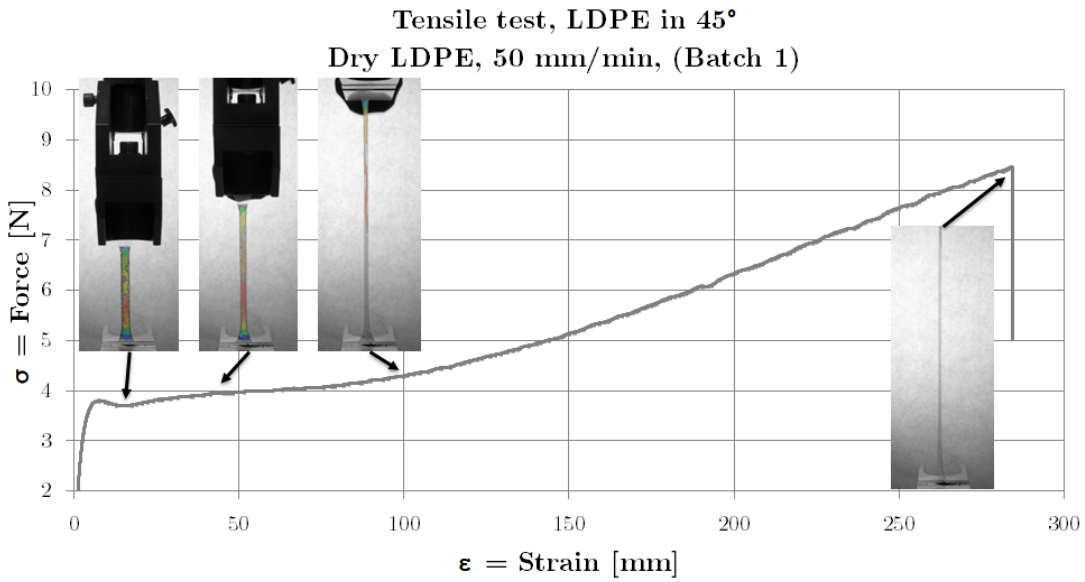

Figure 5.8: *Comparison between tensile test and DIC for a test specimen in 45°.*

LDPE samples processed from blown-film in machine direction are on average stronger than in cross direction. The possible reason for this difference in strength is that the microstructures in the polymer are more align and oriented in the process flow or machine direction, making it stronger but unable to elongate as much than compared to the test samples in cross direction. Tensile tests with different products did not show any significant difference, but as the test samples were only exposed to products for an hour, it is difficult to make a conclusion on the subject.

5.4 Impact on crystallinity

From the product uptake experiment, we have seen that the polymer absorbs the product and therefore we want to investigate if the crystallisation degree is changed. We expect the product to be absorbed in the amorphous parts as described in Figure 2.9. For this thesis two experimental methods have been used to obtain the information on crystallinity and these methods were WAXS and DSC.

WAXS gave an approximate value of percent crystallinity because we were unable to use the associated crystallinity calculation software method and instead have to manually integrate the areas. The results showed little visual difference between all the experimented tests and looking at the obtained data, all samples also got an approximate crystallinity of around 37%. Conclusively, these results tell us that the WAXS technique did not detect any difference or changes in the polymer structure or in the unit cells after exposure with products.

For DSC we want to compare crystallinity from the reference samples with the exposed samples. From the result we can only observe a little difference between reference and exposed samples from the first heating cycle. The reference samples have a crystallinity between 35-37% and samples exposed to sunflower oil, water and orange juice have a similar crystallinity between 33-38%.

From the results of both experimental methods, it is difficult to see any big effect on the crystallinity after exposure of the tested products. For the future it may be interesting to use a more chemically aggressive product or look into other length scale like in the semi-crystalline length scale with SAXS as shown in Figure 2.2.

5.5 SEM on Deformed Samples

SEM was used to further investigate fracture behaviour of blown film extrusion polymers. The images of tensile tested specimen in MD, showed threadlike appearances in the machine direction while the tensile tested specimen in CD instead showed a more clean fracture surface. The threaded strips in the MD sample is believed to be because of the high strength of the MD specimen, which may create a stronger force at fracture.

The specimen in MD also exhibited oriented and structured layers at the edge. Whilst the CD also exhibited layers at the edge, though they were not as oriented and structured compared to the MD specimen. A possible explanation for this could be described from the stress and strain curves. In the process flow or machine direction the polymer layers are believed to be more aligned and oriented which makes the polymer stronger. The specimen in MD does not strain and deform as much as in a CD specimen, resulting in that the edge of the fracture looking more structured and oriented. While, the polymer specimen in CD strain and deform to a longer distance, the layers will look more disoriented and unorganised at fracture.

Chapter 6

Conclusions

In this dissertation, product and polymer interaction have been studied using various experimental techniques and has demonstrated the possibility of combining multiple methods to investigate the chemical, mechanical and physical properties of a blown film extruded polymer.

- From the product uptake test, it was shown that polymers increased by weight with exposure time when subjected to both sunflower oil and orange juice while the polymer exposed to water showed no large impact. However, the test did not last long enough for the curves to stabilise and saturated the whole test samples to be able to assess a conclusion.
- We have shown that the product absorbs into the polymer. From WAXS we have not seen any big change in crystallinity. We can therefore assume that the product absorption occurs in amorphous region. It would be interesting for the future to observe the effect and impact at other length scale, such as the semi-crystalline region with SAXS.
- Furthermore, the thickness measurement showed significant thickness variation in the supplied polymer film sheets. It turned out that the thickness varies greatly with the material orientation and where on the blanket the samples are punched. In addition, the tensile tests showed very scattered results and this is believed to be due to the thickness variation in the punched test samples.
- The samples stamped from MD and CD behaved differently on both the tensile tests and the SEM experiment. MD showed high strength but low elongation while CD showed the opposite with very high elongation but low strength of the test specimen. 45° showed a result between both MD and CD with both a high elongation and strength.
- Finally, DIC made it possible to relate stress and strain curve with both the local displacement and the visual appearance of the test and could be a interesting addition to future tests.

Chapter 7

Future Work

This thesis has shown several experimental setup, method and strategy. There are further possibilities to continue the work in this thesis, by studying more specimen, different polymers, longer exposure time or more settings such as temperature or just use the knowledge in this thesis for other applications.

- **Use SAXS to investigate product interactions at semi-crystalline length scale.** This work has shown that the unit cell size is not affected by product absorption (e.g. 1% uptake of sunflower oil). Therefore, for the future it would be interesting to look into the larger length scale by using SAXS.
- **Perform tensile test and other experiments on exposed samples at longer time.** We were not able to perform enough tensile test on samples exposed to a longer time than 1 hour. Therefore to continue with this thesis in the future, it would be useful to do more regular measurements and better allocate the time between samples. It would also be interesting for the product uptake measurement to measure the uptake at even longer time than ten days to see when the sample is saturated and unable to absorb more product.
- **Improve the test setup for exposure of products.** Because of practical difficulties such as limited space and limited time, it was difficult to expose many samples at the same time. Ideally, it would be best to find glass containers that are a bit smaller but longer so that more samples can fit and it will be easier to work with the test samples. Additionally, in this thesis the test samples are exposed on both sides, while in reality only one side of the polymer is exposed to the product. One solution would be to expose an entire side of polymer film or sheet into the product and then pick it up and punch out test samples.
- **Reduce thickness variation in the test samples.** The thickness variation from suppliers and different batches is hard to eliminate but it is possible to reduce the thickness variation of the test samples by measuring the thickness of the polymer film and punched samples and sort them accordingly. Because the thickness variation was predictable in the machine direction, it is ideal to punch the samples alongside the variation.

Appendix

Raw Data

	Sunflower Oil			Water			Orange Juice		
	Ref (dry)	Exposed	Diff	Ref (dry)	Exposed	Diff	Ref (dry)	Exposed	Diff
10 s	93,2	93,3	0,1	92,7	92,9	0,2	90,8	90,9	0,1
	92,3	92,6	0,3	94,8	94,9	0,1	88,6	88,8	0,2
	93,0	93,2	0,2	93,1	93,2	0,1	91,7	91,9	0,2
	89,9	90,4	0,5	90,0	90,0	0,0	89,4	89,6	0,2
5 min	95,1	95,3	0,2	96,3	96,3	0,0	92,2	92,5	0,3
	97,0	97,2	0,2	94,9	94,8	-0,1	89,8	90,3	0,5
	92,6	93,0	0,4	92,7	92,7	0,0	89,0	89,4	0,4
	93,1	93,2	0,1	93,2	93,5	0,3	87,2	87,6	0,4
10 min	96,2	96,7	0,5	93,9	94,0	0,1	86,1	86,6	0,5
	92,8	92,9	0,1	96,3	96,4	0,1	85,8	86,2	0,4
	93,7	94,2	0,5	95,2	95,4	0,2	89,7	90,1	0,4
	93,2	93,8	0,6	94,6	94,9	0,3	91,4	91,8	0,4
60 min	93,8	94,3	0,5	95,7	96,0	0,3	89,4	89,9	0,5
	93,9	94,6	0,7	92,0	92,0	0,0	87,2	87,6	0,4
	92,4	93,0	0,6	94,7	94,7	0,0	86,0	86,5	0,5
	95,6	96,2	0,6	94,8	94,9	0,1	93,3	93,6	0,3
10 days	93,7	94,8	1,1	95,6	95,4	-0,2	84,6	85,3	0,7
	91,2	92,2	1,0	92,7	92,7	0,0	91,1	91,7	0,6
	92,8	93,9	1,1	92,9	92,7	-0,2	87,6	88,5	0,9
	96,3	97,1	0,8	92,6	92,5	-0,1	88,9	89,4	0,5

Legend
0,8
0,6
0,4
0,2
0
-0,2
-0,4
-0,6
-0,8

Table 1: *Raw data of product uptake measurement.*

		Heating cycle 1		Cooling cycle		Heating cycle 2			
	Sample weight (mg)	Melt peak temp. Tm1(°C)	Melt enthalpy ΔHm1(J/g)	Crystallization peak temp. Tc(°C)	Crystallization enthalpy ΔHc (J/g)	Melt peak temp. Tm2(°C)	Melt enthalpy ΔHm2(J/g)	Crystallinity heat cycle 1 (%)	Crystallinity heat cycle 2 (%)
Pure LDPE, 0h	3,392	112,6	104,5	104,2	93,8	113,2	106,1	35,6	38,6
	2,516	111,9	103,8	104,3	93,1	113,2	106,4	35,4	38,5
	2,420	112,3	104,8	104,4	93,9	112,9	107,4	35,7	38,5
	2,704	111,7	107,4	104,4	95,4	113,0	109,1	36,6	38,5
Sunflower Oil, 1h	2,806	111,8	104,4	104,4	93,8	113,1	107,3	35,6	38,5
	3,072	112,8	101,7	104,0	89,1	113,5	101,9	34,6	38,6
	2,233	111,9	105,5	104,4	95,6	112,9	108,6	35,9	38,4
	2,277	112,2	101,7	104,1	92,3	113,2	105,3	34,6	38,5
Sunflower Oil, 10h	2,303	112,1	98,1	104,0	91,2	113,2	103,8	33,4	38,6
	2,343	111,9	100,6	104,2	91,6	113,2	104,3	34,3	38,5
	2,750	112,3	104,5	104,4	93,9	112,9	107,5	35,6	38,5
	3,002	112,6	103,7	104,3	95,2	113,1	109,0	35,3	38,5
Water, 1h	2,357	-	-	104,3	92,9	113,0	105,6		38,5
	2,491	112,6	100,2	104,2	90,7	113,2	103,5	34,1	38,6
	2,519	111,6	105,1	104,5	93,8	112,9	107,7	35,8	38,5
	2,913	112,3	104,4	104,1	92,3	113,3	106,4	35,6	38,6
Water, 10h	2,509	111,5	106,2	104,4	95,2	112,8	108,6	36,2	38,4
	2,556	111,9	106,9	104,3	94,7	112,9	108,0	36,4	38,5
	2,225	112,7	102,0	104,3	94,3	113,0	106,7	34,7	38,5
	2,739	111,8	106,0	104,4	94,9	112,9	108,6	36,1	38,5
Orange Juice, 1h	2,106	111,6	101,6	103,9	92,6	112,7	104,6	34,6	38,4
	2,832	-	-	-	-	-	-		-
	2,509	111,7	101,4	103,8	92,2	112,8	105,2	34,5	38,4
	2,503	-	-	103,9	95,3	112,7	108,4		38,4
Orange Juice, 10 days	2,202	111,2	104,0	103,9	94,1	112,5	106,8	35,4	38,3
	2,050	112,1	101,2	103,7	91,7	112,9	105,2	34,5	38,5
	2,809	111,6	103,4	103,8	92,0	112,7	105,3	35,2	38,4
	2,703	101,4	111,7	103,7	91,8	112,7	105,3	38,1	38,4

Table 2: *Raw data of DSC measurement.*

Average weight difference (%)							
Time	Sunflower oil	S.D 2σ	Water	S.D 2σ	Orange juice	S.D 2σ	Legend
Ref (dry)	0	0	0	0	0	0	0,00%
10 s	0,30%	0,38%	0,11%	0,18%	0,19%	0,11%	0,25%
5 min	0,24%	0,27%	0,05%	0,37%	0,45%	0,19%	0,50%
10 min	0,45%	0,47%	0,18%	0,20%	0,48%	0,13%	0,75%
60 min	0,64%	0,17%	0,10%	0,30%	0,48%	0,24%	1,00%
10 days	1,07%	0,33%	-0,13%	0,20%	0,77%	0,41%	

Table 3: *Raw data on the average weight difference between all samples from all products.*

Thickness measurement

← Cross direction →	0	2	4	6	8	10	12	14	16	18	20	22	Thick. (µm)
0	50	49	50	49	49	49	50	50	50	50	49	49	
1,5	49	50	50	50	49	49	49	48	48	49	49	49	
3	48	48	47	47	48	48	47	47	47	47	47	47	54
4,5	48	49	49	48	49	48	49	50	49	49	50	50	53
6	50	50	50	50	49	49	49	49	49	49	49	49	52
7,5	51	50	50	50	51	49	50	50	50	49	49	49	51
9	52	52	52	52	52	52	53	53	52	52	51	52	50
10,5	51	52	52	51	51	51	51	51	52	51	51	51	49
12	53	52	52	52	52	51	51	52	52	51	51	51	48
13,5	52	52	52	52	52	53	53	53	53	54	53	52	47
15	50	50	51	52	52	52	51	51	51	51	52	51	46
16,5	50	50	50	51	51	53	52	51	52	52	52	52	
	Machine direction →												

← Cross direction →	0	2	4	6	8	10	12	14	16	18	20	22	Thick. (µm)
0	49	49	50	50	51	50	50	49	48	49	48	48	
1,5	48	48	50	50	50	50	49	49	48	48	48	49	
3	48	48	48	49	47	49	50	49	47	47	48	47	54
4,5	48	48	49	49	48	48	48	48	48	49	49	50	53
6	49	50	49	49	49	48	49	49	49	48	48	49	52
7,5	51	50	51	50	50	51	51	50	49	48	49	49	51
9	53	53	54	51	50	50	50	49	49	50	50	50	50
10,5	50	52	51	50	50	50	50	49	49	49	49	50	49
12	51	50	50	49	51	50	50	50	51	50	50	50	48
13,5	50	50	50	50	49	49	50	49	48	48	49	48	47
15	50	50	50	49	50	50	51	50	50	50	51	51	46
16,5	50	50	51	51	51	52	52	52	52	53	53	53	
	Machine direction →												

← Cross direction →	0	2	4	6	8	10	12	14	16	18	20	22	Thick. (µm)
0	48	48	49	50	49	48	48	48	49	49	49	50	
1,5	49	49	47	48	48	48	47	47	49	49	49	50	
3	48	48	49	47	47	48	48	48	48	49	49	49	54
4,5	50	49	48	47	47	47	47	48	48	49	48	48	53
6	51	51	51	49	49	48	48	49	49	49	49	50	52
7,5	51	51	51	51	50	50	50	50	50	50	51	51	51
9	51	51	51	51	52	52	52	52	51	52	52	51	50
10,5	51	50	50	51	52	51	52	50	50	50	50	50	49
12	51	51	51	52	51	51	52	50	51	51	51	52	48
13,5	54	53	51	53	53	53	53	53	52	51	52	53	47
15	52	52	51	52	52	52	51	52	51	51	51	51	46
16,5	51	51	52	52	53	52	52	53	53	52	52	53	
	Machine direction →												

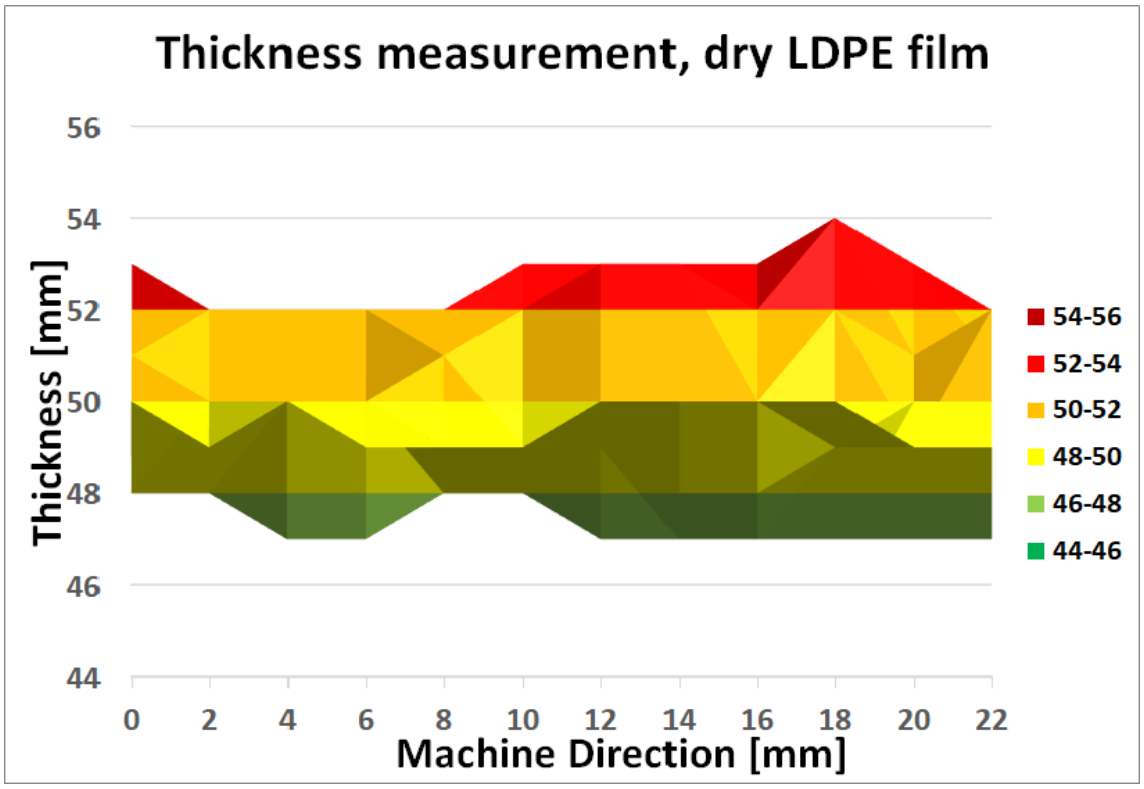
Thickness measurement, dry LDPE film
Thickness [mm]
56
54
52
50
48
46
44
0
2
4
6
8
10
12
14
16
18
20
22
Machine Direction [mm]
54-56
52-54
50-52
48-50
46-48
44-46

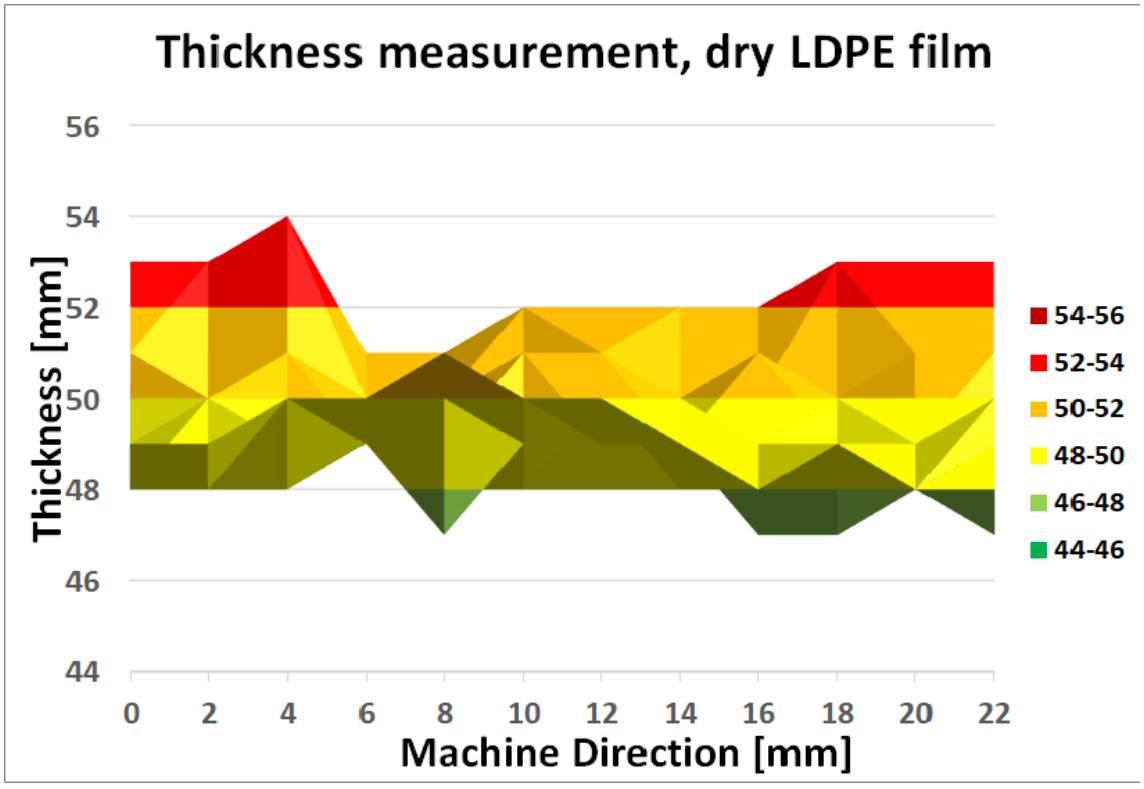
Thickness measurement, dry LDPE film
Thickness [mm]
56
54
52
50
48
46
44
0
2
4
6
8
10
12
14
16
18
20
22
Machine Direction [mm]
54-56
52-54
50-52
48-50
46-48
44-46

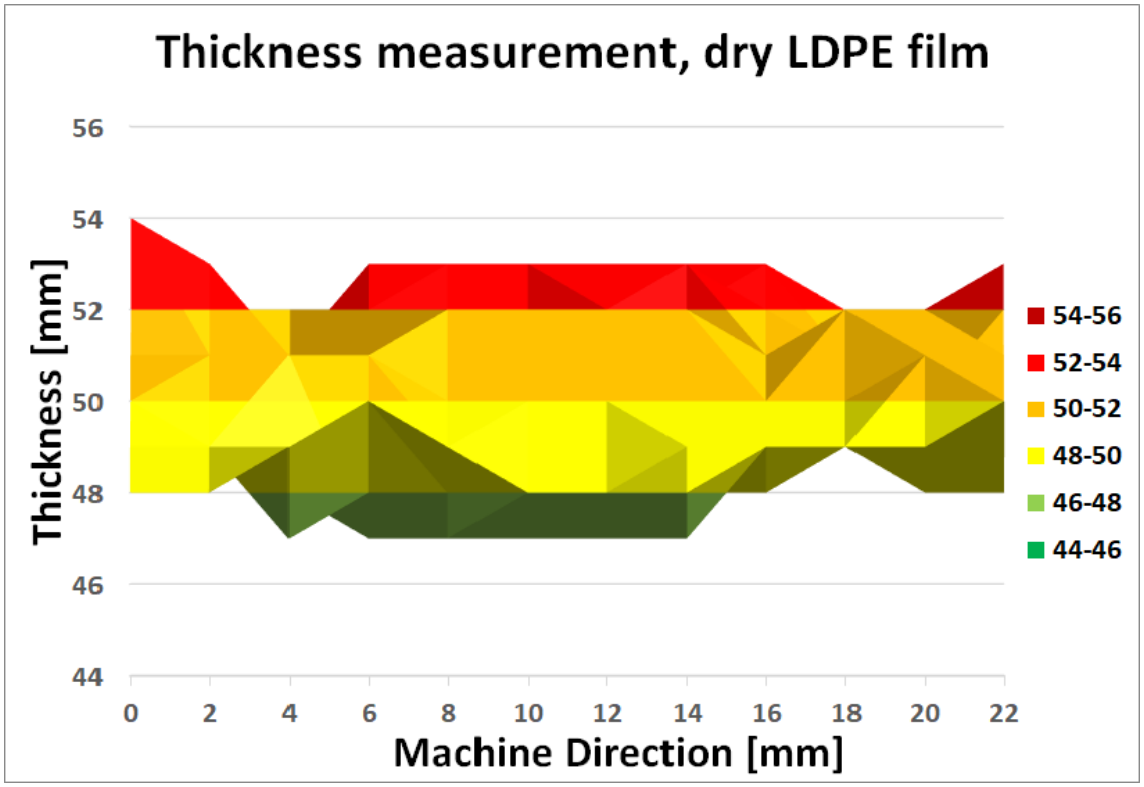
Thickness measurement, dry LDPE film
Thickness [mm]
56
54
52
50
48
46
44
0
2
4
6
8
10
12
14
16
18
20
22
Machine Direction [mm]
54-56
52-54
50-52
48-50
46-48
44-46

DIC

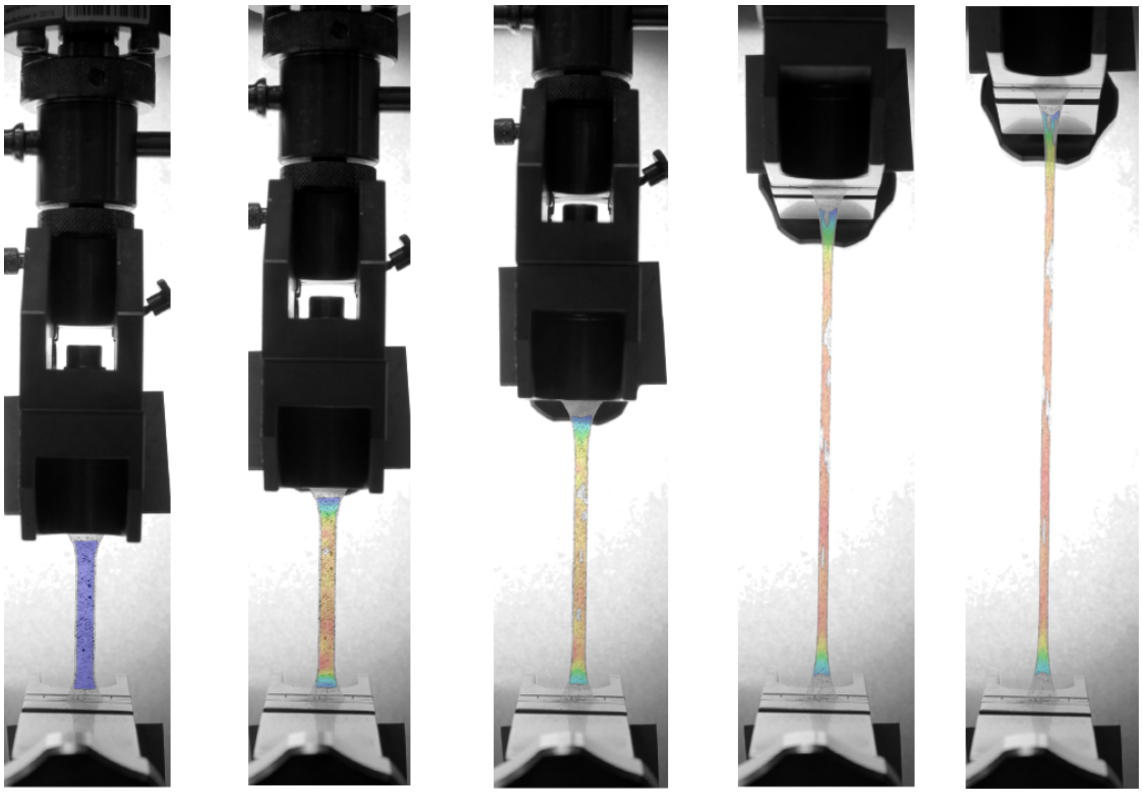
1 0s
2 20s
3 50s
4 125s
5 161s

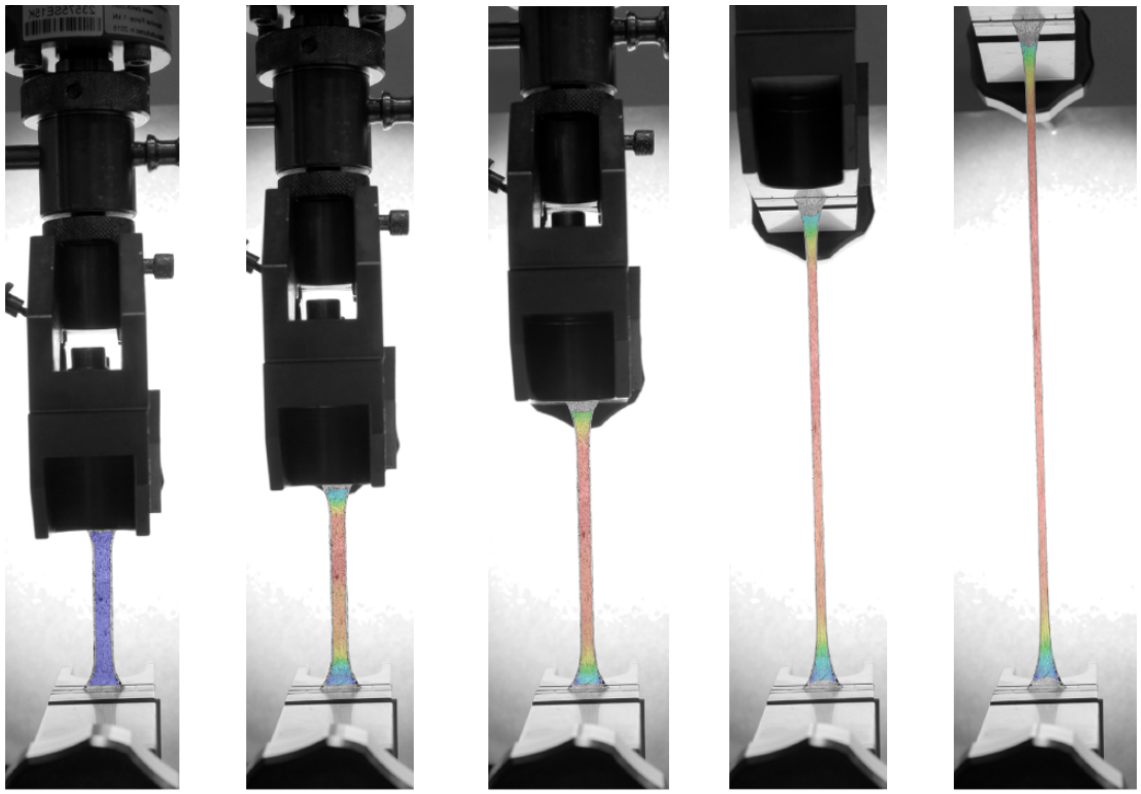

1 0s 2 20s 3 50s 4 125s 5 191s

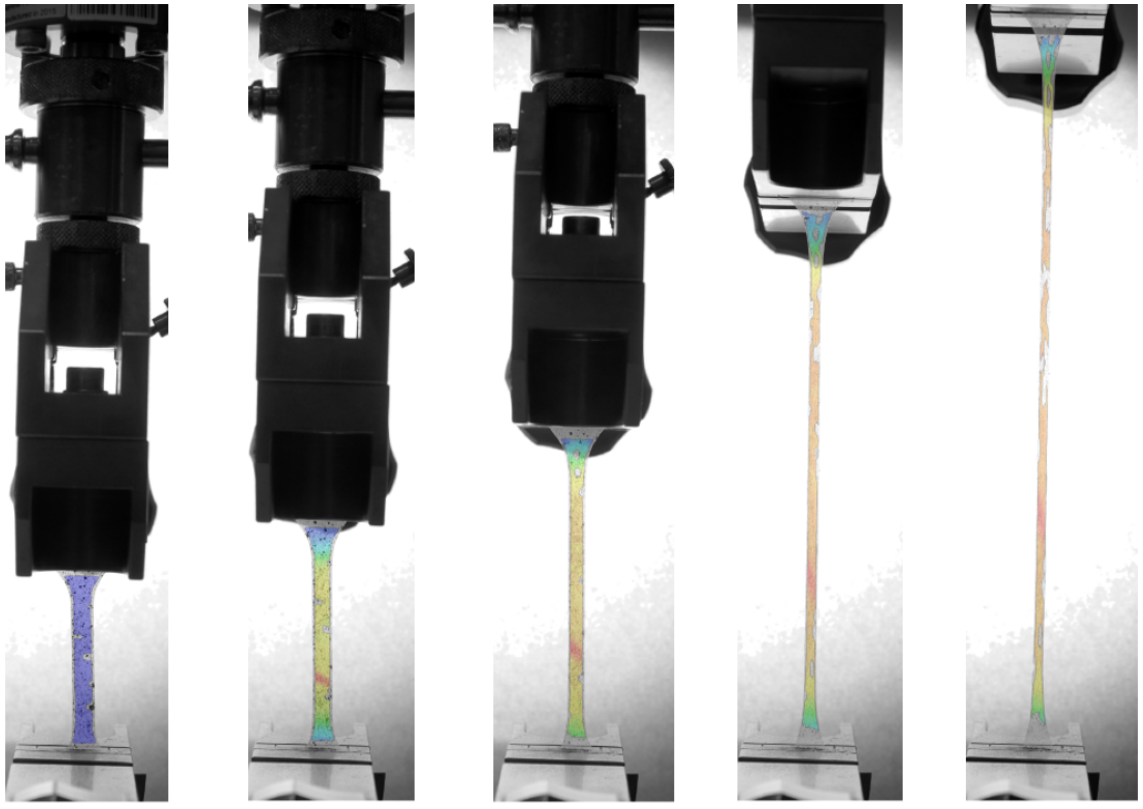

1 0s 2 20s 3 50s 4 125s 5 345s

Bragg's Peaks

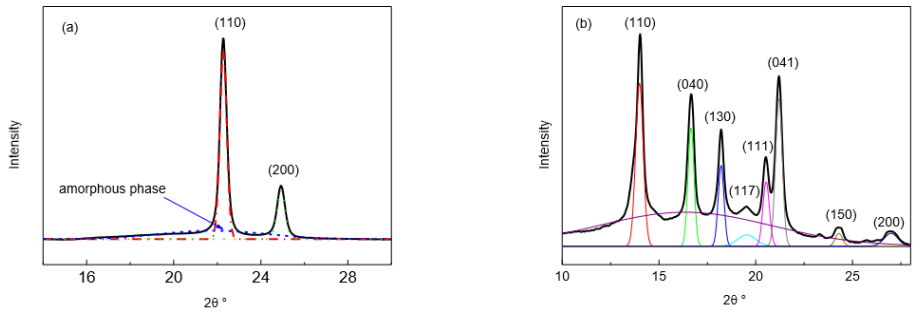

Figure 7. WAXS intensity profiles of (a) polyethylene and (b) polypropylene.

Figure 1: *Bragg's peaks of polyethylene and polypropylene.Xiong (2014)*

Bibliography

Alexander, Z. (2018), 'Unesco', https://www.imc.cas.cz/unescoiupac/lectures/scattering.pdf. (Accessed on 05/31/2018).

Bhadeshia, H. et al. (2018), 'Thermal2', https://www.phase-trans.msm.cam.ac.uk/2002/Thermal2.pdf. (Accessed on 09/25/2018).

Boldon, L. et al. (2015), 'Review of the fundamental theories behind small angle x-ray scattering, molecular dynamics simulations, and relevant integrated application', *Nano reviews* **6**(1), 25661.

Callister, W. & Rethwisch, D. (2011), *Materials science and engineering*, Vol. 5, John Wiley & Sons NY.

Claudionico (2015), 'Electron interaction with matter', https://upload.wikimedia.org/wikipedia/commons/4/49/Electron_Interaction_with_Matter.svg. (Accessed on 11/05/2018).

Elastocon (2018), 'Elastocon sample preparation', https://www.elastocon.com/images/pdf/product-brochures/elastocon-sample-preparation.pdf. (Accessed on 10/24/2018).

Encyclopædia Britannica, i. (2013), 'Adsorption, surface phenomenon', https://www.britannica.com/science/adsorption. (Accessed on 10/19/2018).

Furiouslettuce (2009), 'Bragg plane diffraction', https://upload.wikimedia.org/wikipedia/commons/7/74/BraggPlaneDiffraction.svg. (Accessed on 10/08/2018).

Galarnyk, M. (2018), 'Explaining the 68-95-99.7 rule for a normal distribution', https://tinyurl.com/659599rule. (Accessed on 10/02/2018).

Grant, J. M. & Arrighi, V. (2007), *Polymers: chemistry and physics of modern materials*, CRC press.

Grasmeder, J. (2017), 'Polymer crystallinity, explained part 3', https://tinyurl.com/polymercrystallinity. (Accessed on 10/19/2018).

Jasuja, N. et al. (2018), 'Absorption vs adsorption - difference and comparison', https://www.diffen.com/difference/Absorption_vs_Adsorption. (Accessed on 10/19/2018).

Kim, J. K., Thomas, S. & Saha, P. (2016), *Multicomponent Polymeric Materials*, Vol. 223, Springer.

Liao, D. et al. (2014), 'Validation of shape context based image registration method using digital image correlation measurement on a rat stomach', *Journal of Computational Medicine* **2014**.

Lund University, C. f. A. & Synthesis (2019*a*), 'Stoe powder diffraction system [measurement instrument]'. (Accessed on 31/01/2019).

Lund University, C. f. A. & Synthesis (2019*b*), 'Universal v4.5a ta instruments [measurement instrument]'. (Accessed on 31/01/2019).

Magmar452 (2014), 'Polyethylene repeat unit', https://upload.wikimedia.org/wikipedia/commons/4/45/Polyethylene_repeat_unit.svg. (Accessed on 11/09/2018).

Metrology, P. I. D. (2019), 'Gom correlate', https://www.gom.com/3d-software/gom-correlate.html. (Accessed on 21/01/2019).

Nast, C. (2012), 'Orange juice, raw nutrition facts & calories', https://nutritiondata.self.com/facts/fruits-and-fruit-juices/1971/2. (Accessed on 11/09/2018).

Nilsson, P. (2017), 'Measuring material properties of thin films with dic and tearing test of laminate'.

Pak, T. (2014), 'Tetra pak recognized for outstanding package design', https://tinyurl.com/Outstandingpackagedesign. (Accessed on 10/01/2018).

Piiroja, E. & Lippmaa, H. (1989), 'Thermal degradation of polyethylene', *Makromolekulare Chemie. Macromolecular Symposia* **27**(1), 305–309.
URL: *https://onlinelibrary.wiley.com/doi/abs/10.1002/masy.19890270121*

Podorov, S. et al. (2006), 'A new approach to wide-angle dynamical X-ray diffraction by deformed crystals', *Journal of Applied Crystallography* **39**(5), 652–655.
URL: *https://doi.org/10.1107/S0021889806025696*

Schmacke, S. (2010), Investigations of Polyethylene Materials by Means of X-ray Diffraction: Artificial Ageing of Polyethylene Gas Pipes, PhD thesis, Universitätsbibliothek Technische Universität Dortmund.

Schnablegger, H. & Singh, Y. (2013), 'The saxs guide', *Anton Paar GmbH* .

Schümann, K. et al. (2016), 'Conversion of engineering stresses to cauchy stresses in tensile and compression tests of thermoplastic polymers', *Current Directions in Biomedical Engineering* **2**(1), 649–652.

Sguazzo, C. & Hartmann, S. (2018), 'Tensile and shear experiments using polypropylene/polyethylene foils at different temperatures', *Technische Mechanik* **38**.

Sichina, W. et al. (2000), 'Dsc as problem solving tool: measurement of percent crystallinity of thermoplastics', *Perkin Elmer Instruments, and PETech* **40**.

Smokefoot (2011), 'Triglyceride sunflower', https://upload.wikimedia.org/wikipedia/commons/7/7c/TriglycerideSunflower.png. (Accessed on 11/09/2018).

Swapp, S. (2017), 'Scanning electron microscopy (sem)', https://serc.carleton.edu/research_education/geochemsheets/techniques/SEM.html. (Accessed on 10/03/2018).

TestResources.net (2013), 'Making dogbone tensile test samples', https://www.testresources.net/blog/making-dogbone-tensile-test-samples/. (Accessed on 10/17/2018).

Universitat, H. (2018), 'Differential scanning calorimetry', https://polymerscience.physik.hu-berlin.de/docs/manuals/DSC.pdf. (Accessed on 09/25/2018).

Vu, E. (2019), Selfmade or self taken images, edited with photoshop. (Accessed on 31/01/2019).

Wahlström, I. (2018), Fracture mechanics and damage modeling of injection molded high density polyethylene, diploma thesis, Lund University, Lund.

World, P. (2017), 'Land of milk and neutrons', http://live.iop-pp01.agh.sleek.net/2017/09/16/land-of-milk-and-neutrons/. (Accessed on 05/29/2018).

Xiong, B. (2014), Contribution to the study of elastic and plastic deformation mechanisms of polyethylene and polypropylene as a function of microstructure and temperature, Theses, INSA de Lyon.
URL: *https://tel.archives-ouvertes.fr/tel-01278480*

Xu, J.-t. et al. (2004), 'Simultaneous saxs/waxs/dsc studies on microstructure of conventional and metallocene-based ethylene-butene copolymers', **22**(3), 279–287.

Yikrazuul (2009), 'L-ascorbic acid', https://upload.wikimedia.org/wikipedia/commons/e/e7/L-Ascorbic_acid.svg. (Accessed on 11/09/2018).